

AD736781

AD736781

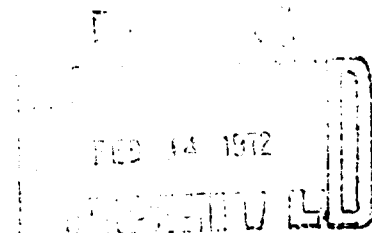
THE ENDOCHRONIC THEORY  
OF VISCOPLASTICITY —  
APPLICATION TO THE MECHANICAL  
BEHAVIOR OF METALS

K. C. Valanis  
Professor of Chemical Engineering  
Stevens Institute of Technology  
Hoboken, New Jersey 07030

Research sponsored by the Air Force Office  
of Scientific Research, ~~Office of Aerospace~~  
Research, United States Air Force, under  
AFOSR Grant ~~Hr~~70-1916.

Reproduced by  
NATIONAL TECHNICAL  
INFORMATION SERVICE  
Springfield, Va 22151

December, 1971



## DOCUMENT CONTROL DATA - R &amp; D

(Security classification of title, body of abstract and indexing annotation must be entered when the overall report is classified)

1. ORIGINATING ACTIVITY (Corporate author) University of Iowa Department of Mechanics and Hydraulics Iowa City, Iowa 52240		2a. REPORT SECURITY CLASSIFICATION Unclassified	
		2b. GROUP	
3. REPORT TITLE  THE ENDOCHRONIC THEORY OF VISCOPLASTICITY - APPLICATION TO THE MECHANICAL BEHAVIOR OF METALS			
4. DESCRIPTIVE NOTES (Type of report and inclusive dates) Scientific Final			
5. AUTHOR(S) (First name, middle initial, last name)  Kirk C. Valanis			
6. REPORT DATE DEC. 1978		7a. TOTAL NO. OF PAGES 128 143	7b. NO. OF REFS 55
8a. CONTRACT OR GRANT NO. AFOSR 70-1916		9a. ORIGINATOR'S REPORT NUMBER(S)	
b. PROJECT NO. 9749			
c. 61102F		9b. OTHER REPORT NO(S) (Any other numbers that may be assigned this report)	
d. 681304			
10. DISTRIBUTION STATEMENT  Approved for public release; distribution is unlimited.			
11. SUPPLEMENTARY NOTES  TECH. OTHER		12. SPONSORING MILITARY ACTIVITY Air Force Office of Scientific Research (NM) 1400 Wilson Boulevard, Arlington, Va. 22209	
13. ABSTRACT  A theory of thermoviscoplasticity is developed, which is firmly founded on the principles of irreversible thermodynamics of internal variables developed previously by the author. It differs from previous theories in the essential axiom that the material senses changes in deformation and temperature in a time scale which is an inherent material property. The theory has thus been termed ENDOCHRONIC.  Material behavior is described in terms of "heredity functions" akin to those in viscoelasticity. Many applications to the mechanical behavior of copper and aluminum are then considered, and many facets of their behavior such as yield, hysteresis, Bauschinger effect, cross-hardening, cyclic hardening, creep and relaxation are predicted and described analytically by the theory, with remarkable accuracy.			

### Final Report

This report is a summary of the work accomplished during the year 1970-1971, under AFOSR Grant 1916-70. The work consists in three main parts:

(a) The development of mathematical constitutive theory for inelastic materials undergoing deformation in a non-isothermal environment.

(b) The application of the theory to certain specific situations, where experimental measurements were made by other people in the past; the purpose part (b) was to establish the physical soundness of the theory and to illustrate its applicability.

(c) The performance of a set of critical experiments with a view to determining the material (heredity) functions that appear in the constitutive equation derived in (a). Knowledge of the material functions will help in their analytical representations necessary for the solution of problems relevant to the analysis and design of aerospace systems.

The development of the theory is based on the principles of Irreversible thermodynamics and the axiom that the stress is determined by the previous history of deformation defined on a time scale which is itself a property of the material at hand.

The foundations are then laid for a class of constitutive equations which govern the behavior of inelastic materials when these are subjected to coupled thermomechanical disturbances. This is done in the first report entitled, "A Theory of Viscoplasticity Without a Yield Surface Part I - General Theory".

Applications of the theory are dealt with in extenso in the second report entitled, "A Theory of Viscoplasticity Without a Yield Surface Part II - Application to Mechanical Behavior of Metals".

A number of problems involving complex deformation of metals under isothermal conditions of small strain, are given analytical solutions for the first time. These solutions are compared with experiments and such comparisons, in all cases favorable, speak eloquently for the power of the theory.

In parallel with the theoretical effort, an experimental program was undertaken to elucidate a number of points which are likely to be of importance in the further development and application of the theory. In particular the physical basis for the assumption of plastic incompressibility was tested; it was found (just as Bridgman did in 1948 but his work went unnoticed) that no such basis exists. Detailed discussion of this aspect of the work is found in Report 3, entitled, "Material Instabilities in the Experimental Study of the Plastic Compressibility of Some Important Metals".

Further, the form of the heredity functions, that appear in the theory, was investigated experimentally for copper and aluminum. Realistic analytical representations of these functions is now possible for the future application and further refinement of the theory. This part of the experimental program is discussed in Report 4 entitled, "Experimental Determination of the Heredity Functions of Copper and Aluminum".

Reports 1 and 2 have already been published in the European Journal, *Archivum Mechaniki Sostowanej*. Published by the Polish Academy of Science. The reference is: *Arch. Mech. Sost.*, 4, (1971).

In summary, visible progress (conceptual as well as analytical) has been made, in this one year in the understanding of the phenomenological description of the mechanical behavior of metals, as a result of this Grant.



K. C. Valanis  
Professor and Principal Investigator

A THEORY OF VISCOPLASTICITY  
WITHOUT A YIELD SURFACE  
PART I - GENERAL THEORY

K. C. Valanis  
Professor of Mechanics  
University of Iowa  
Iowa City

Research sponsored by the Air Force Office  
of Scientific Research, Office of Aerospace  
Research, United States Air Force, under  
AFOSR Grant Nr70-1916.

December, 1970

### ABSTRACT

Herein, we propose a mathematical theory of thermo-viscoplasticity which is a synthesis of experimentally observed material behavior on one hand, and the concepts of irreversible thermodynamics on the other.

The underlying principle is that the history of deformation is defined in terms of a "time scale" which is not measured by a clock, but is in itself a property of the material at hand.

The theory is unifying in the sense that theories of plasticity, viscoelasticity and elasticity can be obtained from it as special cases by imposing suitable constraints on the material parameters involved; furthermore, it does not make use of the idea of a yield surface.

## Section 1. Endochronic Theory of Viscoplasticity

In current theories of plasticity, to explain the observed discontinuities in material behavior upon loading beyond the "yield point" and upon unloading, one has to introduce the concept of a yield surface in stress space as well as a "loading function" to distinguish between loading and unloading. Similarly, in the case of viscoplasticity, the existence of a static stress-strain relation and a yield surface are assumed and the stress increment, with respect to the static value, is related to the strain rate, or more generally to the strain history, by a constitutive equation.

However, the fact that the phenomenon of yield is usually a gradual transition from a linear to a non-linear stress-strain response, makes it difficult to say precisely where yield has occurred, to the extent that different definitions of yield are used for this purpose. Three such definitions, for instance, are (a) the deviation from linearity in the relation between some measure of strain and stress (b) the intersection of the initial part of a stress strain curve and the backward linear extrapolation of the "plastic" part of the curve and (c) a value of "proof" stress corresponding to an arbitrarily defined value of "proof" strain.

Though, from an engineering viewpoint, the initial yield surface is not overly influenced by the definition of yield, it has been found experimentally that subsequent yield surfaces of a strain hardening material are influenced by the definition of yield to an extraordinary degree. (See Appendix I). If we insist that the increment in plastic strain is to be normal to the yield surface, then, for complex stress histories, each such definition will give rise to a different plastic strain history. Only one of these can be the correct one.

The conceptual difficulties that are encountered by the introduction of the yield surface are completely circumvented by our theory of plasticity which is developed on the basis of the observation that the state of stress in the neighborhood of a point in a plastic material depends on the set of all previous states of deformation of that neighborhood, but it does not depend on the rapidity at which such deformation states have succeeded one another<sup>\*</sup>.

The independence of stress of the rapidity of succession of deformation states is achieved by introducing a time scale  $\xi$  which is independent of  $t$ , the external time measured by a clock, but which is intrinsically related to the deformation of the material.

Of course there are many ways of introducing such a time scale. However, it appears almost mandatory that  $\xi$  should be a monotonically increasing function of deformation, otherwise two different states of deformation could exist "simultaneously" i.e. for the same value of  $\xi$ . Furthermore, a positive rate of change  $\frac{dc}{d\xi}$ , of the internal energy density  $c$  with respect to  $\xi$  could not be interpreted unambiguously as a process of increasing  $c$ , if  $d\xi$  could be negative.

A logical definition<sup>\*\*</sup> for  $\xi$  is then given by the relation

---

<sup>\*</sup>In the present Section and in subsequent Sections (with the exception of Section 2) we shall assume that mechanical changes take place in a constant temperature environment, such as an isothermal atmosphere. The thermal changes in the material will, therefore, be mechanically induced and, in general, will remain small. Conversely, only thermal changes of this nature will be considered in this paper.

<sup>\*\*</sup>Alternative but less general definitions have appeared in the literature. For instance, Ilyushin<sup>(1)</sup> and later Rivlin<sup>(2)</sup> defined a "time"  $s$  by the relation  $ds^2 = dC_{ij}dC_{ij}$ . However, we have found that this definition is too narrow to describe, quantitatively, material behavior in the plastic range as will be discussed later. The effect of temperature on  $\xi$ , will at this time, be considered sufficiently small to be negligible. For a more vague allusion to this possibility see also, Schapery (3).



$$d\xi^2 = P_{ijkl} dC_{ij} dC_{kl} \quad (3.1)$$

where  $C_{ij}$  is the Right Cauchy-Green tensor and  $P_{ijkl}$  is a fourth order tensor which could depend on  $C_{ij}$ . The positive definite nature of  $d\xi^2$  requires that  $P_{ijkl}$  be positive definite. In the case of small deformation

$$d\xi^2 = p_{ijkl} d\epsilon_{ij} d\epsilon_{kl}$$

where  $\epsilon_{ij}$  is the small deformation strain tensor and  $p_{ijkl}$  could depend on  $\epsilon_{ij}$ .

Actual materials, on the other hand, do, in general, depend on the history of deformation as well as on the rapidity, or rate, at which deformation states succeed one another. To describe materials of this type one may construct a theory of viscoplasticity by introducing a time scale  $\zeta$  which is related to the external time  $t$ .

It appears logical to define  $\zeta$  by the relationship

$$d\zeta^2 = \alpha^2 d\xi^2 + \beta^2 dt^2$$

where  $\alpha$  and  $\beta$  are scalar material parameters. Henceforth  $d\zeta$  will be called an "intrinsic time measure", and  $\zeta(\zeta)$ , such that  $\frac{d\zeta}{d\zeta} > 0$  ( $0 \leq \zeta < \infty$ ), will be called an "intrinsic time scale".

In our theory, the stress (among other properties) is necessarily, a functional of the strain history, defined with respect to the intrinsic time scale, the latter being a property of the material at hand. As a result we have called our theory an endochronic theory of viscoplasticity.

The theory will now be developed in a general thermodynamic framework in Section 3. Before this is done, however, the thermodynamic foundations are laid in Section 2.

## Section 2. Thermodynamic Foundations

The following are the fundamental laws of thermodynamics, which apply to all continuous media irrespective of their constitutive properties. (For materials that are solid-like, in the sense that they have a memory of their initial configuration, it is more convenient to express these laws in the material coordinate system  $x^i$ ). In differential form, these are the first law of thermodynamics,

$$\dot{\epsilon} = (\rho_0/2\rho) \tau^{ij} \dot{C}_{ij} - h^i_{,i} + \dot{Q}, \quad (2.1)$$

the rate of dissipation inequality,

$$\theta \dot{\gamma} = (\rho_0/2\rho) \tau^{ij} \dot{C}_{ij} - \dot{\psi} - n\dot{\theta} \geq 0 \quad (2.2)$$

and the heat conduction inequality

$$-h^i \theta_{,i} \geq 0. \quad (2.3)$$

The symbols in eq.'s (2.1), (2.2) and (2.3) have the following meaning:  $\rho_0 \epsilon$  is the internal energy per unit mass;  $\rho_0$  and  $\rho$  are the initial and current mass densities respectively;  $\tau^{ij}$  is the stress tensor in the material coordinate system  $x^i$ ;  $C_{ij}$  is the right Cauchy-Green tensor,  $h^i$  is the heat flux vector per unit undeformed area in the material system;  $\rho_0 Q$  is the heat supply per unit mass;  $\theta$  is the temperature,  $\gamma$  the irreversible entropy and  $\psi$  and  $n$  are the free energy and entropy, respectively, per unit undeformed volume finally a subscript following a comma denotes differentiation with respect to the corresponding material coordinate. A dot over a quantity denotes material derivative with respect to time. To avoid repetitious statements, henceforth we shall refer to  $C_{ij}$  as the "deformation".

In the case of dissipative materials the stress, the internal energy and entropy densities (and, therefore, the free energy density) of a material neighborhood depend on the entire history of deformation and temperature of that neighborhood.

In the theory of irreversible thermodynamics the effects of history are taken into account by specifying that the stress and free energy density are functions of the current values of  $C_{ij}$  and  $\theta$  as well as  $n$  additional independent variables  $q_\alpha$ , not necessarily observable, called "internal variables". These may be scalars or components of vectors or tensors in the material frame; whatever their geometric nature they must remain invariant with translation and rotation of the spatial system to satisfy the principle of material indifference. Thus:

$$\psi = \psi(C_{ij}, \theta, q_\alpha) \quad (2.4)$$

$$\tau^{ij} = \tau^{ij}(C_{kl}, \theta, q_\alpha) \quad (2.5)$$

It has been shown elsewhere<sup>(4)</sup> that

$$\tau^{ij} = \frac{2\rho}{\rho_0} \frac{\partial \psi}{\partial C_{ij}} \quad (2.6)$$

$$\eta = - \frac{\partial \psi}{\partial \theta} \quad (2.7)$$

$$\theta \dot{\gamma} = - \frac{\partial \psi}{\partial q_\alpha} \dot{q}_\alpha \geq 0 \quad (2.8)$$

Furthermore the heat flux vector  $h^i$  is a function of  $\theta$ ,  $C_{ij}$  and  $q_\alpha$  i.e.,

$$h^i = h^i(\theta, C_{kl}, q_\alpha) \quad (2.9)$$

subject to the conditions:

$$h^i \Big|_{\theta, i = 0} = 0, \quad h^i \theta, i \leq 0. \quad (2.10 \text{ a, b})$$

Finally eq. (2.1) in conjunction with eq.'s (2.6) and (2.7) yields

$$h^i_{,i} = \theta \left( \frac{\partial \psi}{\partial \theta} \right) \cdot - \frac{\partial \psi}{\partial q_\alpha} \dot{q}_\alpha + \dot{\theta} \quad (2.11)$$

The remarkable property of the above equations is that they apply to all materials irrespective of their constitution. This has not been generally recognized. In fact the constitutive nature of the material follows from the constitutive properties of  $q_\alpha$ . For example, in elastic materials  $q_\alpha = 0$ , whereas in viscoelastic materials  $q_\alpha$  are given by a set of differential equations of the type,

$$\dot{q}_\alpha = f_\alpha (q_\beta, c_{ij}, \theta) \quad (2.12).$$

The question of how  $q_\alpha$  are determined for viscoplastic materials is considered in the next Section.

### Section 3. Constitutive Equations in Viscoplasticity

From the right hand side of eq. (2.8) and the fact that  $\frac{dz}{dt} > 0$  and  $dz/d\tau > 0$ , it follows that

$$-\frac{\partial \psi}{\partial q_\alpha} \frac{dq_\alpha}{dz} \geq 0 \quad (\alpha \text{ not summed}) \quad (3.1)$$

where the inequality is valid unless  $\frac{dq_\alpha}{dz} = 0$ . It also follows from inequality (3.1) that  $\frac{dq_\alpha}{dz}$ ,  $q_\alpha$ ,  $C_{ij}$  and  $\theta$  must be related otherwise  $\frac{\partial \psi}{\partial q_\alpha}$  and  $\frac{dq_\alpha}{dz}$  could be prescribed independently and in such a fashion, that the inequality would be violated. In this event there must exist a set of relations

$$\frac{dq_\alpha}{dz} = f_\alpha(C_{ij}, q_\beta, \theta) \quad (3.2)$$

for all  $\alpha$ , where the functions  $f_\alpha$  are material functions.

It must be noted that, as a result of eq. (3.2)  $q_\alpha$  are indeed functionals of the histories of deformation and temperature with respect, however, to the intrinsic time scale  $z$  which is, itself, a material property.

Thus, at least formally, the constitutive equations of the endochronic theory of viscoplasticity are now complete in the sense that given the material functions  $f_\alpha, \psi$  and  $h^i$  then for some specified deformation and temperature histories,  $q_\alpha$  are found from eq. (3.2) and thus  $\tau^{ij}$  and  $\eta$  are found from eq's. (2.6) and (2.7) respectively; similarly  $h^i$  the heat flux vector is determined from eq. (2.9).

Ideally, one would like to know the thermomechanical three-dimensional response of a material over the whole spectrum of mechanical and thermal conditions, i.e., under all variations in strain, strain rate (or more generally, history of strain) and temperature. However, such a task would be a momentous, if not an impossible, undertaking; the experimental evaluation of the material

functions involved, under wide conditions of strain and temperature, would be impractical.

Fortunately the domain of specification of design conditions is usually limited in some way; for instance usually, (a) large changes of temperature, fast rates of loading, but small strains are prescribed; or (b) small changes in temperature and small rates of loading but large strains and/or displacements prevail. More extreme mechanical as well as thermal conditions are rarer.

It is reasonable to expect that material behavior would be easier to describe mathematically over a narrower domain of environmental conditions, where the applicability or "correctness" of such mathematical formulation would be easier to check experimentally.

In what follows we shall consider situations in which the strain in a material region  $R$  as well as the temperature changes relative to a uniform reference temperature  $\theta_0$  are "small". To make the above statement more precise let  $\epsilon_{ij}(z')$  denote the history of the strain tensor\*, for  $z_0 \leq z' \leq z$  where  $z_0$  is some initial intrinsic time. Set

$$||\epsilon_{ij}(z')|| \equiv \{\epsilon_{ij}(z') \epsilon_{ij}(z')\}^{1/2} \quad (3.3)$$

and let the supremum of  $||\epsilon_{ij}(z')||$  be  $\Delta$ .

Similarly let  $\vartheta(z')$  be the history of the temperature increment relative to the reference temperature  $\theta_0$  and let the supremum of  $|\vartheta(z')|$  be  $\delta$ . The notion of smallness is made precise by stipulating that  $\Delta \ll 1$  and  $\delta \ll 1$ .

Thus, formally

$$\theta = \theta_0 + \vartheta \quad (3.4)$$

---

\* $\epsilon_{ij} = \frac{1}{2} (C_{ij} - \delta_{ij})$

$$\eta = \eta_0 + \chi \quad (3.5)$$

$$||\epsilon_{ij}(z')||_{\text{sup}} = \Delta, \quad |\mathcal{J}(z')|_{\text{sup}} = \delta \quad (3.6)$$

To complete the formalism let  $\chi$  be the entropy change relative and a reference uniform entropy  $\eta_0$ , and let  $\sigma_{ij}$  denote the stress tensor. The reference state is defined by the condition that  $\sigma_{ij} = 0$ ,  $\psi = \mathcal{J} = \chi = 0$ ,  $q_\alpha = 0$ .

Under these conditions, eq.'s (2.4) through (2.9) and eq. (2.10b) become,

$$\psi = \psi(\epsilon_{ij}, \mathcal{J}, q_\alpha) \quad (3.7)$$

$$\sigma_{ij} = \frac{\partial \psi}{\partial \epsilon_{ij}} \quad (3.8)$$

$$\chi = - \frac{\partial \psi}{\partial \mathcal{J}} \quad (3.9)$$

$$\theta_0 \dot{\gamma} = - \frac{\partial \psi}{\partial q_\alpha} \dot{q}_\alpha \geq 0 \quad (3.10)$$

$$h_i = k_{ij} \mathcal{J}_{,j} \quad (3.11)$$

$$h_i \mathcal{J}_{,i} \leq 0 \quad (3.12)$$

where  $k_{ij}$  is the thermal conductivity tensor.

Finally eq. (2.11), becomes

$$h_{i,i} = \theta_0 \left( \frac{\partial \psi}{\partial \mathcal{J}} \right)' - \frac{\partial \psi}{\partial q_\alpha} \dot{q}_\alpha + Q \quad (3.13)$$

It is shown in Appendix II that  $|q_\alpha|$  and  $|\dot{q}_\alpha|$  may stay small in the sense that given two positive numbers  $\delta_1^\alpha$  and  $\delta_2^\alpha$ , however small,  $\Delta$  and  $\delta$  can be chosen small enough such that  $|q_\alpha| < \delta_1^\alpha$  and  $|\dot{q}_\alpha| < \delta_2^\alpha$ .

At this stage one may obtain the corresponding equation for  $q_\alpha$  by linearizing eq. (3.2). However it is physically more meaningful and, a posteriori, more rewarding to examine more closely the rate of change of

irreversible entropy  $\dot{\gamma}$  .

From eq. (3.10),

$$\theta_0 \frac{d\gamma}{dz} = - \frac{\partial \psi}{\partial q_\alpha} \frac{dq_\alpha}{dz} \geq 0 \quad (3.14)$$

It follows from eq.'s (3.14) and (3.2) that  $\frac{d\gamma}{dz}$  may be expressed as a function of  $\frac{dq_\alpha}{dz}$ ,  $\varepsilon_{ij}$  and  $\mathcal{D}$ , subject to the condition that  $\frac{d\gamma}{dz} = 0$  whenever  $\frac{dq_\alpha}{dz} = 0$  for all  $\alpha$ . Thus, if we expand  $\theta_0 \frac{d\gamma}{dz}$  in a Taylor series and ignore terms of order higher than  $O(\delta^2)^*$  and observe the inequality (3.10), thereby eliminating the linear terms in the expansion, then

$$\theta_0 \frac{d\gamma}{dz} = b_{\alpha\beta} \frac{dq_\alpha}{dz} \frac{dq_\beta}{dz} \quad (3.15)$$

Eq.'s (3.14) and (3.15) are simultaneously satisfied if

$$\frac{\partial \psi}{\partial q_\alpha} + b_{\alpha\beta} \frac{dq_\beta}{dz} = 0 \quad (3.16)$$

With eq. (3.16) the constitutive description of a viscoplastic material is now complete.

#### Explicit Constitutive Equations

Explicit constitutive equations for viscoplastic materials under conditions of small strain and small changes in temperature are obtained by expanding  $\psi$  in eq. (3.7) in Taylor Series and omitting terms of order higher than  $O(\delta^2)$ ; \* linear terms must vanish to satisfy the initial conditions.

Before the expansion is carried out, however, it appears desirable to regard  $q_\alpha$  not as scalars but components of second order tensors. This, as will be shown, obviates certain difficulties which arise with the representation of fourth order tensors. For instance, in Ref. (4), we were faced

---

\* $\delta_\alpha$  is the largest of  $\delta_1^\alpha$  and  $\delta_2^\alpha$ . Also,  $\hat{\delta}$  is the largest of  $\delta$ ,  $\Delta$  and  $\delta_1^\alpha$ .



with having to assume, without proof, that a fourth order tensor  $C_{ijkl}$  such that,

$$C_{ijkl} = C_{jikl} = C_{ijlk} = C_{klij}$$

is given by the series

$$C_{ijkl} = \sum_{\alpha} \frac{a_{ij\alpha} a_{kl\alpha}}{a_{\alpha}} \quad (3.17)$$

where  $a_{ij\alpha}$  are second order symmetric tensors and  $a_{\alpha}$  are scalars. Problems such as this are obviated by giving the internal variables a tensorial character. Thus the free energy density and other thermodynamic quantities are now functions of  $\epsilon_{ij}$ ,  $\eta$  and  $n$  internal variables  $q_{ij}^{\alpha}$  ( $\alpha = 1, 2, \dots, n$ ), where  $q_{ij}^{\alpha}$  are symmetric second order tensors, with respect to the material system  $x_i$ . In this notation, eq.'s (3.13) through (3.16) now read,

$$h_{i,i} = \theta_0 \frac{\partial \psi}{\partial \theta} - \frac{\partial \psi}{\partial q_{ij}^{\alpha}} \dot{q}_{ij}^{\alpha} + \dot{Q} \quad (3.18)$$

$$\theta_0 \frac{dy}{dz} = - \frac{\partial \psi}{\partial q_{ij}^{\alpha}} \frac{dq_{ij}^{\alpha}}{dz} \geq 0 \quad (3.19)$$

$$\theta_0 \frac{dy}{dz} = \sum_{\alpha} b_{ijkl}^{\alpha} \frac{dq_{ij}^{\alpha}}{dz} \frac{dq_{kl}^{\alpha}}{dz} \quad (3.20)^*$$

and

$$\frac{\partial \psi}{\partial q_{ij}^{\alpha}} + b_{ijkl}^{\alpha} \frac{dq_{kl}^{\alpha}}{dz} = 0 \quad (3.21)$$

(a not summed)

---

\*Expansions of the type  $b_{ijkl}^{\alpha\beta} \frac{dq_{ij}^{\alpha}}{dz} \frac{dq_{kl}^{\beta}}{dz}$  and  $A_{ijkl}^{\alpha\beta} q_{ij}^{\alpha} q_{kl}^{\beta}$  reduce to the above form. See Ref. 5.

Furthermore, in view of my previous discussion,

$$\begin{aligned} \psi = & \frac{1}{2} A_{ijkl} \epsilon_{ij} \epsilon_{kl} + B_{ijkl}^{\alpha} \epsilon_{ij} q_{kl}^{\alpha} + \frac{1}{2} C_{ijkl}^{\alpha} q_{ij}^{\alpha} q_{kl}^{\alpha} \\ & + D_{ij} \vartheta \epsilon_{ij} + E_{ij}^{\alpha} \vartheta q_{ij}^{\alpha} + \frac{1}{2} F \vartheta^2 \end{aligned} \quad (3.22)$$

Though, in principle, eq.'s (3.8), (3.9), (3.18), (3.21) and (3.22) are sufficient for the derivation of explicit constitutive equations, we shall obtain these only for isotropic material, so as to keep the algebra at a minimum. For such materials

$$\begin{aligned} A_{ijkl} &= A_1 \delta_{ij} \delta_{kl} + A_2 \delta_{ik} \delta_{jl} \\ B_{ijkl}^{\alpha} &= B_1^{\alpha} \delta_{ij} \delta_{kl} + B_2^{\alpha} \delta_{ik} \delta_{jl} \\ C_{ijkl}^{\alpha} &= C_1^{\alpha} \delta_{ij} \delta_{kl} + C_2^{\alpha} \delta_{ik} \delta_{jl} \\ D_{ij} &= D \delta_{ij} \\ E_{ij}^{\alpha} &= E^{\alpha} \delta_{ij} \\ k_{ij} &= k \delta_{ij} \\ b_{ijkl}^{\alpha} &= b_1^{\alpha} \delta_{ij} \delta_{kl} + b_2^{\alpha} \delta_{ik} \delta_{jl} \end{aligned} \quad (3.23 \text{ a-f})$$

It is worth noting that here we consider materials which are "stable" in the sense that straining of the reference configuration under isothermal conditions will increase the free energy density  $\psi$ . Thus  $A_{ijkl}$  and  $C_{ijkl}^{\alpha}$  are positive definite. As a consequence  $A_1$ ,  $A_2$ ,  $C_1^{\alpha}$  and  $C_2^{\alpha}$  are all positive.

Omitting superfluous algebra, the coupled thermomechanical constitutive equations take the following form in terms of the hydrostatic stress  $\sigma = \frac{\sigma_{kk}}{3}$ , the deviatoric stress tensor  $\sigma_{ij}$ , the increment in temperature  $\vartheta$ , the

hydrostatic strain  $\epsilon_{kk}$ , the deviatoric strain tensor  $e_{ij}$  and the entropy increment  $\chi$ ; in terms of the above notation:

$$s_{ij} = 2 \int_{z_0}^z \nu(z-z') \frac{\partial e_{ij}}{\partial z'} dz' \quad (3.24)$$

$$\sigma = \int_{z_0}^z K(z-z') \frac{\partial \epsilon_{kk}}{\partial z'} dz' + \int_{z_0}^z D(z-z') \frac{\partial \vartheta}{\partial z'} dz' \quad (3.25)$$

$$-\chi = \frac{\partial \psi}{\partial \vartheta} = \int_{z_0}^z D(z-z') \frac{\partial \epsilon_{kk}}{\partial z'} dz' + \int_{z_0}^z F(z-z') \frac{\partial \vartheta}{\partial z'} dz' \quad (3.26)$$

where,

$$2 \nu(z) = \left( A_2 - \sum_a \frac{B_2^a B_2^a}{C_2^a} \right) H(z) + \sum_a \frac{B_2^a B_2^a}{C_2^a} e^{-\rho_a z} \quad (3.27)$$

$$K(z) = \left( A_0 - \sum_a \frac{B_0^a B_0^a}{C_0^a} \right) H(z) + \sum_a \frac{B_0^a B_0^a}{C_0^a} e^{-\lambda_a z} \quad (3.28)$$

$$D(z) = \left( D - \sum_a \frac{B_a E_a}{C_a} \right) H(z) + \sum_a \frac{B_a E_a}{C_a} e^{-\lambda_a z} \quad (3.29)$$

$$F(z) = \left( F - \sum_a \frac{E_a E_a}{C_a} \right) H(z) + \sum_a \frac{E_a E_a}{C_a} e^{-\lambda_a z} \quad (3.30)$$

$$A_0 = 1/3 (3A_1 + A_2), \quad B_0 = 1/3 (3B_1 + B_2), \quad C_0 = 1/3 (3C_1 + C_2) \quad (3.31)$$

$$\rho_a = \frac{C_2^a}{b_2^a}, \quad \lambda_a = \frac{C_0^a}{b_0^a} \quad (3.32)$$

$$b_0^a = 3b_1^a + b_2^a \quad (3.33)$$

The heat conduction equation is similarly found to be:

$$\frac{dt}{dz} k \vartheta_{,ii} = \frac{\partial}{\partial z} \int_{z_0}^z C_v(z-z') \frac{\partial \vartheta}{\partial z'} dz' - \theta_0 \frac{\partial}{\partial z} \int_{z_0}^z F(z-z') \frac{\partial \epsilon_{kk}}{\partial z'} dz'$$

$$+ \hat{Q} + \sum_a \left[ b_1^a \hat{q}_{ii}^a \hat{q}_{jj}^a + b_2^a \hat{q}_{ij}^a \hat{q}_{ij}^a \right] \quad (3.34)$$

where

$$C_v(z) = - \theta_0 F(z) \quad (3.35)$$

and a roof over a quantity implies differentiation with respect to  $z$ . The lower limit  $z_0$  denotes the intrinsic time of the reference state.

#### Section 4. Endochronic Theory of Plasticity and its Relation to Present Theories

Our theory of plasticity, which is a rate independent endochronic theory, is obtained by replacing the time measure  $d\zeta$  by  $d\xi$ . The time scale now becomes  $z(\xi)$ , but the form of the constitutive equations remains unaltered. In particular, the "linear" form of our theory is obtained by setting

$$d\xi^2 = p_{ijkl} d\epsilon_{ij} d\epsilon_{kl} \quad (4.1)$$

where  $p_{ijkl}$  is a positive definite fourth order material tensor. We repeat the constitutive equations of the linear theory, in the particular case when the deformation is isothermal so that a comparison may be made with current theories. When  $\vartheta \equiv 0$ , then eq.'s (3.24) and (3.25) become,

$$s_{ij} = 2 \int_{z_0}^z u(z-z') \frac{\partial e_{ij}}{\partial z'} dz' \quad (4.2)$$

$$\sigma_{kk} = 3 \int_{z_0}^z K(z-z') \frac{\partial \epsilon_{kk}}{\partial z'} dz' \quad (4.3)$$

where  $z = z(\xi)$ .

If the material behaves elastically under pressure (so-called plastically incompressible) then  $K(z)$  is a constant and in this case

$$\sigma_{kk} = 3K\epsilon_{kk} \quad (4.4)$$

Whereas,

$$s_{ij} = 2 \int_{z_0}^z u(z-z') d\epsilon_{ij}(z') \quad (4.5)$$

Let now  $u(z)$  consist of a single exponential term i.e.

$$u(z) = u_0 e^{-\alpha z} \quad (4.6)$$

In this event

$$s_{ij} = 2\nu_0 \int_{z_0}^z \frac{-a(z-z')}{\sigma} de_{ij}(z') \quad (4.7)$$

The integral eq. (4.7) is reducible to the differential equation

$$de_{ij} = \frac{a}{2\nu_0} dz s_{ij} + \frac{1}{2\nu_0} ds_{ij} \quad (4.8)$$

Now,  $\frac{1}{2\nu_0} ds_{ij}$  may be identified as the "elastic" component of deviatoric strain of classical plasticity. If one follows the traditional definition of "plastic strain"  $de_{ij}^P$  given below, i.e.,

$$de_{ij}^P = d\epsilon_{ij} - d\epsilon_{ij}^e \quad (4.9)$$

then in view of eq. (4.8)

$$de_{ij}^P = \frac{a}{2\nu_0} dz s_{ij} \quad (4.10)$$

But these are the Prandtl-Reuss relations. Hence our present theory contains these relations as a special case. Where then does it differ from this theory? It does in the interpretation of the proportionality coefficient  $dz$ . In the Prandtl-Reuss theory  $d\epsilon$  may be positive negative or zero, and in fact,  $\epsilon$  has been identified with the yield surface, i.e., plastic action is assumed to occur when  $d\epsilon > 0$ , where

$$\epsilon = \epsilon(s_{ij}) \quad (4.11)$$

but that  $de_{ij}^P$  is zero whenever

$$d\epsilon \leq 0 \quad (4.12)$$

In the present theory  $dz$  is always positive if the material is deforming (it is zero only when deformation does not take place). Thus always,

$$dz \geq 0 \quad (4.13)$$

Furthermore  $dz$  is not given by eq. (4.11) i.e. it is not related to some yield surface but its definition is entirely kinematic. Thus, no yield phenomenon or surface are postulated here. One obtains the stress response by merely monitoring the history of strain.

Also the theory admits a further generality since  $u(z)$  need not consist of a single exponential term.

For instance  $u(z)$  may be of the form

$$u(z) = u_0 + u_1 e^{-\alpha z} \quad (4.14)$$

In this case, however, the differential form of eq. (4.7) becomes:

$$2(u_0 + u_1) de_{ij} + 2u_0 \alpha e_{ij} dz = ds_{ij} + \alpha s_{ij} dz \quad (4.15)$$

The shear modulus  $\mu$ , at  $z = 0$ , (initial modulus), is  $(u_0 + u_1)$ . The "plastic" components of the deviatoric shear strain tensor are given from eq. (4.9), i.e.,

$$de_{ij}^p = \frac{\alpha}{2\mu_1} dz s_{ij} - 2u_0 e_{ij} \quad (4.16)$$

Note that eq. (4.16) does not satisfy the Prandtl-Reuss relations, which are also violated if one adds more exponential terms to the right hand side of eq. (4.14). In fact these relations will be satisfied if and only if  $u(z)$  is given by eq. (4.6), i.e.,  $u$  is represented by a single exponential term only. This situation is not particularly disturbing. Peters et Als<sup>(40)</sup> carried out experiments on thin walled 14S-T4 aluminum alloy cylinders by loading these in combined compression and torsion and found that the Prandtl-Reuss relations were not satisfied, for this particular metal.

### Conclusions

A theory has been presented here, the scope of which is wide enough to allow a rational phenomenological description of mechanical behavior of materials under various histories of strain and temperature. In particular, the viscoplastic behavior of materials is formulated mathematically, without recourse to the dichotomy of the deformation history in plastic and elastic parts and without the necessity of introducing discontinuities in material behavior, such as yield surfaces.

The theory merely asserts that, to every history of deformation gradient and temperature of a neighborhood there corresponds a unique state of stress in that neighborhood. An entirely novel feature of the theory is that these histories are defined with respect to a time scale, which itself is a material property.

In this paper, we have merely presented the framework of the theory without actually evaluating the material functions involved, through the use of experimental data. This, however, will be done in Part II of this paper, where it will be shown that the theory describes experimentally observed plastic behavior of metals with a remarkable degree of accuracy.

### Stipulation

This manuscript is submitted for publication with the understanding that the United States Government is authorized to reproduce and distribute reprints for governmental purposes.



### Appendix I

The following is a short account of the experimental work on (a) the effect of the definition of yield on the shape of the yield surface and (b) of the work on viscoplasticity. The references given are by no means exhaustive and the author wishes to apologize to people of whose work he is not currently aware.

In Ref.'s 6 and 7, aluminum alloy tubes<sup>\*\*</sup> were subjected to shear prestrain by twisting well into the plastic region by a predetermined amount. The yield surface corresponding to this degree of prestrain was established by loading the tubes in combined tension and torsion.

In Ref. 6, Naghdi found that subsequent yield surfaces distorted in the direction of the shear axis with a pronounced Bauschinger effect in shear but there was no effect on the yield stress in tension (i.e. the yield locus did not change in the vicinity of zero shear stress).

On the other hand, in Ref. 7, Ivey observed that the yield surface, in addition to distortion, underwent a large amount of translation in the direction of the shear axis, so that for large prestrains the origin of the stress space was outside the yield surface. However, he was in agreement with Naghdi in that the presence of shear prestrain did not affect the yield stress in tension. Both authors used deviation from linearity in a stress strain diagram as a definition of yield.

Mair and Pugh<sup>(8)</sup> to check the absence of "cross effect", carried out their own experiments on copper with a high degree of isotropy. However they used a different definition of yield, this being the point of intersection of the initial straight part of the stress-strain curve with a backward linear extrapolation of the "plastic" part of the stress-strain curve.

Their results varied significantly from those of Ivey and Naghdi. They found that expansion and distortion of the initial locus took place with a strong cross effect between shear and tension. Also a pronounced Bauschinger effect in torsion was found with large initial positive pretorsion. These authors also observed pronounced "plastic" unloading in shear.

The results of Szczepinski and Miastkowski<sup>(9)</sup> tend to confirm the findings of Mair and Pugh<sup>(8)</sup>. Their results, moreover, were significant in other respects. Specifically, using the proof strain to define yield, they studied aluminum alloy sheets under biaxial tension with the intention of finding the effect of prestrain on the shape of the yield surfaces. They observed, migration, distortion, expansion and sometimes rotation of the initial yield locus.

Similar conclusions\* can be drawn from Szczepinski's paper<sup>(10)</sup>, as well as Miastkowski and Szczepinski's<sup>(17)</sup>, in which tubular brass specimens were subjected to combined axial and circumferential stress.

Initial and subsequent yield loci were plotted when yield was defined (a) as departure from linearity or (b) when it was set to correspond to a certain proof strain. In particular, when definition (a) was used, subsequent yield loci did not contain the initial locus, but when (b) was used, with proof strain set at 0.5% subsequent loci contained the initial locus.

Attempts to describe the change of the yield locus with prestrain, by simple models have not proved satisfactory. Batdorf and Budianski<sup>(13)</sup>, suggested that after prestrain, the yield locus is the minimum surface

---

\* In this connection, see also work of the same general nature by Bertsch and Findley<sup>(11)</sup> and Hu and Bratt<sup>(12)</sup>.

through the point of prestrain and the initial yield locus. This model however does not account for the Bauschinger effect. The kinematic hardening rule\*\* proposed by Prager<sup>(14)</sup>, was partially successful, in so far as it can be of value only when the stress-strain curve of a material in simple tension is bilinear<sup>(15)</sup>. Otherwise subsequent shapes of yield locus must be defined in terms of a parameter that depends on the history of strain<sup>(15)</sup> to obtain realistic unloading behavior.

A more realistic model is the one by Hodge<sup>(16)</sup> which includes translation, expansion and distortion of the yield surface. This model covers all contingencies but does not include the history of stress on the shape and position of the yield locus.

However, every definition of yield gives rise to a different yield surface. If we insist that the increment of plastic strain is to be normal to the yield surface, then, for a complex but specific loading history, each such definition will give rise to a different plastic strain history. Only one of these can be the correct one.

So it appears that through Eisenberg's and Phillip's<sup>(15)</sup> mathematical description of a yield surface has been most promising, we must be prepared to question, if necessary, whether the concept of yield point and yield surface are the only way by which plastic effects may be described, especially in view of the fact that these may take place immediately following the initiation of deformation of material, though they may be negligible in the region of small strains. This would agree with the point of view that dislocations (and, therefore, plastic behavior) originate immediately upon initiation of the loading.

---

\*\* See also Ref. (19).

### Viscoplasticity

The need for the development of the theory of viscoplasticity arises from the recognition of the strain rate sensitivity of metals under dynamic loading.

The difficulty in trying to synthesize a rational "rate" theory from experimental observations, a priori, lies in the fact that under dynamic conditions the inertia effects are significant. In the absence of a constitutive theory, these effects cannot be calculated.\* Therefore, in the case of dynamic theories, such as viscoplasticity, theory and experiment must advance together.

The literature abounds with data on the subject of strain rate sensitivity, particularly in one dimension.<sup>(20-30)</sup> Lindholm<sup>(32)</sup> carried out dynamic experiments in one and two dimensions in an attempt to generalize results which were arrived at, by consideration of thermally activated processes and their relation to dislocation theory in metals. See Ref.'s 35-40.

An early attempt at a theoretical viscoplastic constitutive equation in one dimension is due to Malvern.<sup>(31,32)</sup> This equation assumes the existence of a "static" stress-strain relation and then relates the stress increment, with respect the static value, to the strain rate.

Modifications and generalizations of Malvern's equation were made by Lubliner<sup>(33)</sup> who included a limiting maximum stress-strain curve, and by Perzyna<sup>(34)</sup>, Perzyna and Wojno<sup>(35)</sup> who proposed a multiaxial generalization

---

\* Constant strain rate experiments would appear to be an exception, by being less susceptible to inertia effects. However, Ref. 38 tends to negate this. Long specimens give different responses to short ones, under the same conditions.

for finite strains, assuming the additivity of the elastic and plastic strain components and by Perzyna<sup>(39)</sup> who used concepts of internal coordinates and irreversible thermodynamics to eliminate the above assumptions and to put the theory on sounder foundations.

Though, in his last treatment, Perzyna<sup>(39)</sup> abandoned the additivity of plastic and elastic strains, he still retained the concepts of yield stress (and yield surface) and the hypothesis of a datum plastic stress strain relation, with respect to which "strain history" is to be related to the "excess" stress through the internal coordinates.

Our theory differs from Perzyna's theory in this respect.

We close by mentioning that, with the exception of the papers by Perzyna<sup>(39)</sup>, only a moderate research effort has been made in the area of coupling between a viscoplastic and a thermal process. However, Chidister and Malvern<sup>(25)</sup>, Lindholm<sup>(27)</sup> and Trozera, Sherby and Dorn<sup>(37)</sup>, considered the effect of a change in uniform temperature on viscoplastic behavior, with a view to confirming some results of the dislocation theory.

# Appendix II

The form of eq. (3.22) for isotropic materials, according to eq.'s (3.22 a-e), is

$$\begin{aligned} \psi = & \frac{1}{2} A_1 \epsilon_{ii} \epsilon_{jj} + \frac{1}{2} A_2 \epsilon_{ij} \epsilon_{ij} + B_1^a \epsilon_{ii} q_{jj}^a + B_2^a \epsilon_{ij} q_{ij}^a \\ & + \frac{1}{2} C_1^a q_{ii}^a q_{jj}^a + \frac{1}{2} C_2^a q_{ij}^a q_{ij}^a + D \Theta \epsilon_{jj} + E^a \Theta q_{ii}^a \\ & + \frac{1}{2} F \Theta^2 \end{aligned} \quad (A.2.1)$$

As a result eq.'s (3.8) and (3.9) yield:

$$\begin{aligned} \sigma_{ij} = & A_1 \delta_{ij} \epsilon_{kk} + A_2 \epsilon_{ij} + B_1^a \epsilon_{ij} q_{kk}^a + B_2^a q_{ij}^a \\ & + D \Theta \delta_{ij} \quad (\alpha \text{ summed}) \end{aligned} \quad (A.2.2)$$

$$-\chi = \frac{\partial \psi}{\partial \Theta} = D \epsilon_{ii} + E^a q_{ii}^a + F \Theta \quad (\alpha \text{ summed}) \quad (A.2.3)$$

On the other hand,

$$\begin{aligned} \frac{\partial \psi}{\partial q_{ij}^a} = & B_1^a \epsilon_{kk} \delta_{ij} + B_2^a \epsilon_{ij} + C_1^a \delta_{ij} q_{kk}^a \\ & + C_2^a q_{ij}^a + E^a \delta_{ij} \Theta \quad (\text{not summed}) \end{aligned} \quad (A.2.3)$$

Hence, use of eq. (3.21) in accordance with eq. (3.23f) yields a set of first order differential equations for  $q_{ij}^a$ ; these can be expressed as a set for  $q_{kk}^a$  and another for the deviatoric part of  $q_{ij}^a$ , which we denote by  $p_{ij}^a$ . Thus in the notation of eq.'s (3.31) and (3.33)

$$B_0^a \epsilon_{kk} + C_0^a q_{kk}^a + E^a + b_0^a \frac{dq_{kk}^a}{dz} = 0 \quad (A.2.4)$$

$$B_2^a \epsilon_{ij} + C_2^a p_{ij}^a + b_2^a \frac{dp_{ij}^a}{dz} = 0 \quad (A.2.5)$$

In both eq.'s (A.2.4) and (A.2.5)  $\alpha$  is not summed. It follows from the above two equations that

$$q_{kk}^{\alpha} = - \frac{B_0^{\alpha}}{b_0^{\alpha}} \int_{z_0}^z e^{-\lambda_{\alpha}(z-z')} \epsilon_{kk}(z') dz' - \frac{E^{\alpha}}{b_0^{\alpha}} \int_{z_0}^z e^{-\lambda_{\alpha}(z-z')} \mathcal{G}(z') dz' \quad (A.2.6)$$

$$p_{ij}^{\alpha} = - \frac{B_2^{\alpha}}{b_2^{\alpha}} \int_{z_0}^z e^{-\rho_{\alpha}(z-z')} e_{ij}(z') dz' \quad (A.2.7)$$

where  $\lambda_{\alpha}$  and  $\rho_{\alpha}$  are given by eq. (3.32).

In the light of the tensorial notation that we have adopted for the internal variables, let

$$\left| \left| \epsilon_{ij} \right| \right|_{\sup} = \Delta, \quad \left| \left| e_{ij} \right| \right|_{\sup} = \Delta_1, \quad \left| \epsilon_{kk} \right|_{\sup} = \Delta_0 \quad (A.2.8)$$

where,  $\left| \left| \epsilon_{ij} \right| \right| = \left| \epsilon_{ij} \epsilon_{ij} \right|^{\frac{1}{2}}$ , etc. Evidently,

$$\Delta^2 = \Delta_1^2 + \frac{1}{3} \Delta_0^2 \quad (A.2.9)$$

Then as a result of eq.s (A.2.7) and (A.2.8)

$$\left| \left| p_{ij}^{\alpha} \right| \right| \leq \frac{|B_2^{\alpha}|}{C_2^{\alpha}} \Delta_1 \quad (A.2.10)$$

$$\left| q_{kk}^{\alpha} \right| \leq \frac{|B_0^{\alpha}|}{C_0^{\alpha}} \Delta_0 + \frac{|E^{\alpha}|}{C_0^{\alpha}} \delta \quad (A.2.11)$$

where as before  $\left| \mathcal{G} \right|_{\sup} = \delta$

Also from eq. (A.2.5),

$$(b_2^{\alpha})^2 \left| \left| \frac{dp_{ij}}{dz} \right| \right|^2 = (B_a^2)^2 \left| \left| e_{ij} \right| \right|^2 + (C_a^2)^2 \left| \left| p_{ij} \right| \right|^2 + 2B_a^2 C_a^2 \left| p_{ij} e_{ij} \right| \quad (A.2.12)$$

However, since

$$\left| p_{ij} e_{ij} \right| \leq \left| \left| p_{ij} \right| \right| \left| \left| e_{ij} \right| \right| \quad (A.2.13)$$

it follows from (A.2.12) that

$$b_2^a \left| \left| \frac{dp_{ij}}{dz} \right| \right| \leq 2 \Delta_1 |B_2^a| \quad (\text{A.2.14})$$

Also as a result of eq. (A.2.4)

$$b_0^a \left| \left| \frac{dq_{kk}^a}{dz} \right| \right| \leq 2 |B_0^a| \Delta_0 + 2 |E^a| \delta \quad (\text{A.2.15})$$

At this point we order our internal variables as shown,

$$p_{ij}^1, p_{ij}^2, \dots, p_{ij}^m; q_{kk}^1, q_{kk}^2, \dots, q_{kk}^m.$$

Let  $q_a$  be a typical internal variable. Then, whether it belongs to the p-group or the q-group above, as a result of eq.'s (A.2.10), (A.2.11), (A.2.14) and (A.2.14), given two positive members  $\delta_1$  and  $\delta_2$ , however small, we can choose  $\Delta_0$  and  $\Delta_1$  (and therefore  $\Delta$ ) and  $\delta$  such that

$$|q_a| \leq \delta_1 \text{ and } \left| \left| \frac{dq_a}{dz} \right| \right| \leq \delta_2.$$



# References

1. Ilyushin A. A., "On the relation between stresses and small deformations in the mechanics of continuous media," Prikl. Math. Meh., 18, 641, (1954).
2. Rivlin R. S., "Nonlinear viscoelastic solids," SIAM Review 7, 323, (1965).
3. Schapery, R. A., "On a thermodynamic constitutive theory and its application to various non-linear materials," Proceedings, IUTAM Symposium, East Kilbride, 259, (1968).
4. Valanis, K. C., "A unified theory of thermomechanical behavior of viscoelastic materials," Mechanical Behavior of Materials Under Dynamic Loads, Ed. U. S. Lindholm, Springer-Verlag, N. Y. (1968).
5. Valanis, K. C., "Thermodynamics of large viscrelastic deformations, J. Math and Phys., 45, 197, (1966).
6. Naghdi, P. M., Essenburgh, F. and Koff, W., "An experimental study of initial and subsequent yield surfaces in plasticity," J. App. Mech., 25, 201, (1958).
7. Ivey, H. J., "Plastic stress-strain relations and yield surfaces for aluminum alloys," J. Mech. Eng. Sc., 3, 15, (1961).
8. Mair W. M. and Pugh, H. L. 1. D., "Effect of prestrain on yield surfaces in copper," J. Mech. Eng. Sc., 6, 150 (1964).
9. Szczepinski, W. and Miastkowski, J., "An experimental study of the pre-staining history on the yield surfaces of an aluminum alloy," J. Mech. ph. Sol. 16, 153, (1968).
10. Szczepinski, W. "On the effect of plastic deformation on the yield condition," Bulletin de l'academie polonaise des sciences, Serie des sciences techniques, 11, 463, (1963).
11. Bertsch, P. K. and Findley, W. N., "An experimental study of subsequent yield surfaces, normality, Bauschinger and allied effects," Proc. 4th U. S. Congr. App Mech., Berkley (1962).
12. Hu, L. W. and Bratt, J. F., J. App. Mech. 25, 441 (1958).
13. Batdorf, S. F. and Budianski, B., "Polyaxial stress-strain relations of strain-hardening metal," J. App. Mech., 21, 323, (1954).
14. Prager, W., "The Theory of plasticity: a survey of recent achievements Proc. Inst. Mech. Eng., 169, 41, (1955).
15. Eisenberg, M. A. and Phillips, A., "On nonlinear kinematic hardening," Acta Mechanica, 5, 1, (1968).

16. Hodge, P. G., J. App. Mech., Trans. Amer. Soc. Mech. Eng. 79, 482 (1957).
17. Miastkowski J. and Szczepinski W., "An experimental study of yield surfaces of prestrained brass," Int. J. Solids Structures, 1, 189, (1965).
18. Naghdi P. M. and Rowley J. C., "An experimental study of biaxial stress-strain relations in plasticity," J. Mech. Phys. Solids, 3, 63, (1954).
19. Shield T. R. and Ziegler H., "On Prager's hardening rule," Zamp, 9, 260, (1958).
20. Bell, J. F., "Single, Temperature-dependent stress-strain law for the dynamic plastic deformation of annealed F. C. C. metals," J. App. Phys. 34, 134, (1963).
21. Rosen A. and Bodner, S. R., "The influence of strain rate and strain aging on the flow stress of commercially pur aluminum," J. Mech. Ph. Solids 15, 47, (1967).
22. Manjoine, M. J., "Influence of rate of strain and temperature on yield stresses of mild steel," Trans. ASME, 66, A211, (1944).
23. Hanser F. E., Simmons J. A. and Dorn J. E., "Strain rate effects in plastic wave propagation," University of California MRL publication, Series 133, Issue 3, (1960).
24. Marsh K. J. and Campbell J. D., "The effect of strain rate on the post yield flow of mild steel," J. Mech. Phys. Solids, 11, 49, (1963).
25. Chidister J. L. and Malvern, L. E., "Compression-impact testing of aluminum at elevated temperatures," Exp. Mech. 3, 81, (1963).
26. Lindholm, U. S., "Some experiments with the split Hopkinson bar," J. Mech. Phys. Solids, 12, 317, (1964).
27. Lindholm, U. S. and Yeakley, L. M., "Dynamic deformation of single and polycrystalline aluminum," J. Mech. Phys. Solids, 13, 41, (1965).
28. Lindholm, U. S., "Some experiments in dynamic plasticity under combined stress," Symposium on Mechanical Behavior of Materials under Dynamic Loads, San Antonio, Texas (1967).
29. Krafft, J. M., Sullivan, A. M. and Tipper, C. F., "The effect of static and dynamic loading and temperature on the yield stress of iron and mild steel in compression," Proc. Royal Soc. Land. A 221, 114 (1954).
30. Larsen, T. L. et Als, "Plastic stress/strain-rate/temperature relations in H. C. P. Ag-Al under impact loading," J. Mech. Ph. Solids, 12, 361, (1964).
31. Malvern, L. E., "Plastic wave propagation in a bar of material exhibiting a strain rate effect," Q. App. Math. 8, 405, (1950).

32. Malvern, L. E., "The propagation of longitudinal waves of plastic deformation in a bar of material exhibiting a strain rate effect," J. App. Mech. 18, 203, (1951).
33. Lubliner, J. "A generalized theory of strain rate dependent plastic wave propagation in bars," J. Mech. Ph. Solids, 12, 59, (1964).
34. Perzyna, P., "On the thermodynamic foundations of viscoplasticity," Symposium on the mechanical behavior of materials under dynamic loads, San Antonio, Texas (1967).
35. Perzyna, P. and Wojno, W., "Thermodynamics of rate sensitive plastic material," Arch. Mech. Stos. 20, (1968).
36. Perzyna, P. and Wojno, W., "Thermodynamics of a rate sensitive plastic material," Arch. Mech. Stos. 5, 500, (1968).
37. Trozera, T. A., Sherby, O. D. and Dorn, J. E., "Effect of strain rate and temperature on the plastic deformation of high purity aluminum," Trans. ASME, 49, 173, (1957).
38. Eddington J. W., "Effect of Strain rate on the Dislocation Substructure in deformed Niobium single crystals," Mechanical Behavior of Materials under Dynamic Loads, Ed. V. S. Lindholm, Springer-Verlag, N. Y. (1968).
39. Perzyna, P., "On Physical Foundations of Viscoplasticity," Polskiej Akademii Nauk, IBTP Report 28/1968.
40. Peters, R. W. et Als, "Preliminary for testing basic assumptions of plasticity theories," Proc. Soc. Exp. Stress Anal. 7, 27, (1949).

A THEORY OF VISCOPLASTICITY  
WITHOUT A YIELD SURFACE  
PART II - APPLICATION TO MECHANICAL  
BEHAVIOR OF METALS

K. C. Valanis  
Professor of Mechanics  
University of Iowa  
Iowa City,  
Iowa

Research sponsored by the Air Force Office  
of Scientific Research, Office of Aerospace  
Research, United States Air Force  
under AFOSR Grant No. 70 - 1916

January 1971.

# ABSTRACT

The endochronic theory of viscoplasticity developed previously by the author is used to give quantitative analytical predictions on the mechanical response of aluminum and copper under conditions of complex strain histories. One single constitutive equation describes with remarkable accuracy and ease of calculation diverse phenomena, such as cross-hardening, loading and unloading loops, cyclic hardening as well as behavior in tension in the presence of a shearing stress, which have been observed experimentally by four different authors.

## 1. Introduction

In Part I of this work, a theory of viscoplasticity (of which the theory of plasticity was a part) was developed on the basis of the concept that the current state of stress is a functional of the entire history of deformation and temperature,

but the history was defined with respect to a time scale which is in itself a property of the material at hand.

In particular for the case of strain-rate-independent materials under isothermal conditions, which is the topic of this part of our work, it was shown that within the restriction of small strains

$$\sigma_{ij} = \delta_{ij} \int_0^t \lambda(z-z') \frac{\partial \epsilon_{kk}}{\partial z'} dz' + 2 \int_0^t \mu(z-z') \frac{\partial \epsilon_{ij}}{\partial z'} dz' \quad (1.1)$$

where

$$\lambda(z) = \lambda_\infty + \sum_{r=1}^n \lambda_r e^{-\rho_r z} \quad (1.2)$$

$$\mu(z) = \mu_\infty + \sum_{r=1}^n \mu_r e^{-\alpha_r z} \quad (1.3)$$

where  $\lambda_\infty$ ,  $\lambda_r$ ,  $\mu_\infty$ ,  $\mu_r$ ,  $\rho_r$  and  $\alpha_r$  are positive constants and

$$z=z(\zeta); \frac{dz}{d\zeta} > 0, z \geq 0. \quad (1.4 \text{ a,b})$$

The symbol  $z$  denotes a positive monotonically increasing time scale with respect to a time measure  $d\zeta$  such that

$$d\zeta^2 = p_{ijkl} d\epsilon_{ij} d\epsilon_{kl} \quad (1.5)$$

where  $p_{ijkl}$  is a material tensor, which is positive definite and which, for

the isotropic materials envisioned in Eq. (1.1), has the form

$$P_{ijkl} = k_1 \delta_{ij} \delta_{kl} + k_2 \delta_{ik} \delta_{jl} \quad (1.6)$$

where  $k_1$  and  $k_2$  are material constants, such that  $k_1 + \frac{k_2}{3} \geq 0$ ,  $k_2 \geq 0$ .

It is evident from Eq. (1.5) that  $d\epsilon$  is independent of the natural time scale given by a clock and thus materials described by Eq. (1.1) are strain history dependent but strain-rate independent.

The derivation of constitutive equation (1.1) was given in detail and its relation to classical theory of plasticity was examined, in some of its aspects, in Part I.

In the present paper we shall be concerned with the real behavior of metals under conditions of room temperature and slow straining. By examining data on copper and aluminum which were obtained in the laboratory by various experimenters, we shall show that Eq. (1.1) does indeed have the capability of explaining quantitatively and with remarkable accuracy such diverse phenomena as cross-hardening i.e. hardening in tension due to torsion, loading-unloading loops, and hysteresis loops during repetitive tension-unloading - compression-unloading histories, as well as behavior in tension in the presence of shear stress due to torsion.

## 2. Discussion of Equation (1.1)

At the present time one cannot find sufficient experimental data in the literature to determine the functions  $z(\zeta)$ ,  $f(z)$  and  $\mu(z)$ . Therefore in order to use the theory at all, with the object of interpreting available experimental data, we have to seek other avenues, essentially heuristic, to determine the form of the above functions.

With regard to  $z(\zeta)$ , we recall that the rate of dissipation  $\hat{\gamma}$  was given by Eq. (3.15) of Part I, i.e.,

$$\theta_0 \hat{\gamma} = (b_1^a + \frac{b_2^a}{3}) \hat{q}_{ii}^a \hat{q}_{ij}^a + b_2^a \hat{p}_{ij}^a \hat{p}_{ij}^a, \quad (2.1)$$

(a summed)

where a roof over a quantity represents its derivative with respect to  $z$ , and  $p_{ij}^a$  is the deviatoric component of the tensorial internal variable  $q_{ij}^a$ .

For the sake of argument let

$$\theta_0 \hat{\gamma}_D = b_2^a \hat{p}_{ij}^a \hat{p}_{ij}^a. \quad (2.2)$$

(a summed)

Then as a result of Eq. (2.2)

$$\theta_0 \frac{d\gamma_D}{dz} = \frac{b_2^a}{(dz/d\zeta)} \frac{dp_{ij}^a}{d\zeta} \frac{dp_{ij}^a}{d\zeta}. \quad (2.3)$$

(a summed)

Equation (2.3) may now be written in the form,

$$\theta_0 \frac{d\gamma_D}{d\zeta} = b_2^a f(\zeta) \frac{dp_{ij}^a}{d\zeta} \frac{dp_{ij}^a}{d\zeta} \quad (2.4)$$

(a summed)

where, it will be recalled,

$$\zeta = \int_0^z p_{ijkl} (dc_{ij} dc_{kl})^{1/2} \quad (2.5)$$

i.e.  $\zeta$  is a FUNCTIONAL of the strain history, and

$$dz = \frac{d\zeta}{f(\zeta)}. \quad (2.6)$$

Of course if we set,



$$\hat{\sigma}_o \hat{\gamma}_v = (b_1^a + \frac{b_2^a}{3}) \hat{q}_{ii}^a \hat{q}_{jj}^a \quad (2.7a)$$

(a summed)

then,

$$\sigma_o \frac{d\gamma_v}{d\zeta} = (b_1^a + \frac{b_2^a}{3}) f(\zeta) \frac{dq_{ii}^a}{d\zeta} \frac{dq_{jj}^a}{d\zeta} \quad (2.7b)$$

(a summed)

At this point various possibilities present themselves. The simplest is to take  $f(\zeta) = \text{constant}$ , in which case,

$$z = \zeta_1 \zeta + \zeta_o \quad (2.7c)$$

where  $\zeta_o$  and  $\zeta_1$  are constants. However it can be shown (and will be demonstrated in later sections) that this choice eliminates "cross-hardening" in the sense that a change in the uniaxial stress-strain behavior due to shear prestrain cannot be accommodated. This effect has been observed in practically all experiments on metals that have ever been reported. Therefore, though Eq. (2.7) is convenient, it is not very useful.

This observation applies to Ilyushin's and Rivlin's theory, where  $z = \zeta + \zeta_o$  and

$$\zeta = \int_0^{\zeta} (dc_{ij} dc_{ij})^{\frac{1}{2}} \quad (2.7d)$$

Note that Eq. (2.7d) is a particular case of Eq. (2.6); also note the absence of the material constants  $k_1$  and  $k_2$  from Eq. (2.7d), which renders  $\zeta$  independent of the material at hand. In other words their theories are not endochronic.

The next natural choice is to consider  $f(\zeta)$  to be a linear function of  $\zeta$  i.e.

$$f(\zeta) = 1 + B\zeta \quad (2.8)$$

where  $\beta$  is a positive constant. Note that  $\beta > 0$  because  $b_2^a > 0$ , as well as  $\frac{dy_D}{d\zeta} > 0$ , thus necessitating that  $f(\zeta) > 0$ , for all  $\zeta$ . As a result of Eq.'s (2.7) and (2.8),

$$z = \frac{1}{\beta} \log (1 + \beta \zeta) \quad (2.9)$$

an expression which has been found to give excellent agreement in the cases of some significant experiments, as will be shown in subsequent Sections.

In the absence of experimental data, the question of the form of the "relaxation" functions  $\lambda(z)$  and  $\mu(z)$  is equally difficult.

There are two simplifying assumptions, however, which lead to a relation between  $\lambda(z)$  and  $\mu(z)$ , so that one is left with the problem of finding the form of only one of these functions. One is that of an elastic hydrostatic response and the other is the assumption of constant Poisson's ratio.

Efficient use of the first assumption is made by writing Eq. (2.1) in terms of the hydrostatic and deviatoric components of  $\sigma_{ij}$ , in which case

$$\sigma_{kk} = 3 \int_0^z K(z-z') \frac{\partial \epsilon_{kk}}{\partial z'} dz' \quad (2.10)$$

$$\sigma_{ij} = 2 \int_0^z \mu(z-z') \frac{\partial \epsilon_{ij}}{\partial z'} dz' \quad (2.11)$$

where  $K(z)$  is the bulk modulus. Elastic hydrostatic response implies that  $K(z) = K_H(z)$ , in which case Eq. (2.10) becomes,

$$\sigma_{kk} = 3K_{kk} \quad (2.12)$$

The assumption of constant Poisson ratio leads to the conclusion that  $\mu(z)$  and  $K(z)$  differ by a multiplicative constant, and can both be written

in terms of a single function  $G(z)$ , such that

$$K(z) = K_0 G(z) \quad (2.13)$$

$$\nu(z) = \nu_0 G(z) \quad (2.14)$$

where  $G(0) = 1$ .

This assumption has the added advantage that, under condition of plane stress, or uniaxial strain, the strain in the unstressed direction is related to the strains in the stressed directions by a multiplicative constant. Thus the strain increments in the direction of zero stress may be easily eliminated from the expression for  $d\epsilon$  so that the latter may be expressed solely in terms of the strain increments in the stressed directions.

### 3. Crosshardening in Tension-torsion

It has been observed that in aluminum and copper as well as in other metals, prestraining in torsion, well into the plastic range, has a significant hardening effect on the stress strain curve in tension.

In this Section we shall analyze data by Mair and Pugh, who have investigated this effect on annealed copper. Their experiments were performed accurately and with care, on very thin circular cylinders which were twisted well into the plastic region, so that upon unloading there remained a permanent residual shear strain. The effect of initial shear prestrain on the tensile response was then obtained by loading the cylinders in tension.

The constitutive equations pertinent to the above situation are easily found to be:

$$\sigma = \int_0^z E(z-z') \frac{de}{dz'} dz' \quad (3.1)$$

$$\tau = 2 \int_0^z \mu(z-z') \frac{d\eta}{dz'} dz' \quad (3.2)$$

where  $\sigma$  and  $\epsilon$  are the axial stress and strain, respectively, and  $\tau$  and  $\eta$  are the respective shear stress and torsional shear strain; the moduli  $E(z)$  and  $\mu(z)$  are interrelated through the bulk modulus  $K(z)$ . Their relating is best expressed through their Laplace transforms:

$$\bar{E} = \frac{3\bar{\mu}}{1 + \frac{\bar{\mu}}{3\bar{K}}} \quad (3.3)$$

To deal with the effect of cross-hardening analytically, we have assumed a constant poisson ratio. As a result Eq. (3.3) reduces to the form:

$$E(z) = E_0 G(z) \quad (3.4)$$

where

$$E_0 = \frac{3\mu_0}{1 + \frac{\mu_0}{3K_0}} \quad (3.5)$$

Regarding the form of  $G(z)$  we have taken the simplest possible view by assuming that

$$G(z) = e^{-\alpha z} \quad (3.6)$$

Despite these simplifications we have been able to obtain excellent agreement with experimental data that have hitherto lacked analytical representation.

### Analysis

In the tension-torsion test the effect of constant poisson ratio is to

reduce  $d\zeta^2$  to the form

$$d\zeta^2 = k_1 d\epsilon^2 + k_2 d\eta^2 \quad (3.7)$$

where  $k_1$  and  $k_2$  are material constants, not the same as those in Eq. (1.6).

During torsion ( $\epsilon=0$ ),

$$\zeta = k_2 \eta \quad (3.8)$$

whereas during tension ( $\eta=\eta_0$ ) and after pretension

$$\zeta = k_2 \eta_0 + k_1 \epsilon \quad (3.9)$$

where  $\eta_0$  is the maximum shear prestrain.

Equation (3.1) may now be written in the form

$$\sigma = E_0 \int_{\zeta_0}^{\zeta} G[z(\zeta) - z(\zeta')] \frac{\partial \epsilon}{\partial \zeta'} d\zeta' \quad (3.10)$$

(where  $\zeta_0 = k_2 \eta_0$ ) when allowance is made of the fact that  $\epsilon = 0$  in the range  $0 \leq \zeta \leq k_2 \eta_0$ . Thus cross-hardening is taken fully into account by Eq. (3.10), through the shear prestrain parameter  $\zeta_0$ , which appears as a lower limit on the integral on the right hand side of Eq. (3.10). If, in particular, we assume that  $G(\zeta)$  is given by Eq. (3.6) and use of this is made in Eq. (3.10) the latter becomes

$$\sigma = E_0 e^{-a\zeta(\zeta)} \int_{\zeta_0}^{\zeta} e^{a\zeta(\zeta')} \frac{\partial \epsilon}{\partial \zeta'} d\zeta' \quad (3.11)$$

The integral in the right hand side of Eq. (3.11) can be evaluated explicitly by using Eq. (2.9) and noting that during monotonically increasing extension  $\frac{d\epsilon}{d\zeta} = k_1$ . Omitting the algebra,

$$\sigma = \frac{E_0(1+\beta\zeta)}{k_1\beta n} \left( 1 - \left( \frac{1+\beta\zeta}{1+\beta\zeta_0} \right)^{-n} \right) \quad (3.12)$$

where

$$n = 1 + \frac{\alpha}{\beta} \quad (3.13)$$

and

$$\zeta_0 \leq \zeta = \zeta_0 + k_1 \epsilon \quad (3.14)$$

Equation (3.12) represents a family of stress strain waves in tension, in terms of the prestrain parameter  $\zeta_0$  and the "cross-hardening" parameter\*  $\beta$ .

To determine the material parameters in Eq. (3.12) we note that in the absence of shear prestrain ( $\zeta_0 = 0$ ),

$$\sigma = \frac{E_0(1+\beta_1\epsilon)}{\beta_1 n} \left( 1 - (1+\beta_1\epsilon)^{-1} \right) \quad (3.15)$$

where  $\beta_1 = k_1\beta$ .

It may be verified that as  $\epsilon \rightarrow 0$ ,  $\sigma = E_0\epsilon$  i.e.  $E_0$  is the initial slope of the stress-strain curve. Also as  $\epsilon$  increases,  $\sigma$  tends asymptotically to the linear expression

$$\sigma = \frac{E_0}{\beta_1 n} (1+\beta_1\epsilon) \quad (3.16)$$

---

\* There is ample justification for calling  $\beta$  the cross-hardening parameter.

Indeed in the limit of  $\beta = 0$ , and using Eq. (3.9) Eq. (3.12) becomes:

$$\sigma = \frac{E_0}{k_1\alpha} (1 - e^{-\alpha\epsilon})$$

which is independent of  $\zeta_0$ ; in other words cross-hardening cannot take place when  $\beta = 0$ , as pointed out earlier.

If  $E_t$  is the slope (tangent modulus) of the asymptotic straight line, then

$$n = \frac{E_o}{E_t} \quad (3.17)$$

Also, as shown in Fig. 1, if one extrapolates backwards the asymptotic straight line to intersect the stress axis one obtains an intercept  $\sigma_o$  from which  $\beta_1$  is determined by the relation

$$\beta_1 = \frac{E_t}{\sigma_o} \quad (3.18)$$

Similarly integration of Eq. (3.2) yields an equation analogous to Eq. (3.16); this is

$$\tau = \frac{2\mu_o(1+\beta_2 n)}{\beta_2 n} \{1 - (\beta_2 n)^{-n}\} \quad (3.19)$$

where  $\beta_2 = k_2 \beta$ . Thus,  $\beta_2$  and  $\mu_o$  may be determined from Eq. (3.19).

Finally we observe from Eq. (3.12) that the intercepts  $\sigma_o'$  in the presence of shear prestrain  $\tau_o$  are given from the expression

$$\sigma_o' = \sigma_o (1 + \beta \tau_o) = \sigma_o (1 + \beta_2 n_o) \quad (3.20)$$

Equation (3.20) was used to confirm the self-consistency of the theory. However Eq.'s (3.12), (3.1) and (3.19) can only yield the ratio  $\frac{k_1}{k_2}$  but the constants  $k_1$  and  $k_2$  cannot be evaluated. In this sense, and for these experiments one may choose  $k_2$  arbitrarily; we chose  $k_2 = 1$ .

Experimental data obtained by Mair and Pugh that illustrate the effect of cross-hardening are given in Fig. 2.

Curve 0 is the virgin stress strain curve for the type of copper they used. The circles on the curves A, B and C are experimental points corres-

ponding to initial shear prestrains of  $.25 \times 10^{-2}$ ,  $1.5 \times 10^{-2}$  and  $3 \times 10^{-2}$  respectively.

From curve 0,  $E_0 = 14 \times 10^6$  lb/in<sup>2</sup>,  $\beta_1 = .53 \times 10^2$ ,  $n = 46$ . With  $k_2 = 1$ , Eq. (3.20) was used to give  $k = 1.00$ . The curves A, B and C were then calculated and plotted as shown. Without a doubt the agreement between theory and experiment is remarkable.

#### 4. Repetitive loading-unloading cycles

The tensile strain history  $\epsilon(\zeta)$  corresponding to a typical tensile loading-unloading sequence is shown in Fig. 3. We use the terms "straining" and "unstraining" in the following sense:

The ranges  $0 \leq \zeta < \zeta_1$ ,  $\zeta_2 \leq \zeta < \zeta_3$ ,  $\zeta_B \leq \zeta < \zeta_5$ ,  $\zeta_D \leq \zeta$  represent straining in tension.

The ranges  $\zeta_1 \leq \zeta < \zeta_2$ ,  $\zeta_3 \leq \zeta < \zeta_A$ ,  $\zeta_5 \leq \zeta < \zeta_C$  represents unstraining in tension.

The ranges  $\zeta_A \leq \zeta < \zeta_4$ ,  $\zeta_{C-} \leq \zeta < \zeta_6$ ,  $\zeta_7 \leq \zeta < \zeta_8$  represent straining in compression.

The ranges  $\zeta_4 \leq \zeta < \zeta_B$ ,  $\zeta_6 \leq \zeta < \zeta_7$ ,  $\zeta_8 \leq \zeta < \zeta_D$  represent unstraining in compression.

Points on the  $\zeta$ -axis denoted by  $\zeta_r$  ( $r=1,2,\dots$ ) represent points of discontinuity in  $\frac{d\epsilon}{d\zeta}$ , brought about by reverting from straining to unstraining histories, or vice-versa.

A perusal of experimental data on copper, shows that the constitutive equation of the metal varies depending on its previous history of manufacture and subsequent annealing. The single term form of  $G(\zeta)$  that explained Mair and Pugh's data<sup>(2)</sup> so well was found inadequate to explain data by Lubahn<sup>(3)</sup>



and by Wadsworth<sup>(4)</sup>.

We found however, that the adoption of a single extra term for  $G(z)$  suffices to describe quantitatively broad trends of their data. In effect we took

$$G(z) = E_1 + G_2 e^{-\alpha z} \quad (4.1)$$

or

$$E(z) = E_1 + E_2 e^{-\alpha z} \quad (4.2)$$

Let  $\zeta_n$  ( $n = 1, 2, \dots$ ) be the last point of discontinuity in  $\frac{d\epsilon}{d\zeta}$ . Then using Eq's. (2.9), (3.11) and (4.1) and in the range  $\zeta_m \leq \zeta$

$$\sigma = (1+\beta\zeta)\sigma_0 \left\{ (-1)^m - \frac{1}{(1+\beta\zeta)^n} + 2 \sum_{r=1}^m (-1)^{r+1} \frac{(1+\beta\zeta_r)^n}{1+\beta\zeta_r} \right\} + E_1 \epsilon \quad (4.3)$$

The quantities  $\zeta_r$  may be evaluated explicitly in terms of  $\epsilon_r$  (the values of strain corresponding to  $\zeta_r$ ) by the formula

$$\zeta_r = 2k_1 \sum_{s=1}^r (-1)^{s-1} \epsilon_s + k_1 (-1)^r \epsilon_r \quad (4.4)$$

The effect of  $E_1$  on the unstraining characteristics is remarkable, especially since its effect on the shape of the straining part of the stress-strain curve is minimal. Let the history  $\epsilon(z)$  be one of continuous straining. Then Eq. (4.3) becomes:

$$\sigma = E_1 \epsilon + \frac{E_2 (1+\beta_1 \epsilon)}{n\beta_1} \{ 1 - (1+\beta_1 \epsilon)^{-n} \} \quad (4.5)$$

From Eq. (4.5) we obtain the following relations in the notation of Section 3.

$$E_1 + E_2 = E_0 \quad (4.6a)$$

$$\frac{E_2}{\beta_1^n} = \sigma_0 \quad (4.6b)$$

$$E_1 + \sigma_0 \beta_1 = E_t \quad (4.6c)$$

Equations (4.6a-c) do not suffice for the determination of the four unknown material constants  $E_1$ ,  $E_2$ ,  $n$ ,  $\beta_1$ . It has been found that a fourth relation can be obtained by considering the "unloading" portion of the stress-strain history.

Fig. 4. shows the stress-strain relation for a uniaxial specimen which has been strained in tension to a strain value  $\epsilon_1$ ; whereupon it is unloaded and compressed until the final strain is zero.

The strain-intrinsic time measure history  $\epsilon(\zeta)$  corresponding to the above stress-strain history is also shown in Fig. 5.

Equation (4.3) in conjunction with the above history yields the relation, at  $\epsilon = 0$ :

$$\sigma = \sigma_0 (1 + 8\zeta) \left\{ -1 + \frac{2(1 + 8\zeta_1)^n - 1}{(1 + 8\zeta)^n} \right\} \quad (4.7)$$

If the value of  $\epsilon_1$  is sufficiently large (in the case of copper this value was found to be  $50 \times 10^{-3}$ , or so) then  $\sigma_0^c$  is given very nearly by the expression

$$\sigma_0^c = -\sigma_0 (1 + 28\zeta_1) = -\sigma_0 (1 + 28\beta_1 \epsilon_1) \quad (4.8)$$

The constant  $\beta_1$  can now be obtained from Eq. (4.8) and the constants  $E_1$ ,  $E_2$  and  $n$  can be found from Eq's. (4.6a-c).

We illustrate the points made in the above discussion in Fig. 6 where stress

strain curves for three different materials are given when these are subjected to the same strain history shown in Fig. 5.

The constants for these materials are given in the following table:

	$E_1$	$E_2$	$\beta$	$n$
1	0	$6.14 \times 10^6$	$.4 \times 10^2$	25
2	$.24 \times 10^6$	$5.9 \times 10^6$	0	$\infty$
3	$.12 \times 10^6$	$6.02 \times 10^6$	$.2 \times 10^2$	50

What is remarkable is that changing  $\beta$  results in these materials having indistinguishable stress-strain curves during straining but wildly differing ones during unstraining.

In Fig. 7 we illustrate an attempt to predict analytically the loading-unloading-loading response of copper in simple tension. The solid line is an experimental curve obtained by Lubahn<sup>(3)</sup> for a copper specimen which had already undergone similar strain cycles. We have assumed, however, that these have a negligible effect in the response shown because they occurred sufficiently far in the distant "past".

The triangular points shown, were obtained theoretically from Eq. (4.3) by assuming that the specimen was continually extended (without unstraining) until the strain  $\epsilon = 51.6 \times 10^{-3}$  was reached. The unstraining-straining cycle was then applied.

Despite the fact that  $E(z)$  was approximated by two terms, as in Eq. (4.2) the agreement between theory and experiment is remarkable. The constants employed were,  $\sigma_0 = 6 \times 10^3$ ,  $E_1 = .125 \times 10^6$ ,  $\beta = .02 \times 10^3$ ,  $n = 160$ .

In fact we are not aware of another instance where an attempt was made to describe such experimental data analytically by means of one single

constitutive equation. In addition we can say with assurance that the observed difference between theory and observation can be reduced further by including more exponential terms in the series representation for  $E(z)$ . We conclude this Section by considering the effect of work hardening under cyclic straining. In particular we shall examine the work of Wadsworth's<sup>(4)</sup> and show that our theory again provides an excellent analytical basis for his results.

In this work single copper crystals were tested under conditions of uniaxial cyclic strain; The data was presented in terms of the resolved shear stress and strain in the plane of slip.

Fig. 8 gives the first few cycles of his straining program, in which a crystal was cycled under fixed limits of resolved shear strain of  $7 \times 10^{-3}$ . The "peak stresses" corresponding to the extreme values of tensile and compressive strain increased monotonically with the number of cycles.

In Fig. 9 the values of peak tensile and compressive stresses have been plotted by Wadsworth against  $|\ln|$ . It is rather interesting that he felt that such a plot was meaningful, without further elaboration on this point. Of course  $|\ln|$ , but for a scalar factor, is our intrinsic time measure.

The history of the resolved shear strain versus  $\xi$  is shown in Fig. 10. From this Figure it follows that  $\xi_m = (2m-1)\Delta k_1$ . Equations (4.6c) and (4.8) were now utilized to find  $\beta k_1$ , which we denote by  $\beta_1$ , and  $E_1$ . It was found that  $\beta_1 = 12.3$  and  $E_1 = 2 \times 10^9 \frac{\text{dyn}}{\text{cm}^2}$ . At this point  $n$  could not be determined because the initial slope of the stress-strain curve corresponding to  $\xi_1$  could not be evaluated accurately.

However letting  $\tau_m = \tau|_{\xi=\xi_m}$ , it was found that as  $m \rightarrow \infty$ , Eq. (4.3)

yields the asymptotic expression:

$$\tau = n\beta\tau_0 \Delta + E_1 \Delta \quad (4.9)$$

Hence, from the tensile experimental curve of Fig. 4 of Ref. 4,  $n$  could be determined explicitly and was found to be equal to 225. For this value of  $n$  the term  $\frac{1}{(1+\beta\tau_0 \Delta)^m}$  was found to be negligible for  $m \geq 1$ .

Thus for the history in Fig. 10, Eq. (4.3) gives

$$\tau_{m+1} = \tau_0 [1+\beta_1(2m+1)\Delta] (-1)^{m+2} \sum_{r=1}^m \left[ \frac{1+(2r-1)\beta_1 \Delta}{1+(2m+1)\beta_1 \Delta} \right]^n (-1)^{r+1} + E_1 \epsilon \quad (4.10)$$

The above equation can be simplified further for large values of  $m$ . In particular for  $m \geq 50$ , it was found that the series in the bracket on the right hand side of Eq. (4.10) degenerates into the geometric series

$$\sum_{r=1}^m (-u)^r \sim -\frac{u}{1+u} \quad (4.11)$$

where

$$u = \left\{ \frac{1+(2m-1)\beta_1 \Delta}{1+(2m+1)\beta_1 \Delta} \right\}^n \quad (4.12)$$

Equation (4.10) may now be written in an asymptotic form in terms of the absolute value of the shear stress as follows:

$$|\tau_m| = [1+\beta(2m+1)\Delta] \tau_0 \left( -1 + \frac{2}{1+u} \right) + E_1 \Delta \quad (4.13)$$

For very large values of  $m$  ( $m \gg n$ ) Eq. (4.13) simplifies further and becomes

$$|\tau_m| = \frac{n\beta_1 \tau_0 \Delta}{1 - \frac{n}{m}} + E_1 \Delta \quad (4.14)$$

Thus,

$$\lim_{m \rightarrow \infty} |\tau_m| = n\beta_1 \tau_0 \Delta + E_1 \Delta \quad (4.15)$$

In Fig. 11 a plot has been made of the theoretical relation between  $|\tau_m|$  and  $m\Delta$  obtained from Eq. (4.13). The experimental points obtained by Wadsworth are also shown. The following comments are in order. Though our theory does give values for  $\tau_m$  which are different in tension from those in compression, the difference is not as great as the experimental data indicate, and is too small to be plotted on the scale shown. However, the theoretical curve lies very close to, and is in fact bounded by the experimental points, which indicate a deviation between the values of compressive stress and those of tensile stress which increases with  $m$  but is never greater than 5.5%.

This is the first time that a theory of plasticity has provided a rational explanation for the phenomena of cyclic hardening.

##### 5. Tensile response in the presence of initial shear stress

In Section 3 we obtained a theoretical prediction of the effect of prestrain in torsion on the stress strain curve in tension. In this Section we shall examine theoretically, in the light of our endochronic theory, the effect of initial constant prestress in torsion on the stress-strain curve in tension. To do this, we have assumed, just as we did in Section 3, that  $E(z)$  and  $\nu(z)$  are proportional to some relaxation function  $G(z)$ , and furthermore that  $G(z)$  consists of a single exponential term i.e. it is given by Eq. (3.6). Thus

$$E(z) = E_0 e^{-\alpha z} \quad (5.1)$$

In the light of Eq. (5.1) and bearing in mind Eq. (2.9), the constitutive Eqs (3.1) and (3.2) can be reduced to the differential equations

$$\epsilon_0 \frac{d\epsilon}{d\zeta} = \frac{\alpha\sigma}{1+\beta\zeta} + \frac{d\sigma}{d\zeta} \quad (5.2)$$

$$2\mu_0 \frac{d\eta}{d\zeta} = \frac{\alpha\tau}{1+\beta\zeta} + \frac{d\tau}{d\zeta} \quad (5.3)$$

where, as in Section 3,

$$d\zeta^2 = k_1 d\epsilon^2 + k_2 d\eta^2 \quad (5.4)$$

As mentioned above the test to be discussed consists of applying an initial stress  $\tau^0$  corresponding to an initial strain  $\eta_0$ ; then keeping  $\tau^0$  constant, a axial strain  $\epsilon$  is applied and the axial stress  $\sigma$  is measured. The object at hand is to deduce from Eq.'s (5.1-5.4) the relation between  $\sigma$  and  $\epsilon$ , and compare with the experimental data obtained by Ivey<sup>(5)</sup>.

To accomplish this we proceed as follows. From Eq. (5.4) it is clear that the axial straining process begins at  $\zeta = \zeta_0$  where

$$\zeta_0 = k_2 \eta_0 \quad (5.5)$$

During this process  $\frac{d\tau}{d\zeta} = 0$ , so that from Eq. (5.3)

$$d\eta = \frac{\alpha\tau^0}{2\mu_0} \frac{d\zeta}{1+\beta\zeta} \quad (5.6)$$

Equations (5.4) and (5.6) now combine to show that during the axial straining process,

$$d\zeta^2 = k_1^2 d\epsilon^2 + k_2^2 \left( \frac{\alpha\tau^0}{2\mu_0} \right)^2 \frac{d\zeta^2}{(1+\beta\zeta)^2} \quad (5.7)$$

At this point we introduce the variable  $\theta$  such that

$$\zeta = k_1 \theta \quad (5.8)$$

Also let  $(\frac{k_2}{k_1}) = k$ ,  $k_1 \beta = \beta$  and  $c = (k\alpha\tau^0/2\mu_0)$ . Then, in terms of  $\theta$  and as a result of Eq. (5.7)

$$d\theta \left\{ 1 - \frac{c^2}{(1+\beta_1\theta)^2} \right\}^{\frac{1}{2}} = d\epsilon \quad (5.8)$$

Equation (5.8) may be integrated subject to the initial condition that at

$$\zeta = k_2 n_0, \epsilon = 0; \text{ or, } \theta = \theta_0 = k n_0, \epsilon = 0.$$

Equation (5.2) may now be integrated with respect to  $\theta$  to yield

$$\sigma = \frac{E_0}{(1+\beta_1\theta)(\alpha/\beta_1)} \int_{\theta_0}^{\theta} (1+\beta_1\theta')^{(\alpha/\beta_1-1)} \sqrt{(1+\beta_1\theta')^2 - c^2} d\theta' \quad (5.9)$$

We introduce now a change of variable by the relation

$$1 + \beta_1 \theta = c \cosh \phi \quad (5.10)$$

whereupon Eq. (5.9) becomes:

$$\sigma = \frac{E_0 c}{\beta_1 \cosh^{n-1} \phi} \int_{\phi_0}^{\phi} (\cosh^n \phi' - \cosh^{n-2} \phi') d\phi' \quad (5.11)$$

where as before,  $n = 1 + \frac{\alpha}{\beta_1}$ .

Now,

$$\int \cosh^n x dx = \frac{n-1}{n} \int \cosh^{n-2} x dx + \frac{1}{n} \cosh^{n-1} x \sinh x \quad (5.12)$$

Since for asymptotically large  $n$  (say  $n \geq 30$ ),  $\frac{n-1}{n} \sim 1$ , it follows from Eq. (5.12) that in this instance

$$(\cosh^n x - \cosh^{n-2} x) dx \sim \frac{1}{n} \cosh^{n-1} x \sinh x \quad (5.13)$$



The result of Eq. (5.13) can be utilized to obtain a closed form solution for  $\sigma$  which now becomes,

$$\sigma = \frac{E_0 c}{\beta_1 n} \left\{ \sinh \phi - \left( \frac{\cosh \phi_0}{\cosh \phi} \right)^{n-1} \sinh \phi_0 \right\}. \quad (5.14)$$

Equation (5.8) may also be integrated with respect to  $\phi$  to yield

$$\epsilon = \frac{c}{\beta_1} (F(\phi) - F(\phi_0)) \quad (5.15)$$

where

$$F(\phi) \equiv \sinh \phi - \tan^{-1} (\sinh \phi) \quad (5.16)$$

Thus  $\sigma$  and  $\epsilon$  are related parametrically through  $\phi$  and  $\phi_0$  such that

$$\phi_0 = \cosh^{-1} \left( \frac{(1 + \beta_1 k \eta_0)}{c} \right) \quad (5.17)$$

The relation between  $\sigma$  and  $\epsilon$  has been calculated with the following values of the constants:

$$k = 1, \sigma_0 = \frac{E_0}{\beta_1 n} = 17.4 \times 10^3 \text{ lb/in}^2, \beta = 20, n = 33.$$

The result was compared with one of Ivey's experiments in which  $\tau^0 = 14 \times 10^3 \text{ lb/m}^2$ ,  $\eta_0 = 2.35 \times 10^{-3}$ . The predicted and experimental stress-strain responses compare very favorably. See Fig. 12.

### Conclusion

On the evidence of the results presented above it appears that the endochronic theory of plasticity can predict accurately the mechanical response of metals under complex straining histories. The full implications of the theory will be investigated further in our future work.

### References

1. Valanis, K. C., "A Theory of Viscoplasticity without a yield surface, Part I - General Theory", Mechanics Report 1.01, University of Iowa, Dec. 1970.
2. Mair, W. M. and Pugh, H. L. D., "Effect of Prestrain on Yield Surfaces in Copper", J. Mech. Eng. Sc., 6, 150, (1964).
3. Lubahn, J. D., "Bauschinger Effect in Creep and Tensile Tests on Copper", J. of Metals, 205, 1031, (1955).
4. Wadsworth, N. J., "Work Hardening of Copper Crystals under Cyclic Straining", Acta Metallurgica, 11, 663, (1963).
5. Ivey, H. J. "Plastic Stress Strain Relations and Yield Surfaces for Aluminum Alloys", J. Mech. Eng. Sc., 3, 15, (1961).

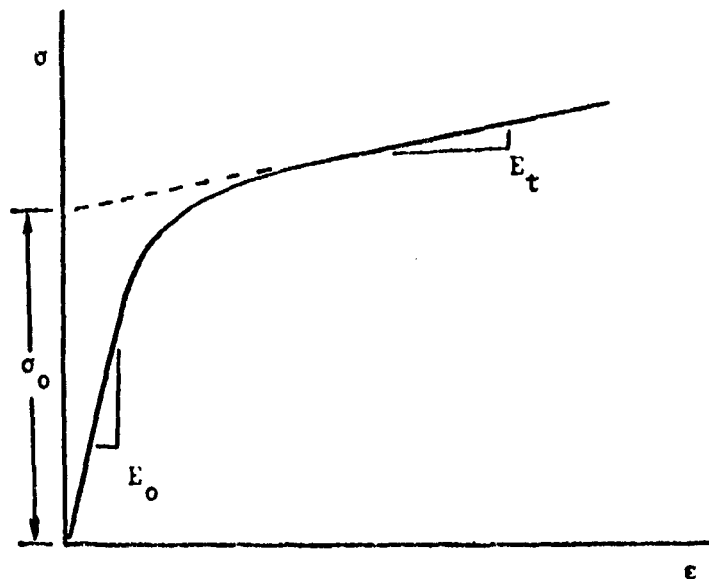


Fig. 1. Typical stress-strain curve

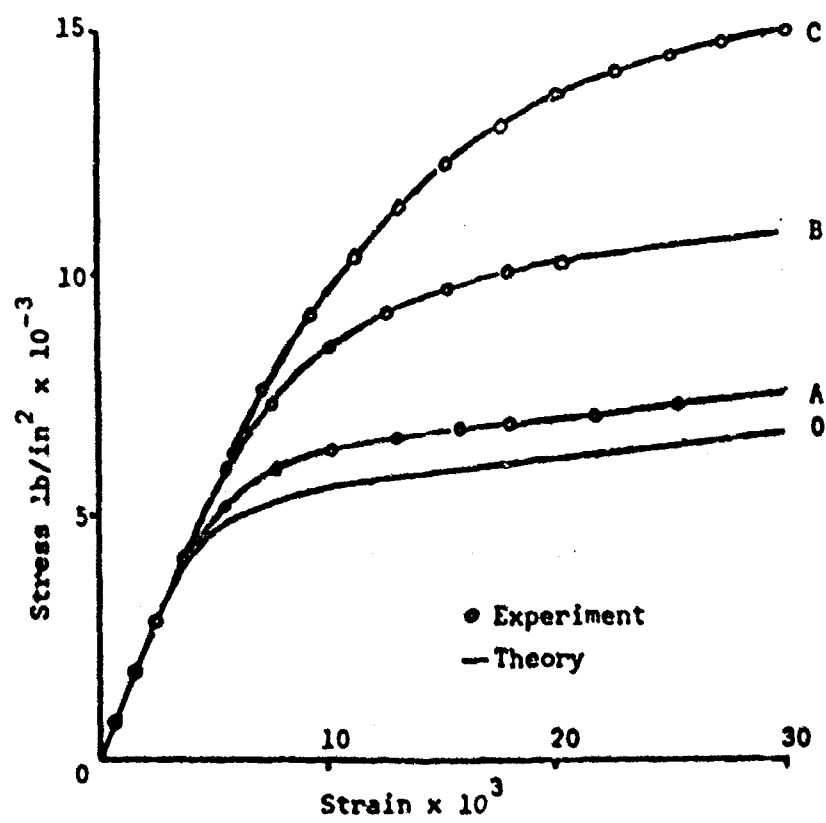


Fig. 2. Hardening due to shear prestrain

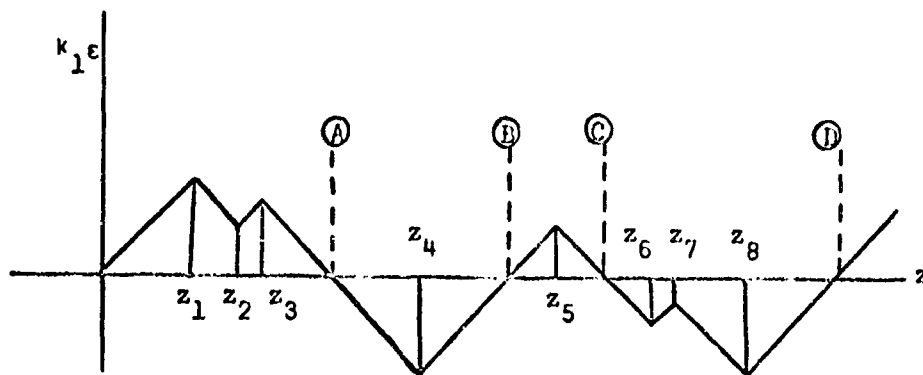


Fig. 3. Typical loading - unloading - loading sequence

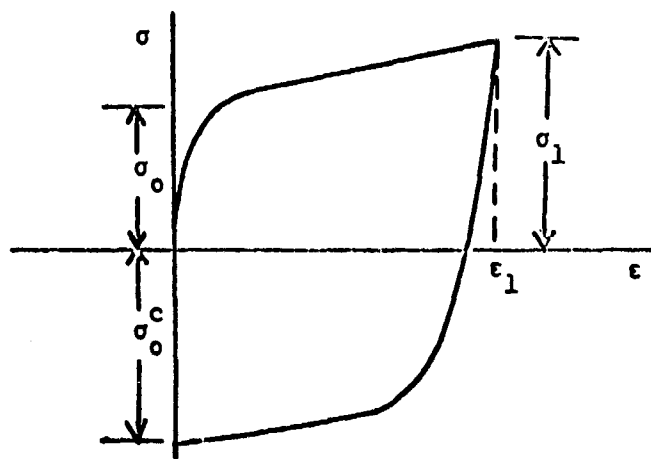


Fig. 4. Tension - Compression test

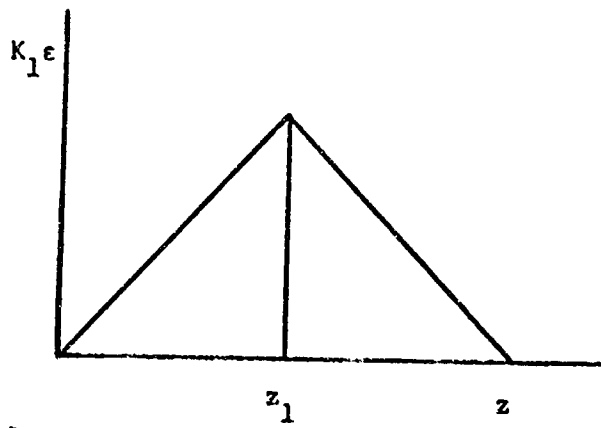


Fig. 5. Strain history of Fig. 6.

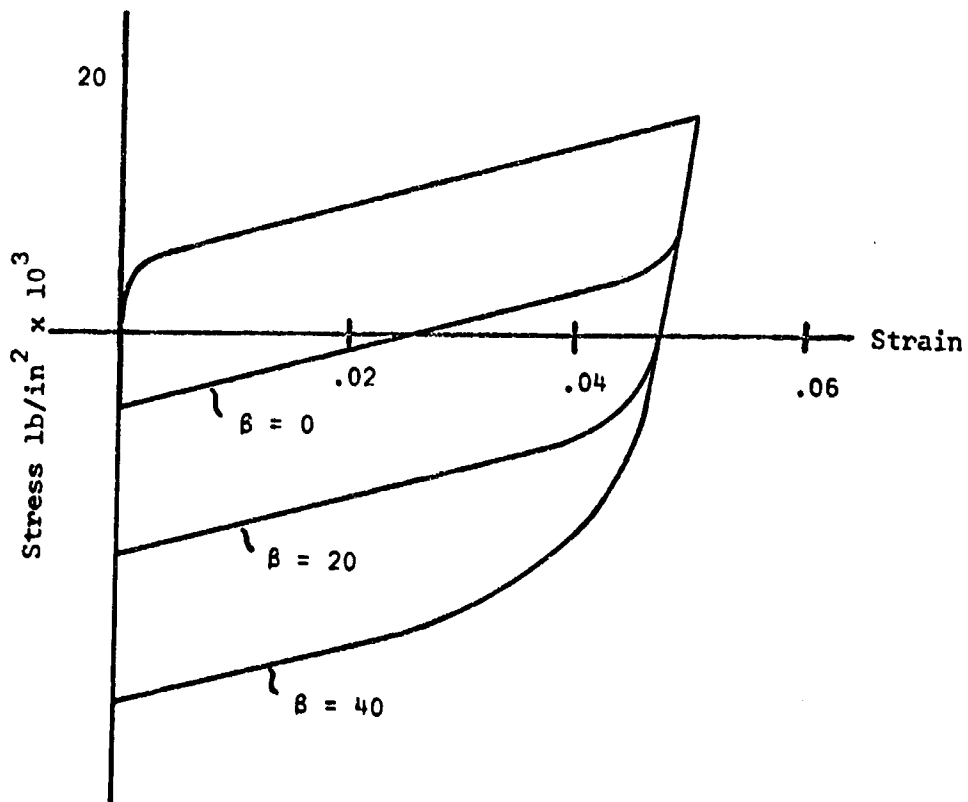


Fig. 6. Bauschinger effect and its relation to  $\beta$

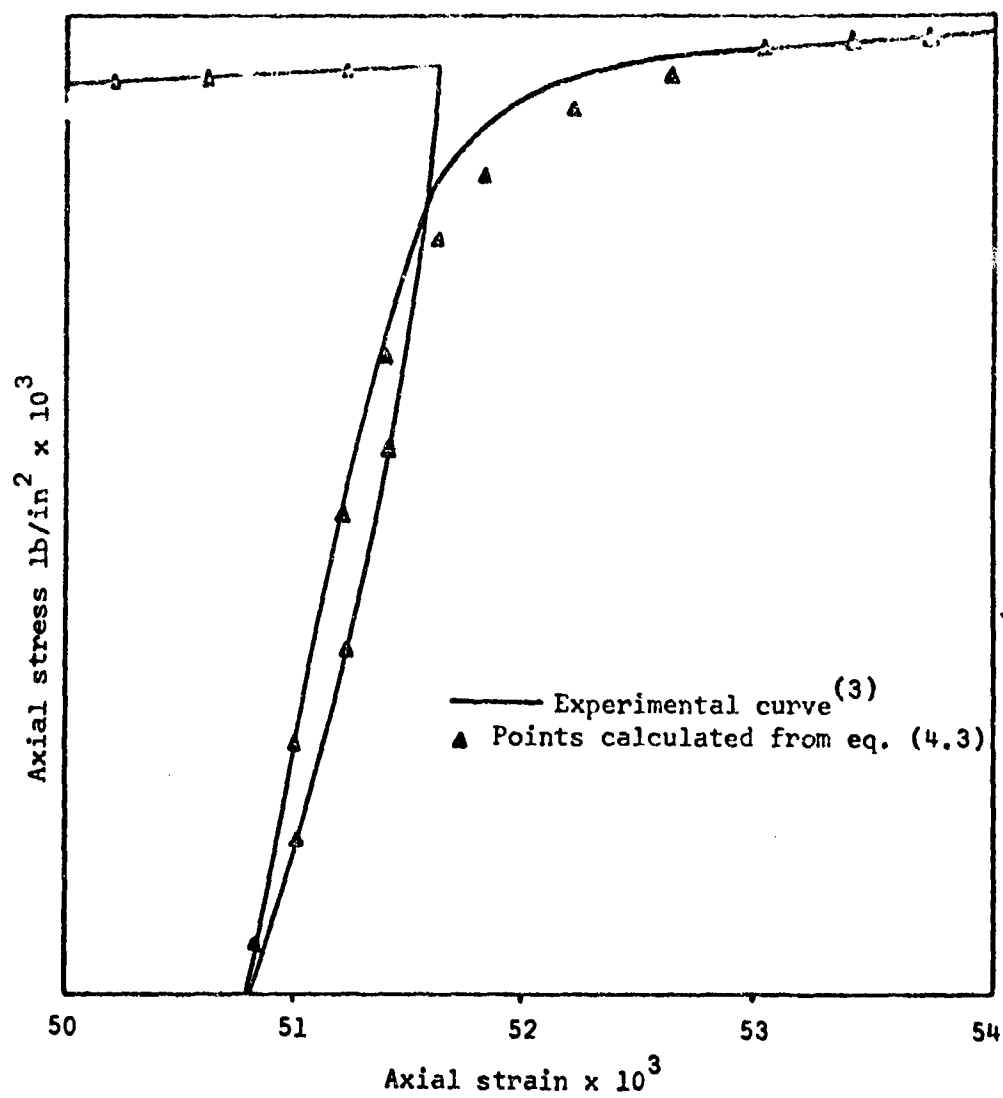


Fig. 7. Unloading - loading loop

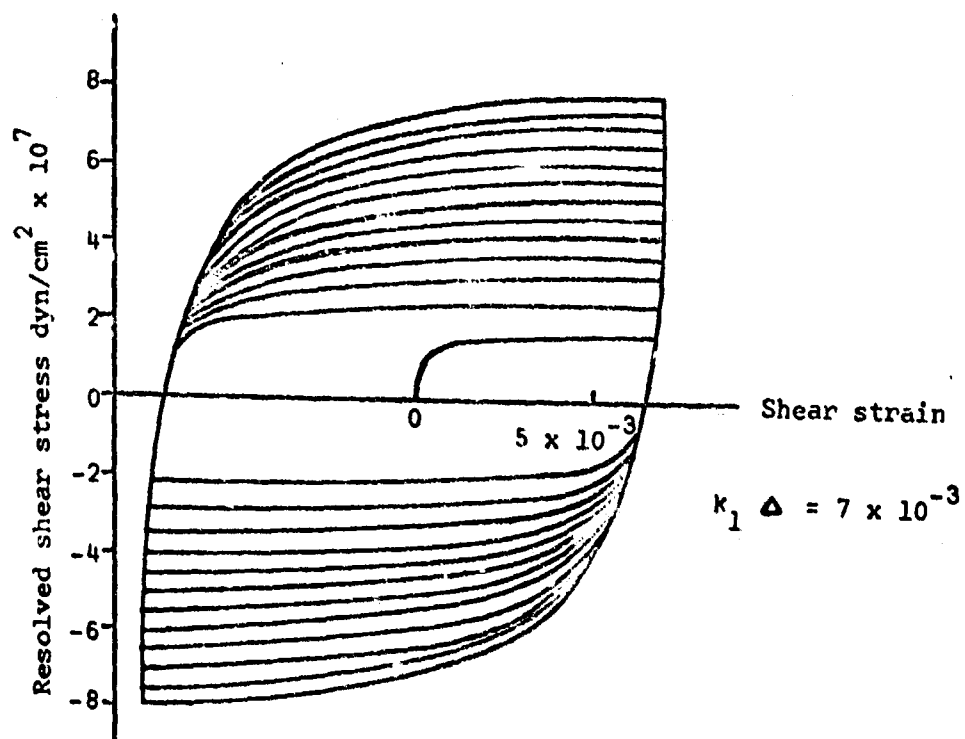
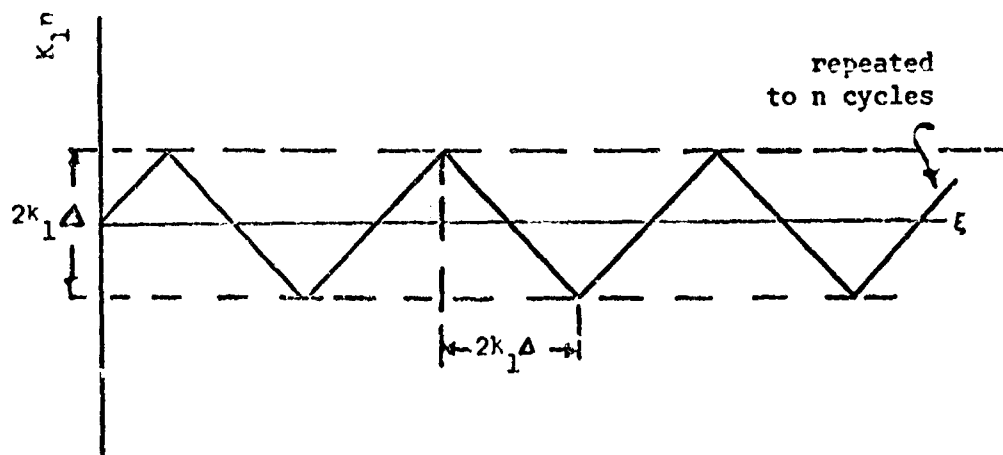


Fig. 8. Cyclic straining

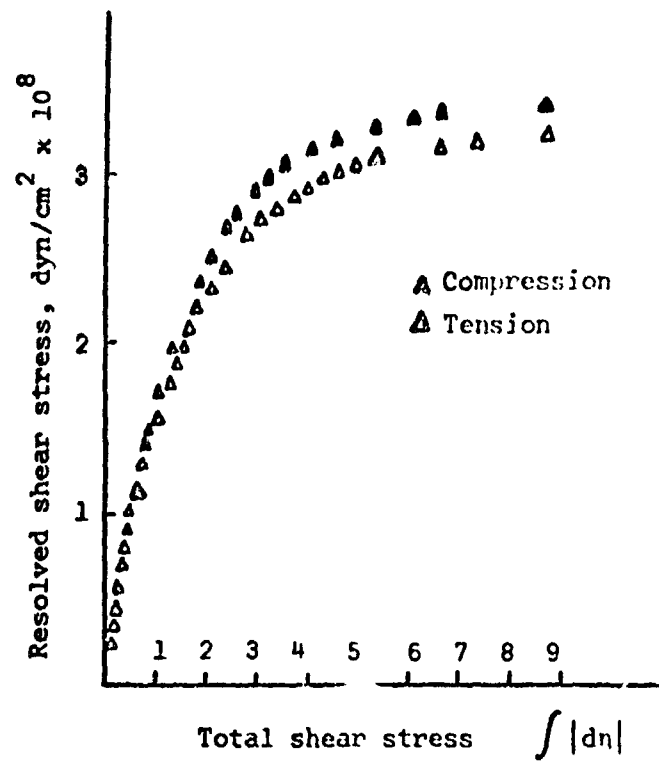


Fig. 9. Peak stresses due to cyclic straining

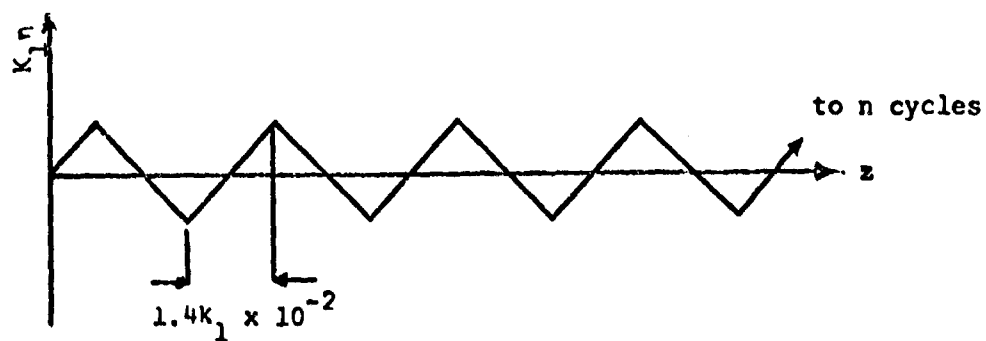


Fig. 10. History of resolved shear strain



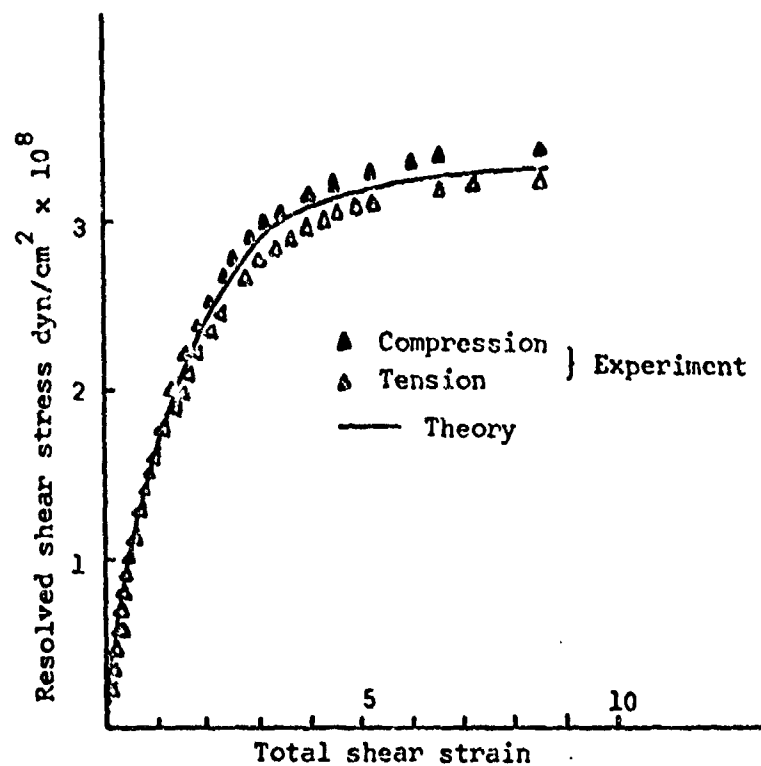


Fig. 11. Theoretical prediction of cyclic hardening

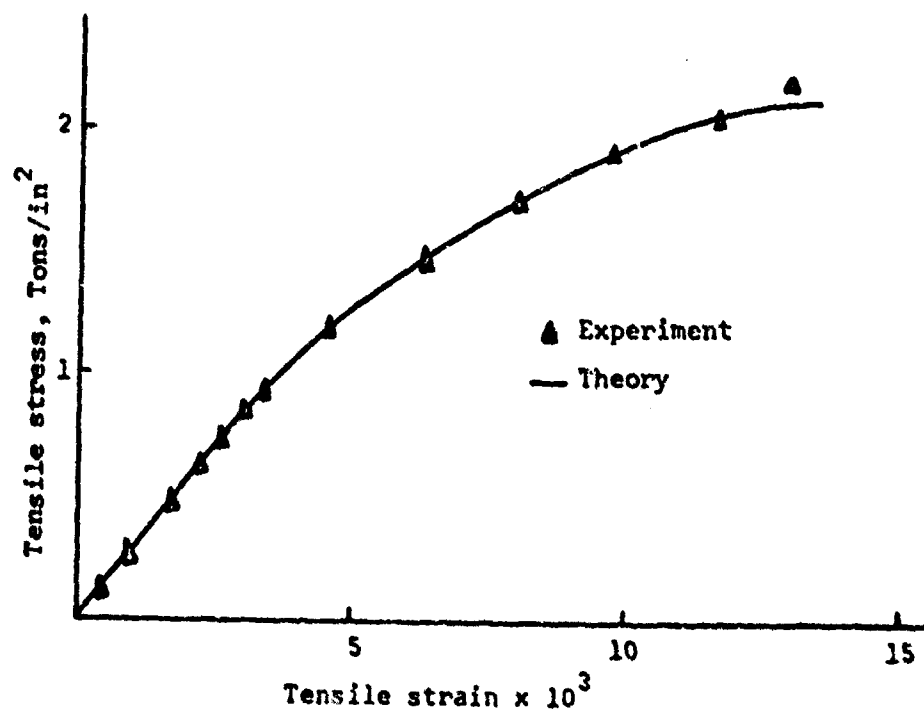


Fig. 12. Theoretical prediction of effect of shear prestress

Security Classification

## DOCUMENT CONTROL DATA - R &amp; D

(Security classification of title, body of abstract and indexing annotation must be entered when the overall report is classified)

1. ORIGINATING ACTIVITY (Corporate author) University of Iowa Department of Mechanics and Hydraulics Iowa City, Iowa 52240		2a. REPORT SECURITY CLASSIFICATION unclassified	
		2b. GROUP	
3. REPORT TITLE MATERIAL INSTABILITIES IN THE EXPERIMENTAL STUDY OF THE PLASTIC COMPRESSIBILITY OF SOME IMPORTANT METALS			
4. DESCRIPTIVE NOTES (Type of report and inclusive dates) Technical Report (Final)			
5. AUTHOR(S) (First name, middle initial, last name) K. C. Valanis and Han-Chin Wu			
6. REPORT DATE August 1971	7a. TOTAL NO. OF PAGES 50	7b. NO. OF REFS 5	
8a. CONTRACT OR GRANT NO. AFOSR 70-1916	9a. ORIGINATOR'S REPORT NUMBER(S) M & H 1.03		
b. PROJECT NO. J452	9b. OTHER REPORT NO(S) (Any other numbers that may be assigned this report)		
c.			
d.			
10. DISTRIBUTION STATEMENT 1. This document has been approved for public release and sale; its distribution is unlimited.			
11. SUPPLEMENTARY NOTES TECH.		12. SPONSORING MILITARY ACTIVITY Air Force Office of Scientific Research(NR) 1400 Wilson Boulevard Arlington, Virginia 22209	
13. ABSTRACT <p>The hypothesis of plastic incompressibility, which is pivotal in the development of the classical theory of plasticity has been tested by means of a series of simple tension tests on aluminum, copper and low carbon steel. The experimental measurements show conclusively that these metals are plastically compressible, the compressibility increasing with straining in the plastic region.</p> <p>A new phenomenon, termed lateral instability, has also been observed, consisting in an abrupt plastic flow in the transverse direction either immediately preceding or immediately following yield in the longitudinal direction, during a simple tension test on low carbon steel. To a less pronounced extent such a phenomenon has also been observed in the case of commercially pure aluminum.</p>			

DD FORM 1473  
NOV 68

Security Classification

14 KEY WORDS	LINK A		LINK B		LINK C	
	ROLE	WT	ROLE	WT	ROLE	WT
Plasticity, Compressibility, Material Instability, Poisson's Ratio, Metals.						

Report No. M & H 1.03

MATERIAL INSTABILITIES  
IN THE EXPERIMENTAL STUDY OF THE  
PLASTIC COMPRESSIBILITY OF SOME IMPORTANT METALS

K. C. Valanis and Han-Chin Wu  
Department of Mechanics and Hydraulics  
University of Iowa, Iowa City

Research sponsored by the Air Force Office  
of Scientific Research, Office of Aerospace  
Research, United States Air Force, under  
AFOSR Grant Nr70-1916.

August, 1971

### Abstract

The hypothesis of plastic incompressibility, which is pivotal in the development of the classical theory of plasticity has been tested by means of a series of simple tension tests on aluminum, copper and low carbon steel. The experimental measurements show conclusively that these metals are plastically compressible, the compressibility increasing with straining in the plastic region.

A new phenomenon, termed lateral instability, has also been observed, consisting in an abrupt plastic flow in the transverse direction either immediately preceding or immediately following yield in the longitudinal direction, during a simple tension test on low carbon steel. To a less pronounced extent such a phenomenon has also been observed in the case of commercially pure aluminum.

## I. Introduction

One of the assumptions of the classical theory of plasticity is that the material remains plastically incompressible while it undergoes plastic deformation. This implies that the hydrostatic response of the material remains elastic, (linearly, for small strains) even after yielding has occurred. This assumption also leads to the conclusion that Poisson's ratio\* tends to  $\frac{1}{2}$  as the plastic strain increases<sup>[1,2]</sup>.

In the present investigation the above assumption is evaluated critically by means of a series of simple tension tests on aluminum, copper and low carbon steel. We shall show in the following, that our experimental data do not support the hypothesis of plastic incompressibility. Moreover, Poisson's ratio does not tend to  $\frac{1}{2}$  as the plastic strain increases but, on the contrary, its value decreases and becomes smaller than its "elastic" value.

A newly observed form of material instability. The above statements on the observed behavior of Poisson's ratio, are true for copper and broadly true for aluminum and mild steel. However, in the case of mild steel (and to a lesser extent, aluminum) an unusual phenomenon, which we shall call LATERAL INSTABILITY, was observed for what is believed to be the first time. At least, to our knowledge no such phenomenon has ever been reported in the literature in the past.

---

\*It must be pointed out that, in this report, we do not regard Poisson's ratio as some fundamental physical property or function, but simply as the ratio of the algebraic values of the transverse and longitudinal strains, in a uniaxial test. On the other hand because the experiments reported here were carried out in the small strain range, Poisson's ratio is a convenient quantity to work with, since it can be used to relate directly the uniaxial to the volumetric strain; the latter is an important parameter in our investigation.

Lateral instability is defined by one of the following two observed sequences of events during a simple tension test.

- (a) As the yield point of a low carbon steel specimen is reached, the material begins to flow longitudinally (i.e., in the direction of applied stress) and one observes the usual increase in longitudinal strain while the longitudinal stress remains constant. However an abrupt occurrence of plastic flow in the transverse direction has also been observed, just after longitudinal flow has ceased and strain-hardening has begun.
- (b) Abrupt transverse flow occurred just before the onset of longitudinal flow.

It is significant that no transverse flow has been observed during the process of longitudinal flow. A more detailed discussion of this phenomenon will be given in text.

In the case of aluminum the onset of lateral plastic flow was not abrupt, but what was observed amounted to a significant increase in the transverse strain during a relatively small increment in longitudinal strain. A quantitative plot of these events is shown in later figures.

Loading-unloading loops have also been observed in some of the tests. It will be shown in later sections that loops are also obtained in plots of transverse strain versus longitudinal strain, and hydrostatic stress versus volumetric strain.

## II. Materials and Specimens

Altogether three metallurgically important metals were tested. They were commercially pure aluminum, electrolytic tough pitch copper and low-carbon steel. The aluminum specimens were sheared from an 1100-0 aluminum sheet, all the copper specimens were cut out of an electrolytic tough pitch copper 110 (99.9<sup>+</sup>% copper) bus bar, and the steel specimens were cut from a cold drawn C 1018 flat. The nominal dimension of all the aluminum and copper specimens was  $\frac{1}{8}$ " x  $\frac{3}{4}$ " x 15" and that of all the low-carbon steel specimens was  $\frac{1}{8}$ " x  $\frac{1}{2}$ " x 12". All the specimens of the same metal were considered to be identical prior to the heat treatment. These specimens have been divided into several groups, according to the annealing temperatures and purposes of study. They are listed in Table I.



### III. The Equipment and Strain Measurements

All tests were conducted at room temperature on a Tinius Olsen Lo Cap universal testing machine with strain gage load cell weighing and equipped with a Tinius Olsen Model 51 electronic recorder. The load readings on the dial indicator were calibrated against a Tinius Olsen proving ring with the electrical vibrating reed.

A Tinius Olsen S-400-2AB extensometer was used to measure the longitudinal strains of all the specimens except those of group III of aluminum. This is an averaging type extensometer with a gage length of two inches. The accuracy of the extensometer is  $\pm 0.0001$  in/in as guaranteed by the manufacturer and was calibrated against the SR-4 electric strain gages of type A-7 which have the accuracy of  $2 \times 10^{-5}$  in/in. The load vs. longitudinal strain  $\epsilon_x$  curves were plotted by the Model 51 recorder during experiments.

To measure the transverse strains  $\epsilon_y$ , a SR-4 electric strain gage of type A-7 was transversely put on one side of each specimen. The transverse strain was then read directly from a SR-4 portable strain indicator at the accuracy of  $2 \times 10^{-5}$  in/in.

The strain measurements of the specimens of group III of aluminum were specially arranged for greater accuracy. A-7 type strain gages were longitudinally and transversely glued on both sides of each specimen belonging to this group, in order to cancel out the bending effect. The strain reading of each gage was then obtained from a SR-4 portable strain indicator with the help of a BLH Model 225 switching and balancing unit. Finally, the average value of the readings of the two longitudinally arranged strain gages gives us the longitudinal strain  $\epsilon_x$ , and the average value of the

readings of the two transversely arranged strain gages gives us the transverse strain  $\epsilon_y$ .

#### IV. Description of Tests and Results

##### Experiments on Aluminum

The first group of aluminum specimens was tested under the "as-received" condition. During the tests, the Tinius Olsen machine was operated at a constant rate of crosshead separation. The rate was  $8 \times 10^{-4}$  in/sec, which corresponds to a strain-rate of approximately  $5 \times 10^{-5}$  in/in/sec for the specimens used. The recorder traced out the load versus  $\epsilon_x$  curve as readings of load and of transverse strain were taken simultaneously at predetermined readings of load, at small longitudinal strains, and at predetermined readings of longitudinal strains, when the strain was large.

The stress-strain curves are shown in Fig. 1, in which the curve for specimen #1 is identical to that for specimen #2. Fig. 2 shows the relations between the transverse and the longitudinal strain, and Fig. 3 shows the hydrostatic stress ( $\times 3$ ) versus the volumetric strain curve for aluminum of group I. A loading-unloading loop was generated at the end of each test, and we obtain loops, which is similar to the hysteresis loops, in the curves of Figures 2 and 3 (not shown). More observations and discussions of the loops will be presented later in this report. The large increase of  $-\epsilon_y$  at a longitudinal strain of approximately 2.5% (see Fig. 2) corresponds to a case of "mild" lateral instability as compared to the "strong" lateral instability observed in low-carbon steel. We shall make more observations later about the lateral instability of aluminum.

The second group of aluminum specimens was tested exactly in the same way as those of group I, except that the specimens were first annealed at a temperature of 600°F for two hours and then oven cooled to the room temperature before testing. This annealing process removes most of the effects due

to cold work, and the material can thus be considered as isotropic. The stress-strain curves for specimens Al #3 and Al #4 are shown in Fig. 4, in which the two curves are indistinguishable. We notice, however, that the material is considerably softened due to the heat treatment.

To see the sudden increase in magnitude of the transverse strain at a longitudinal strain of approximately 2.2%, which has been an observed fact in the test of group I, this series of tests was carried out to the extent that the longitudinal strain at the time of termination of the test was approximately 9%. Here, again, we have observed a sudden increase in  $-\epsilon_y$  at a longitudinal strain of approximately 2.2%. This phenomenon has been observed both for specimens Al #3 and Al #4.

The  $-\epsilon_y$  vs.  $\epsilon_x$  curves are plotted in Fig. 5, and the  $\sigma_{kk}$  vs.  $\epsilon_{kk}$  curves are given in Fig. 6. The sudden increase of the transverse strain in Fig. 5 gives rise again to the sudden decrease of the volumetric strain in Fig. 6 which corresponds to the lateral instability mentioned earlier. In this series of test, the loopings of the curves are once more present in all the figures concerned (not shown). These loopings are due to the loading-unloading test conducted at the end of each study.

It is important to point out, that aside of the sudden change of Poisson's ratio immediately following yielding, Poisson's ratio remains approximately constant throughout the range tested. Poisson's ratio in the plastic range is defined in the present investigation by the expression

$$\nu = - \frac{\epsilon_y}{\epsilon_x}$$

which, in fact, is also used in elasticity (see footnote in the introduction).

Group III of the aluminum specimens was tested quasi-statically, i.e., readings were taken after the machine had been stopped and time of 5 minutes

had already elapsed. By doing this, it is believed that the results obtained are time independent. As it has already been described earlier in this report that four strain gages were applied to each specimen of this series to eliminate the bending effect due to the possible eccentricity of the loading arrangement. The comparison of the present results (shown in Figures 7-12) with those obtained earlier in groups I and II of the aluminum specimens shows that reliable data can be obtained without the complicated strain gage set-ups of group III. In fact, the grips of the Tinius-Olsen machine are of the self-aligning type, therefore, eccentricity is to be expected at its minimum.

Loops are again present in all the figures concerned (Figures 7-12). It is seen from Figures 9 and 10 that Poisson's ratio decreases again drastically immediately following yielding.

The fact that all the curves in Figures 3, 6, 11 and 12 bend over toward the  $\epsilon_{kk}$ -axis leads to the conclusion that aluminum is plastically compressible, at least when the hydrostatic stress is of a tensile nature. The assumption of plastic incompressibility in the classical theory of plasticity would lead to a linear relation between hydrostatic stress and volumetric strain; this apparently is not the case.

#### Experiments on Copper

The experiments on group I of the copper specimens were designed to further study the loops which we had observed in the tests of aluminum specimens. These specimens of copper were tested under the "as-received" condition. The rate of crosshead motion was kept constant ( $8 \times 10^{-4}$  in/sec) during this series of test. The loading-unloading curves for specimens Cu #1 and Cu #2 are shown in Figures 13 and 14, and the corresponding  $-\epsilon_y$  versus  $\epsilon_x$  curves are shown in Figures 15 and 16. We see here again that loops are definitely in existence and that, after a loop has been completed, the curve of  $-\epsilon_y$

versus  $\epsilon_x$  is virtually a continuation of the original  $-\epsilon_y$  versus  $\epsilon_x$  curve. The plots of  $\sigma_{kk}$  vs.  $\epsilon_{kk}$  for these specimens are given in Figures 17 and 18.

The copper specimens of group II were tested in exactly the same way as those of the aluminum specimens of group II, except that the annealing temperature was 750°F. The results are shown in Figures 19, 20 and 21. We remark that in contrast with the aluminum specimens we do not observe the sudden increase in the magnitude of the transverse strain for all the copper specimens concerned. As a result, Poisson's ratio is approximately a constant throughout the range tested.

Experiments were conducted on group III of the copper specimens under quasi-static conditions, i.e. readings were taken after the machine had been stopped and 5 minutes had elapsed. The results of this series are given in Figures 22, 23 and 24. We again observe no sudden increase in the magnitude of the transverse strain and that Poisson's ratio is virtually constant throughout the range tested.

The tests on copper specimens of groups I, II and III show conclusively that copper is also plastically compressible, as it is seen easily from Figures 17, 18, 21 and 24; otherwise these plots would have been straight lines.

#### Experiments on Low Carbon Steel

The same experimental procedure as described above was followed when the five low-carbon steel specimens were tested. All the five specimens were annealed, prior to tests, at a temperature of 1250°F for one hour and then oven cooled to room temperature. Thus, all the specimens can be considered to be identical and the material can be considered to be isotropic.

The tests were carried out under quasi-static conditions, and a typical stress-strain curve for these specimens is given in Fig. 25. In Fig. 26, the

relation between the transverse strain and the longitudinal strain is plotted for all the five specimens. It is seen that aside of the portion reflecting "lateral instability" the curve is almost a straight line. Of all the specimens tested in this series, three of them (#1, #2 and #4) showed lateral instability before the occurrence of the longitudinal plastic flow, and follow the path OABDE in Fig. 26. The rest of the specimens (#3 and #5) experienced lateral instability immediately after the longitudinal plastic flow had been accomplished, i.e., lateral instability had occurred before the material strain-hardened. In this case, curve OACDE of Fig. 26 is followed.

We conjecture that had the material been homogeneous as well as isotropic then longitudinal and transverse flow would have taken place simultaneously. Since in practice this is rarely true, the order in which these flows occur must then be decided by slight differences in the directional properties of the specimen.

To ensure the correctness of our observation about the lateral instability as a material property of low-carbon steel. The transverse dimension of all specimens was measured after the experiments by means of a micrometer. The permanent transverse strains were then calculated referring to the original dimensions of the specimens. The results checked favorably (with less accuracy, of course) with those obtained by means of electric strain gages. Two of the five experiments (#2 and #4) were terminated right after the occurrence of the transverse plastic flow and before much longitudinal flow had occurred, in order for us to study the lateral instability more closely. Measurements by means of both electric strain gages and micrometer showed that large amount of plastic flow did occur transversely at yielding. If it was not for the transverse plastic flow, the transverse permanent strains would have been very small for these two specimens.

The relation between the hydrostatic stress and the volumetric strain is shown in Figures 27-31. The alphabetical order of letters in the figures denotes successive states of the material during the tests. The last letter in the figure gives us the position where the corresponding test was terminated. It is seen that the lateral instability corresponds to a sudden decrease of volumetric strain. In the case when lateral instability occurs before the longitudinal plastic flow, the volumetric strain could become negative! A very strange result!

However, a similar phenomenon was observed by Bridgman<sup>[6]</sup>. He investigated, by means of a dilatometer, volume changes during simple compression in the plastic range, in various materials, such as mild steel, Norway iron, cast iron and rock (soapstone, marble and diabase). He observed an increase in volume under conditions of compressive hydrostatic stress, when the axial compressive stress exceeded its yield value.



#### V. On the Accuracy of the Experimental Measurements

It is to be noted that it is impossible to glue a strain gage on the specimen such that the strain gage makes an angle of exactly  $90^\circ$  degrees with the longitudinal direction of the specimen. Slight errors are always possible, and these errors tend to make the readings of transverse strain smaller than it should be. These are, however, small since the gages are in the principal strain directions. According to Perry and Lissner<sup>[3]</sup>, a 2 degree error in gage alignment would only result in an error of less than 1%.

Our purpose in the present experimental study is not the determination of the exact value of Poisson's ratio. Our primary concern is the trend in the variation of Poisson's ratio as the longitudinal strain increases. For this reason, the above mentioned deviations due to the misalignment of the transverse strain gages are not important, since they hardly affect the broad trends in the variation of Poisson's ratio, which are of interest here.

Slight scattering of some of our experimental data for different specimens may be attributed partially to the above mentioned misalignments of the transverse strain gages. We notice, however, that our data are very consistent in general, and the slight scattering of data occurs only in the case of copper specimens #5 and #6. Even in these cases where data are scattered slightly, the curve for each specimen is itself smooth, which indicates that scattering is due to a large extent to variability in the properties of the specimens.

Of course corrections must also be made on the readings of the transverse strain  $\epsilon_y$  due to the effect of transverse sensitivity of the electric strain gages. The transverse sensitivity factor for A-7 strain gage is given by

Perry and Lissner<sup>[3]</sup> as  $k = -0.01$ . The error, which is defined by  $e = \frac{\epsilon_c - \epsilon}{\epsilon}$ , where  $\epsilon_c$  is the apparent strain and  $\epsilon$  is the true strain, is 3% for a Poisson's ratio of 0.3 and is 2.6% for a Poisson's ratio of 0.33. It is equivalent to saying that  $\epsilon = 0.971 \epsilon_c$  for material with Poisson's ratio of 0.3 and  $\epsilon = 0.984 \epsilon_c$  for material with Poisson's ratio of 0.33. We have thus seen that the true transverse strain is 2.9% smaller than the apparent transverse strain when  $\nu = 0.30$ , and is 1.6% smaller than the apparent transverse strain when  $\nu = 0.33$ . This correction is however in a different direction from the one due to the misalignment of the strain gages, therefore some of the errors should cancel out.

Stang, Greenspan and Newman<sup>[4]</sup> reported in as early as 1946 their experimental study on Poisson's ratio of aluminum alloys 24 ST and 24 SRT, chrome-molybdenum steel plate and structural and fully killed low-carbon steel plate. In all cases these authors reported the increase of Poisson's ratio beyond its initial (elastic) value throughout the longitudinal strain range tested. This observation is not in agreement with the present findings.

We like to mention that the above discussed misalignment in the transverse strain gages also existed in the tests by Stang et al<sup>[4]</sup>. In addition to this, as it was pointed out by these authors themselves in their report, there were large discrepancies in the values of Poisson's ratio obtained by them for two nominally identical specimens.

Finally, from a thermodynamic point of view the hydrostatic stress versus volumetric strain curve should bend over toward the  $\epsilon_{kk}$ -axis<sup>[5]</sup>; this agrees with our own observations.

## VI. Conclusions

The following conclusions can be drawn from the present experimental study:

- (1) The curve of hydrostatic stress versus volumetric strain bends over toward the volumetric strain axis for all three materials tested. This implies that the commercially pure aluminum, the electrolytic tough pitch copper and the low-carbon steel are plastically compressible, (at least when the hydrostatic stress is of a tensile character) and that the most important assumption in the classical theory of plasticity concerning the plastic incompressibility of material lacks experimental justification.
- (2) Lateral instability occurs weakly in the case of aluminum and occurs strongly in the case of low-carbon steel. Lateral instability always follows the longitudinal plastic flow for aluminum, whereas two possibilities arise in the case of low-carbon steel—lateral instability may precede or follow the longitudinal plastic flow as dictated by the anisotropy of the material. No phenomenon of lateral instability has been observed for the copper specimens tested.
- (3) The lateral instability corresponds to a decrease in volume due to a slight increase in load for the case of aluminum, and corresponds to a sudden decrease in volume while the load remains constant for the case of low-carbon steel. Where the lateral instability occurs, Poisson's ratio has a large increase.
- (4) Poisson's ratio for the commercially pure aluminum decreases considerably after yield has occurred, from an initial value of 0.30 to a

value as low as 0.06 corresponding to a longitudinal strain of approximately 2%; beyond this point it increases continuously and at an axial strain of 3% it reaches a value of 0.15 which remains approximately constant up to  $\epsilon_x = 9\%$ .

- (5) For the electrolytic copper, Poisson's ratio decreases continuously with  $\epsilon_x$  from a value of 0.35 to a value of 0.3 at  $\epsilon_x = 9\%$ .
- (6) For the low-carbon steel, two possibilities prevail. If the lateral instability occurs before the longitudinal plastic flow then Poisson's ratio increases suddenly at yielding from its initial value of 0.29 to a value as high as 6.0. It then decreases gradually and reaches a value of 0.3 at  $\epsilon_x = 3\%$ . Beyond this point, Poisson's ratio remains approximately constant up to  $\epsilon_x = 9\%$ . If the lateral instability occurs after the longitudinal plastic flow, then Poisson's ratio decreases considerably after yield has occurred from an initial value of 0.29 to a value as low as 0.02 corresponding to a longitudinal strain of approximately 2.5%, beyond this point, it increases continuously and at an axial strain of 3% it reaches a value of 0.3 which remains approximately constant thereafter.
- (7) Loops similar to the hysteresis loops are present in curves obtained by plotting  $-\epsilon_y$  against  $\epsilon_x$  and also in curves of  $\sigma_{kk}$  against  $\epsilon_{kk}$  for all three materials tested.

Acknowledgement

The authors wish to express their appreciation to Mr. Hyo Kim of his very capable assistance with the experimental work and the preparation of the graphs.

References:

- [1] Hill, R., "The mathematical theory of plasticity", Oxford, 1950.
- [2] Naghdi, P. M., "Stress-strain relations in plasticity and thermo-plasticity", PLASTICITY, edited by E. H. Lee and P. S. Symonds, Pergamon Press, London, 1960.
- [3] Perry, C. C. and Lissner, H. R., "The strain gage primer", McGraw-Hill, New York, 1962.
- [4] Stang, A. H., Greenspan, M. and Newman, S. B., "Poisson's ratio of some structural alloys for large strains", Journal of Research, National Bureau of Standards, 37, 211-221, 1946.
- [5] Valanis, K. C., "A theory of viscoplasticity without a yield surface", Archives of Mechanics - Archiwum Mechaniki Stosowanej, 23, 4 (1971) (in press).
- [6] Bridgman, P. W., "Volume changes in simple compression", J. App. Phys. 20, 1241, (1949).

TABLE I

Metal	Group	Specimen	Heat Treatment	Remarks
Al 1100-0	I	#1	No	Constant strain-rate test
		#2		
	II	#3	Annealed at 600°F for 2 hrs. and then oven cooled to room temperature	Constant strain-rate test
		#4		
	III	#5	Annealed at 600°F for 2 hrs. and then oven cooled to room temperature	Quasi-static test, loading- unloading loops observed strain gages on both sides of specimens.
		#6		
Cu 110	I	#1	No	Constant strain-rate test, loading-unloading loops observed.
		#2		
	II	#3	Annealed at 750°F for 2 hrs. and then oven cooled to room temperature	Constant strain-rate test
		#4		
	III	#5	Annealed at 750°F for 2 hrs. and then oven cooled to room temperature	Quasi-static test
		#6		
Low- Carbon Steel C1018		#1		
		#2		
		#3	Annealed at 1250°F for 1 hr. and then oven cooled to room temperature	Quasi-static test, lateral instability observed
		#4		
		#5		

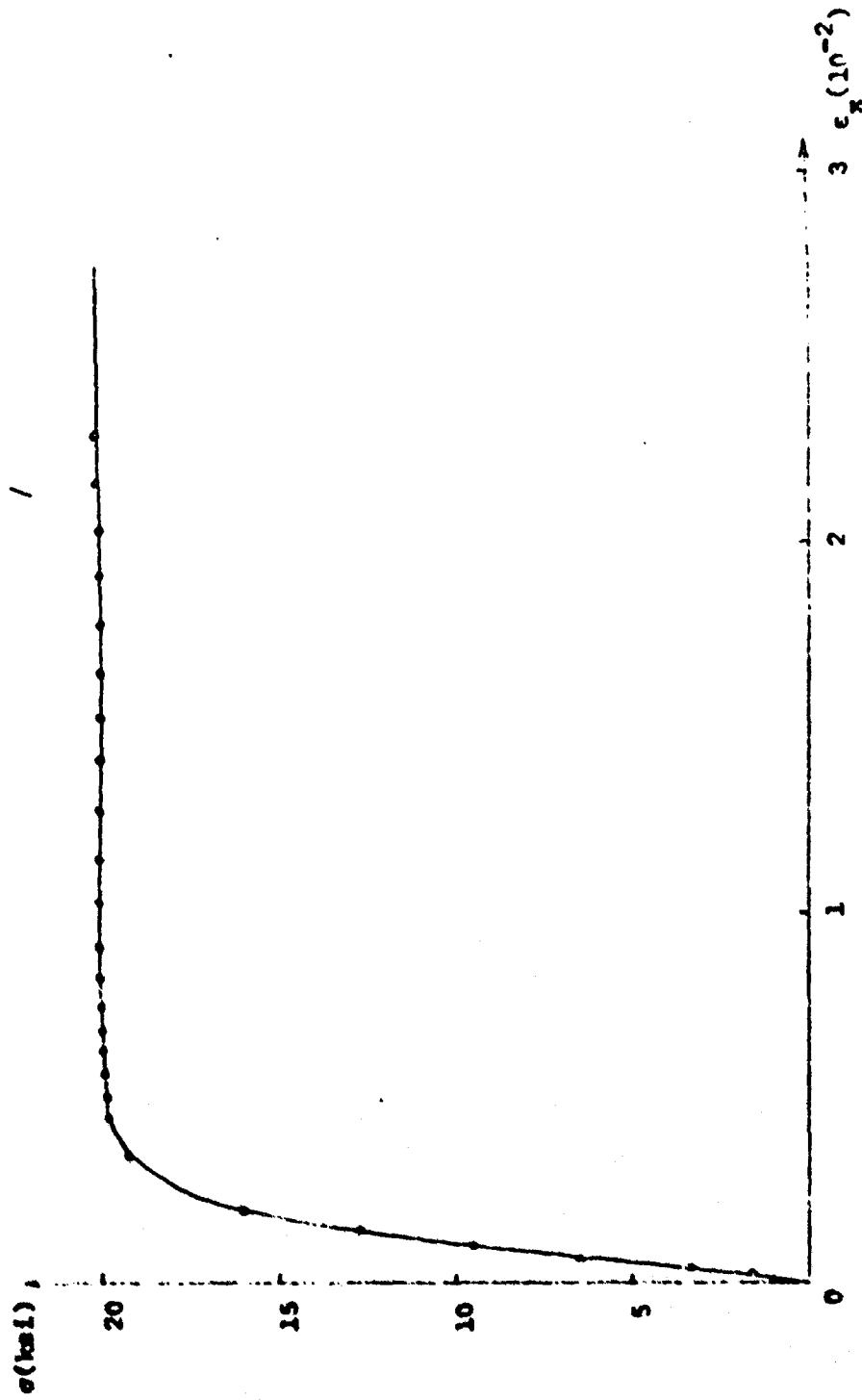


Figure 1 The stress-strain curve for aluminum of group I



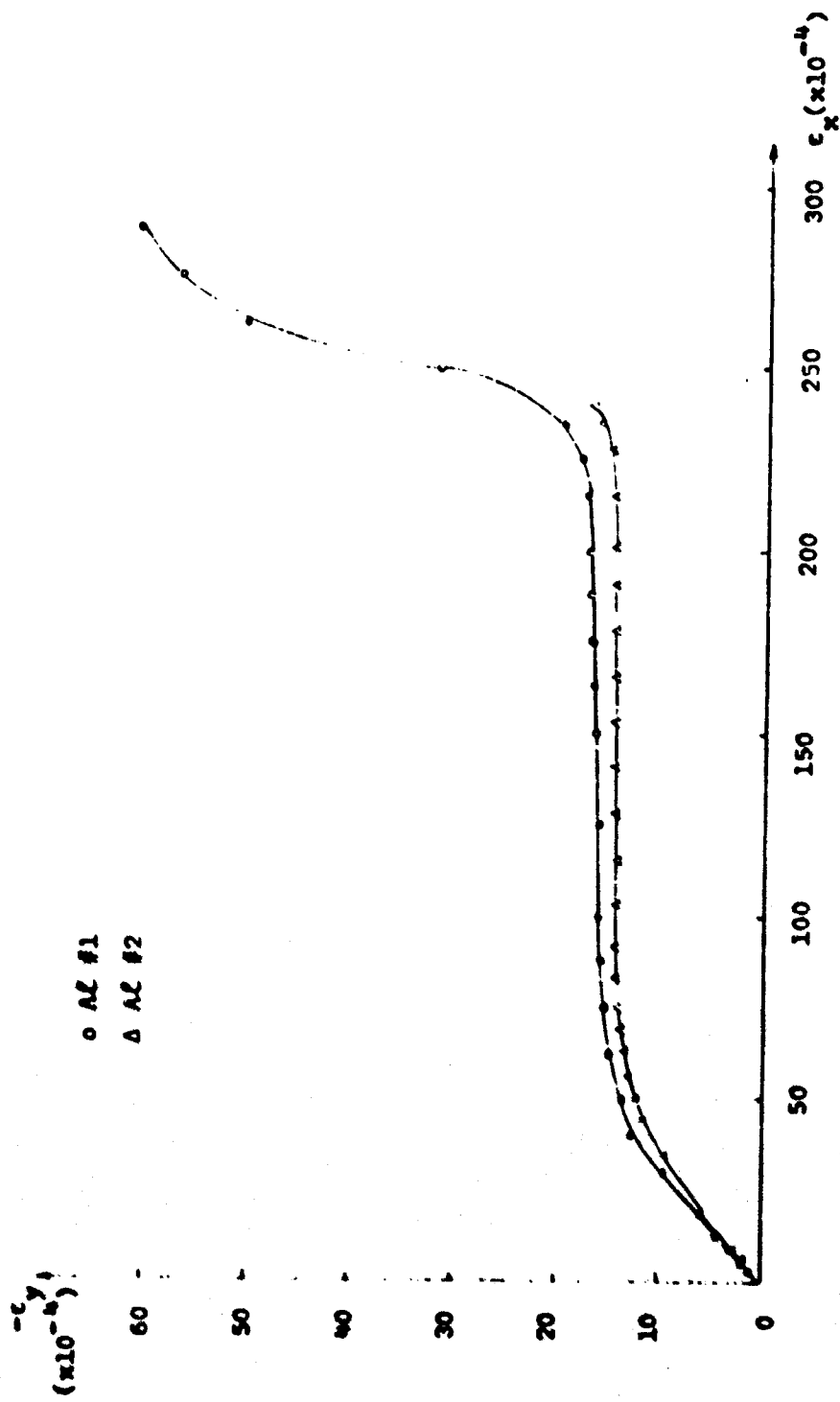


Figure 2. Relations between transverse and longitudinal strain for aluminum of group I

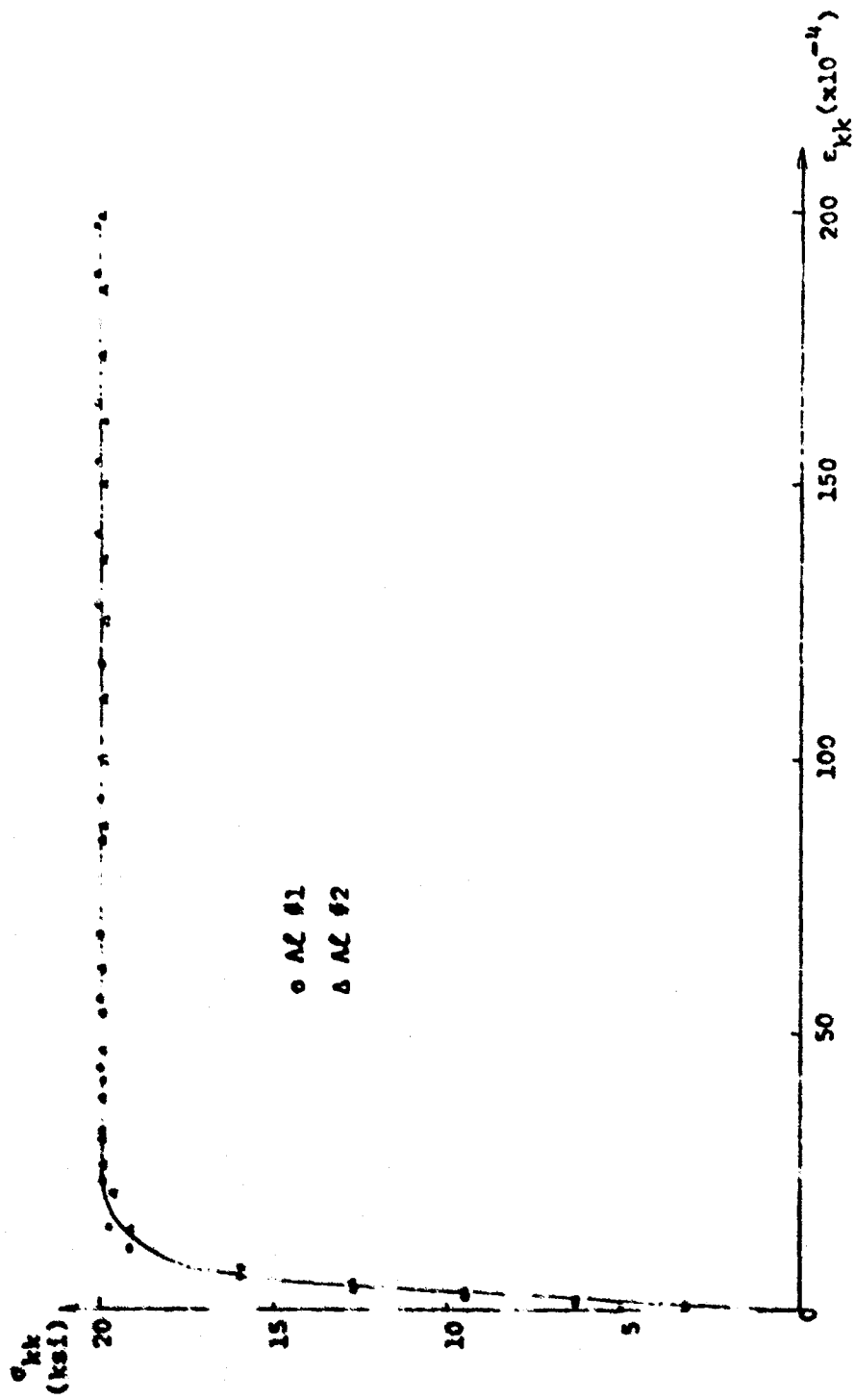


Figure 3 Hydrostatic stress ( $\times 3$ ) versus volumetric strain for aluminum of group I

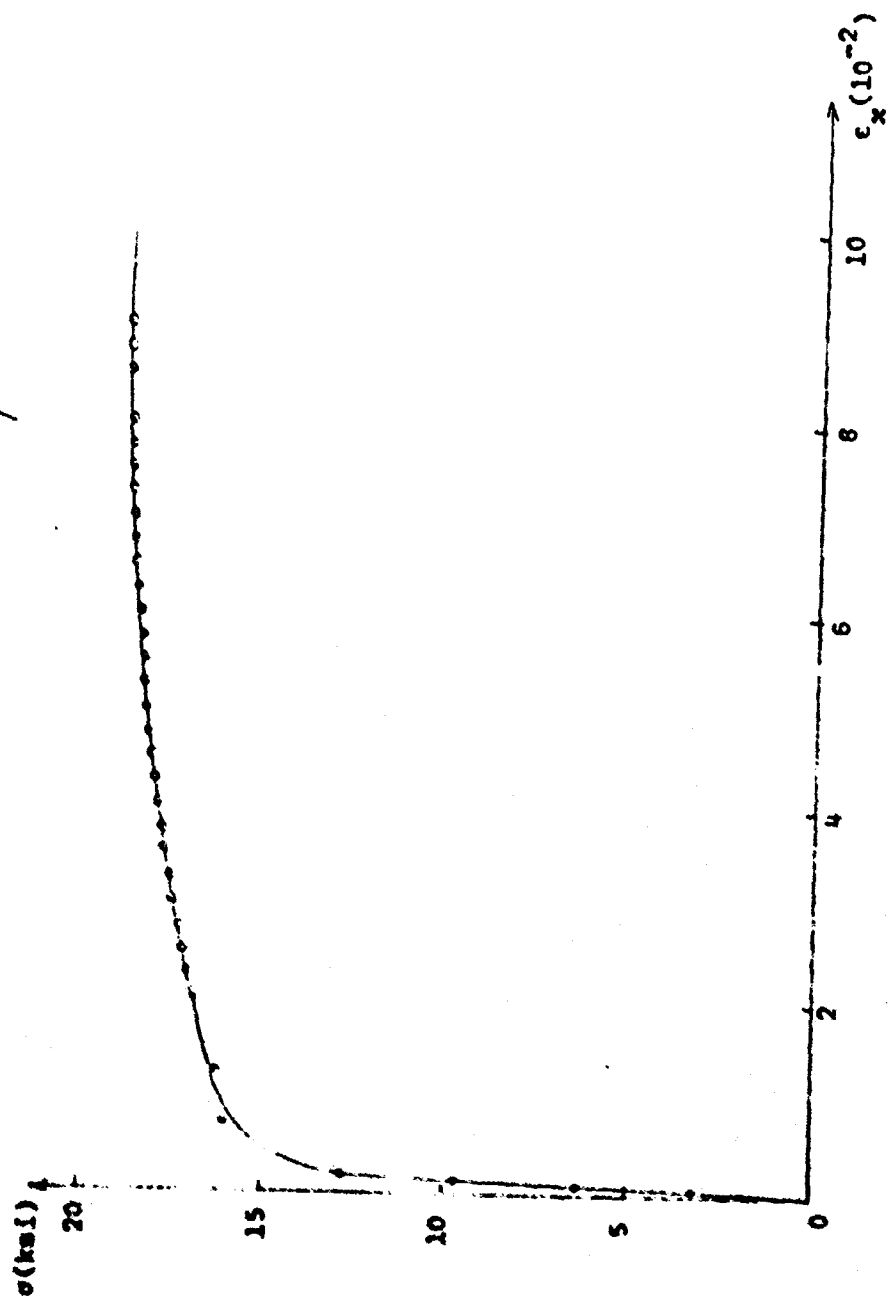


Figure 4 The stress-strain curve for aluminum of group II

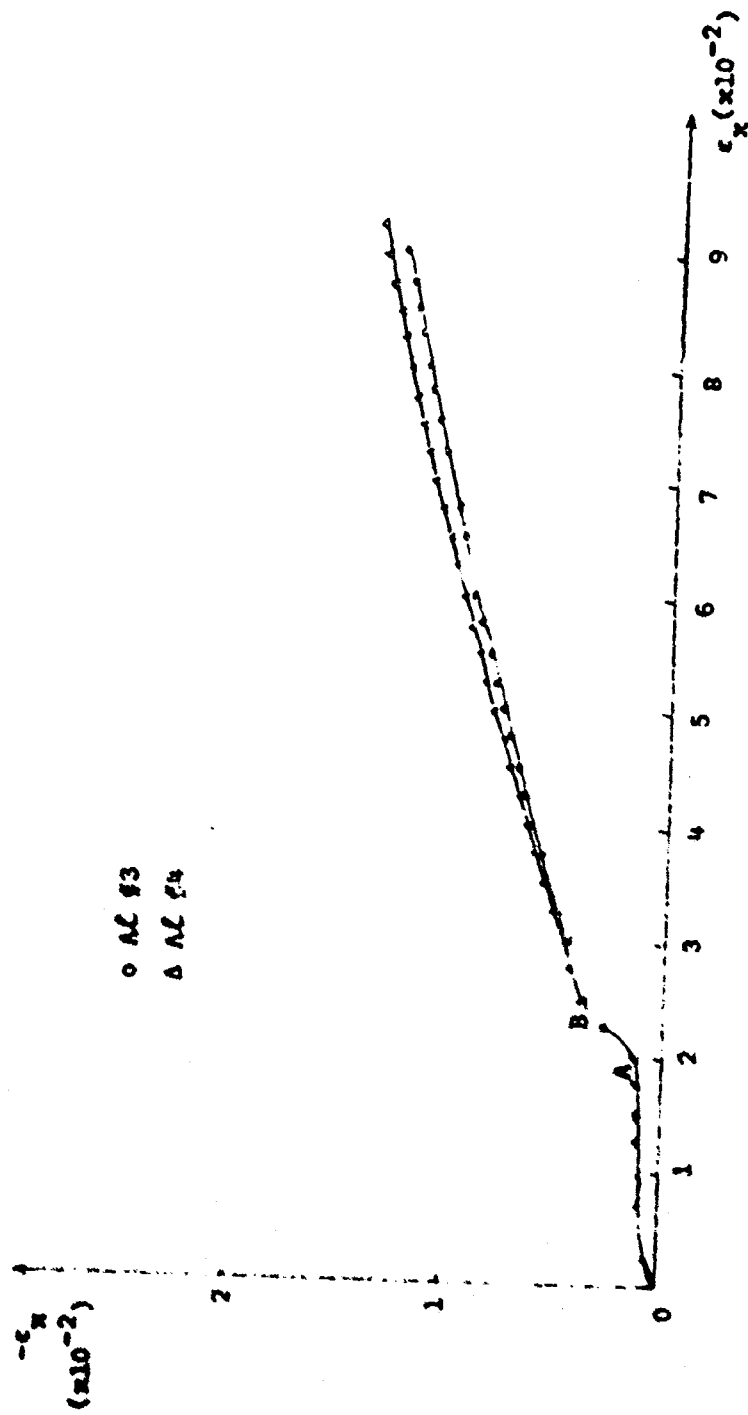


Figure 5 Relations between transverse and longitudinal strain for aluminum of group II

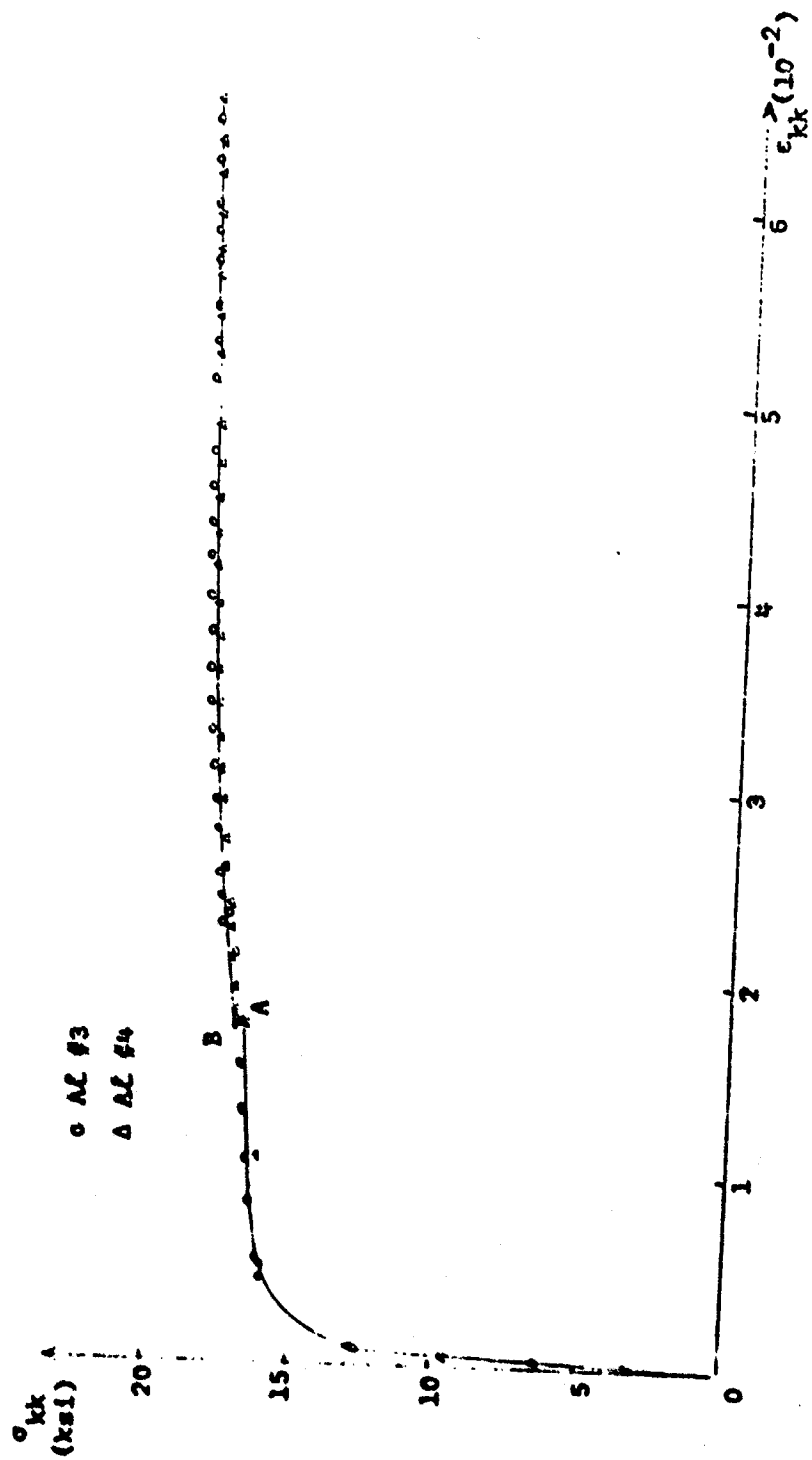


Figure 6 Hydrostatic stress ( $\times 3$ ) versus volumetric strain for aluminum of group II

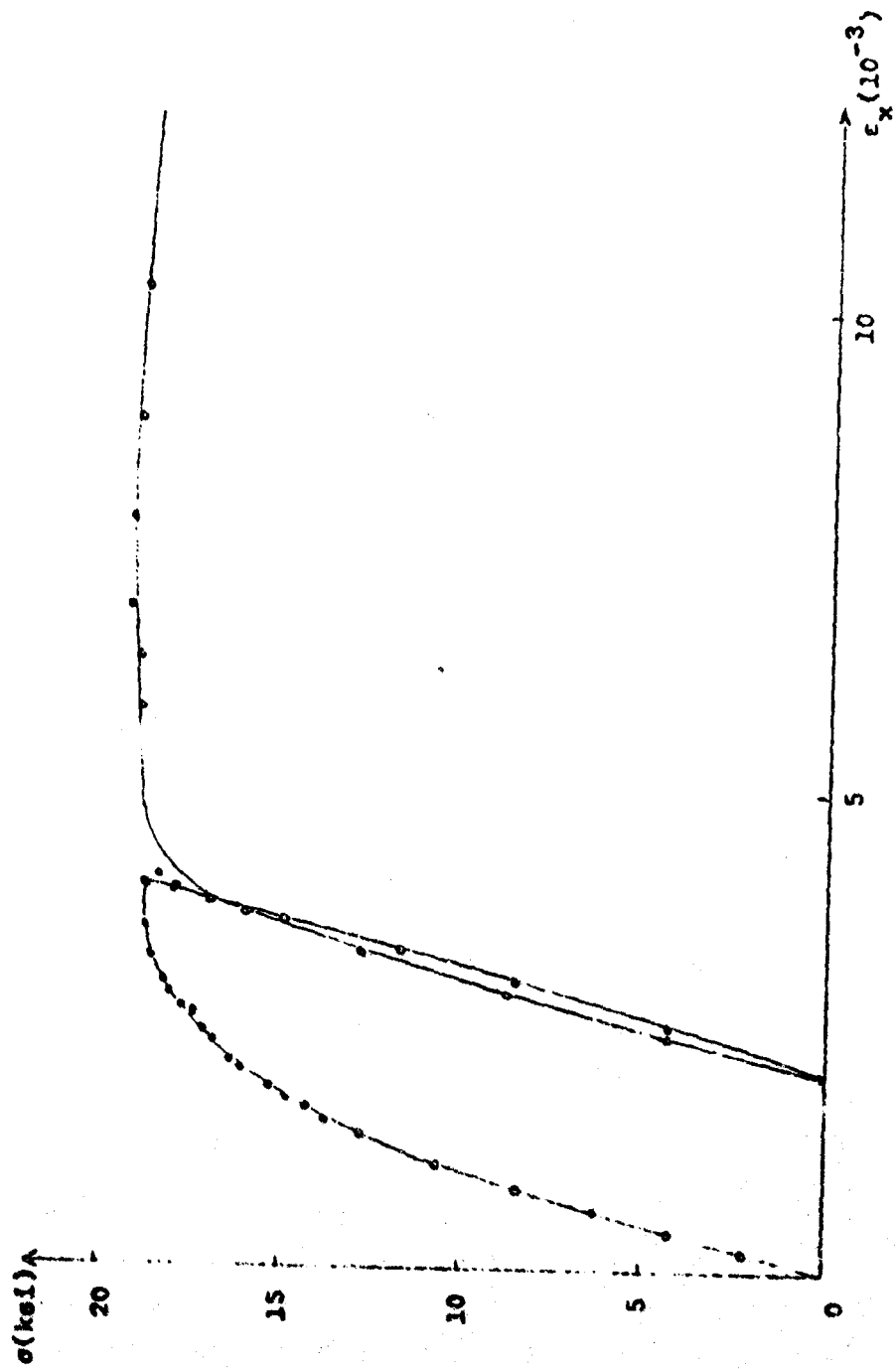
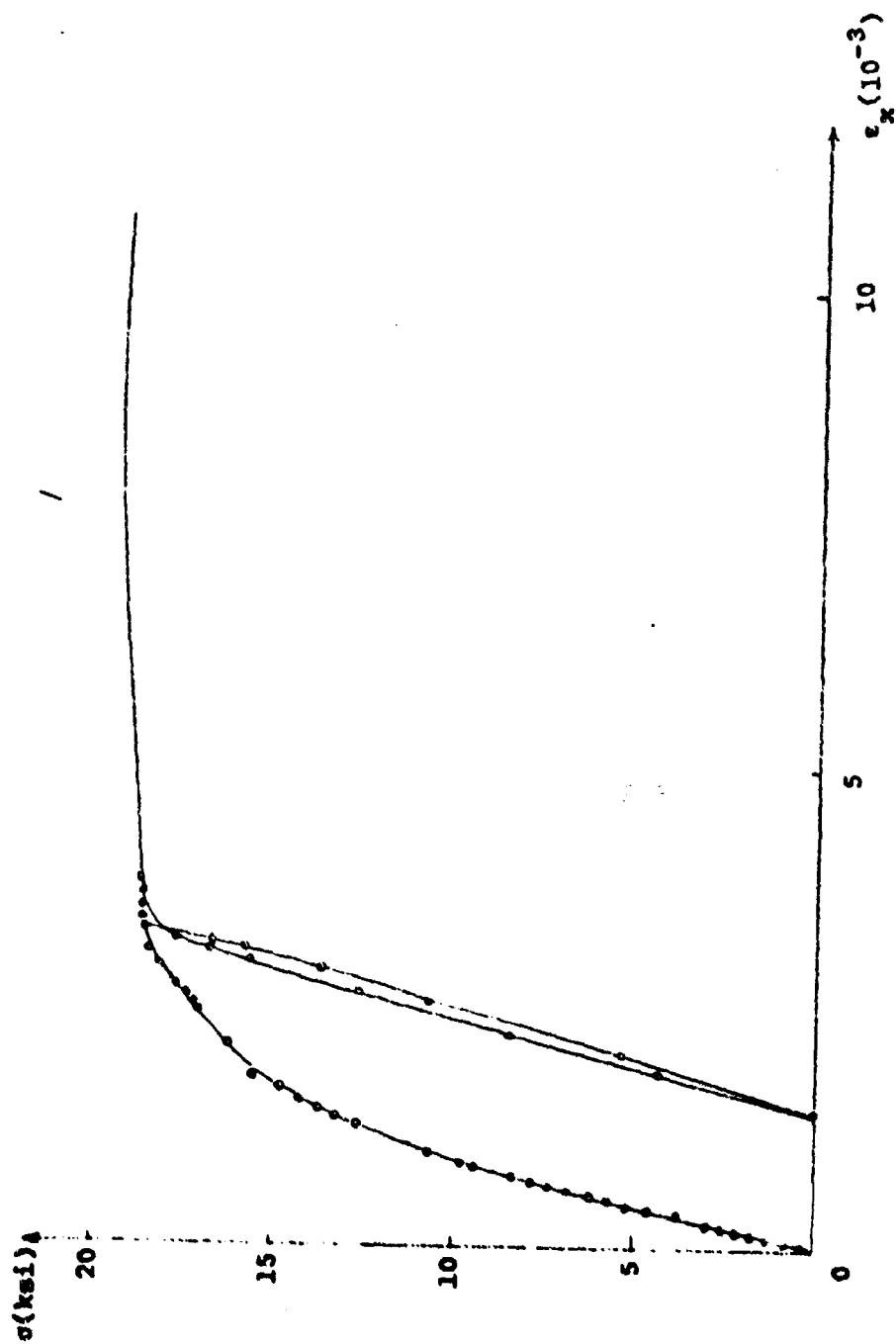


Figure 7 The stress-strain curve of aluminum specimen #5



**Figure 8** The stress-strain curve of aluminum specimen #6

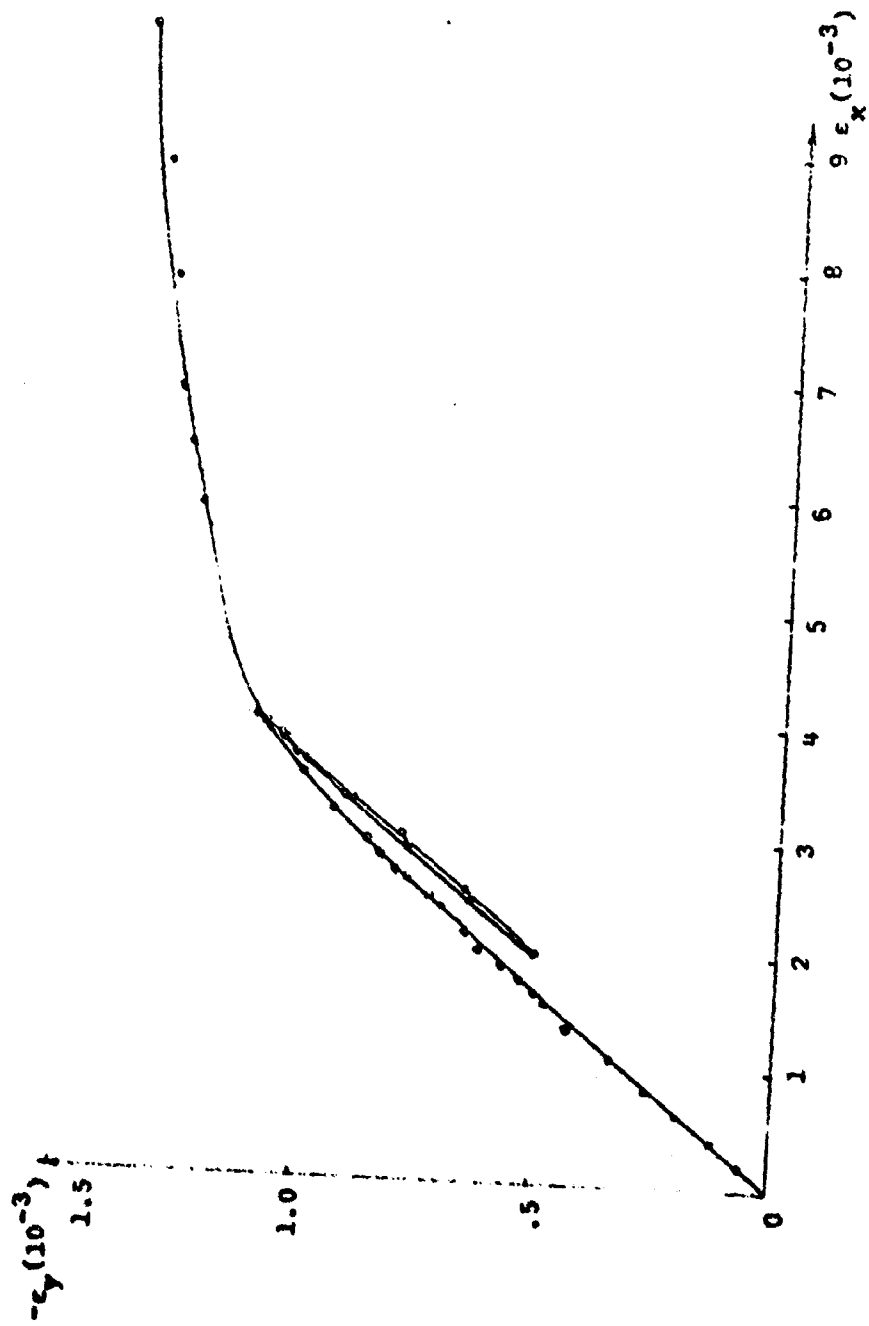


Figure 9 Relation between transverse and longitudinal strain for aluminum specimen #5



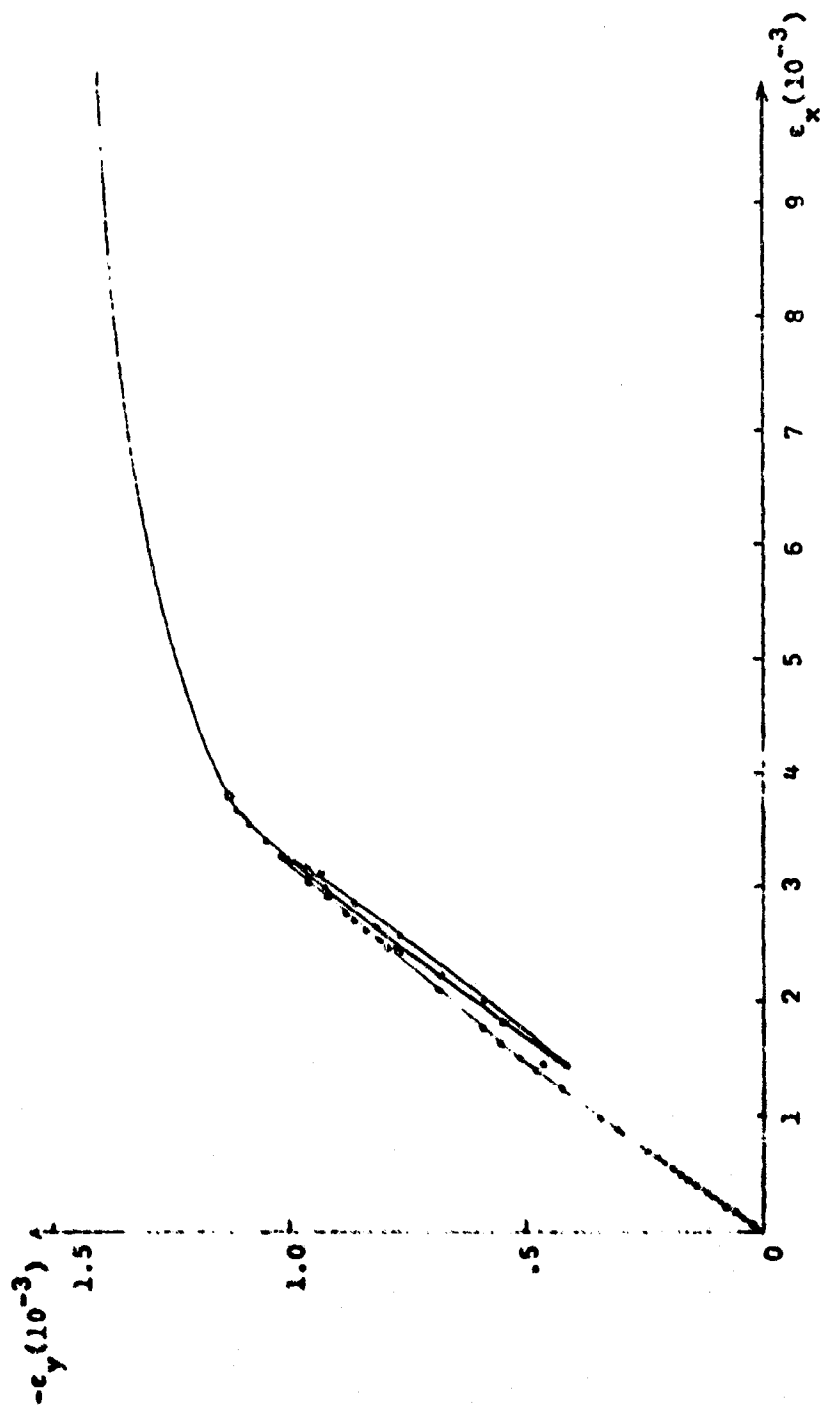


Figure 10 Relation between transverse and longitudinal strain for aluminum specimen #6

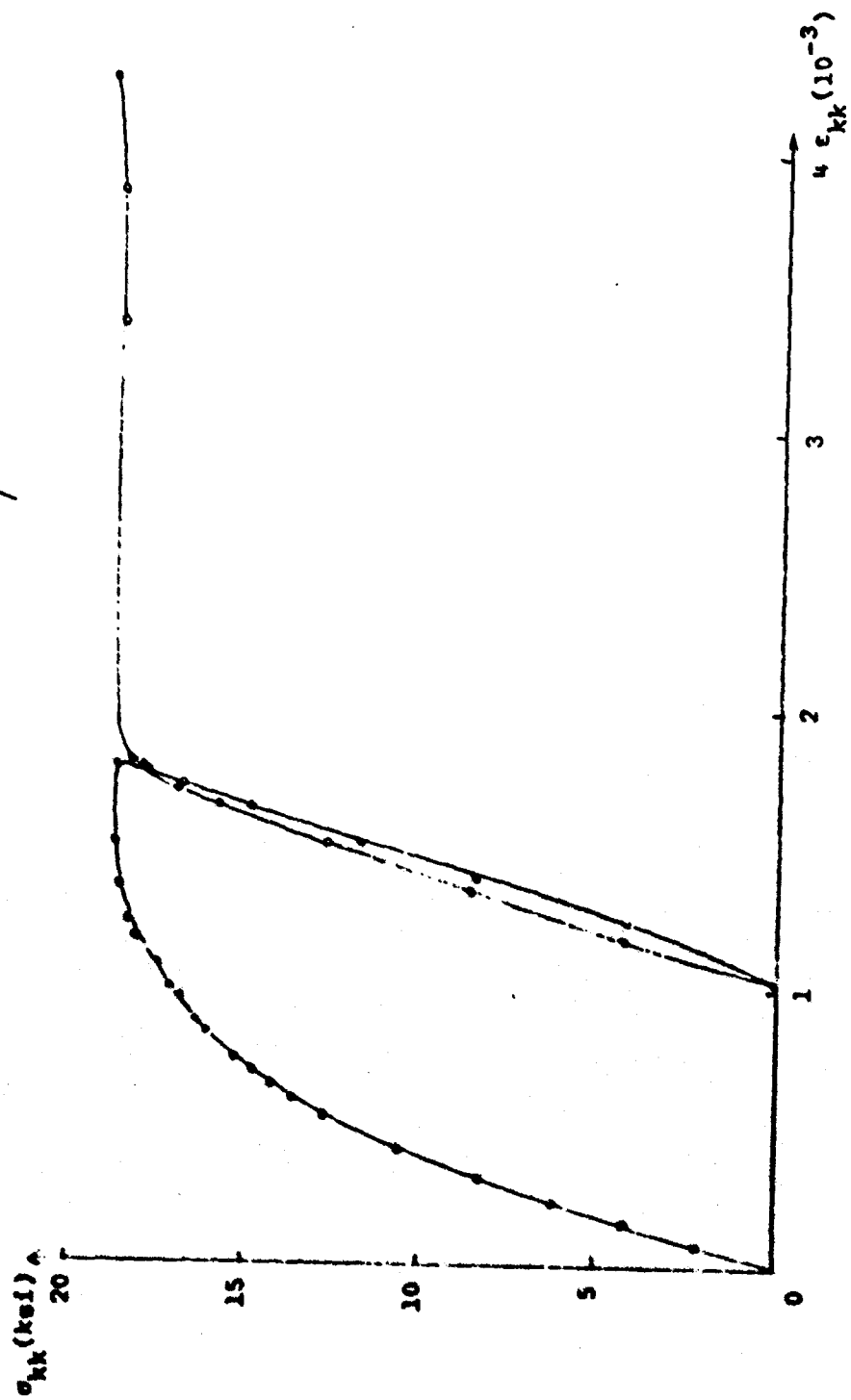


Figure 11 Hydrostatic stress ( $\times 3$ ) versus volumetric strain for aluminum specimen #5

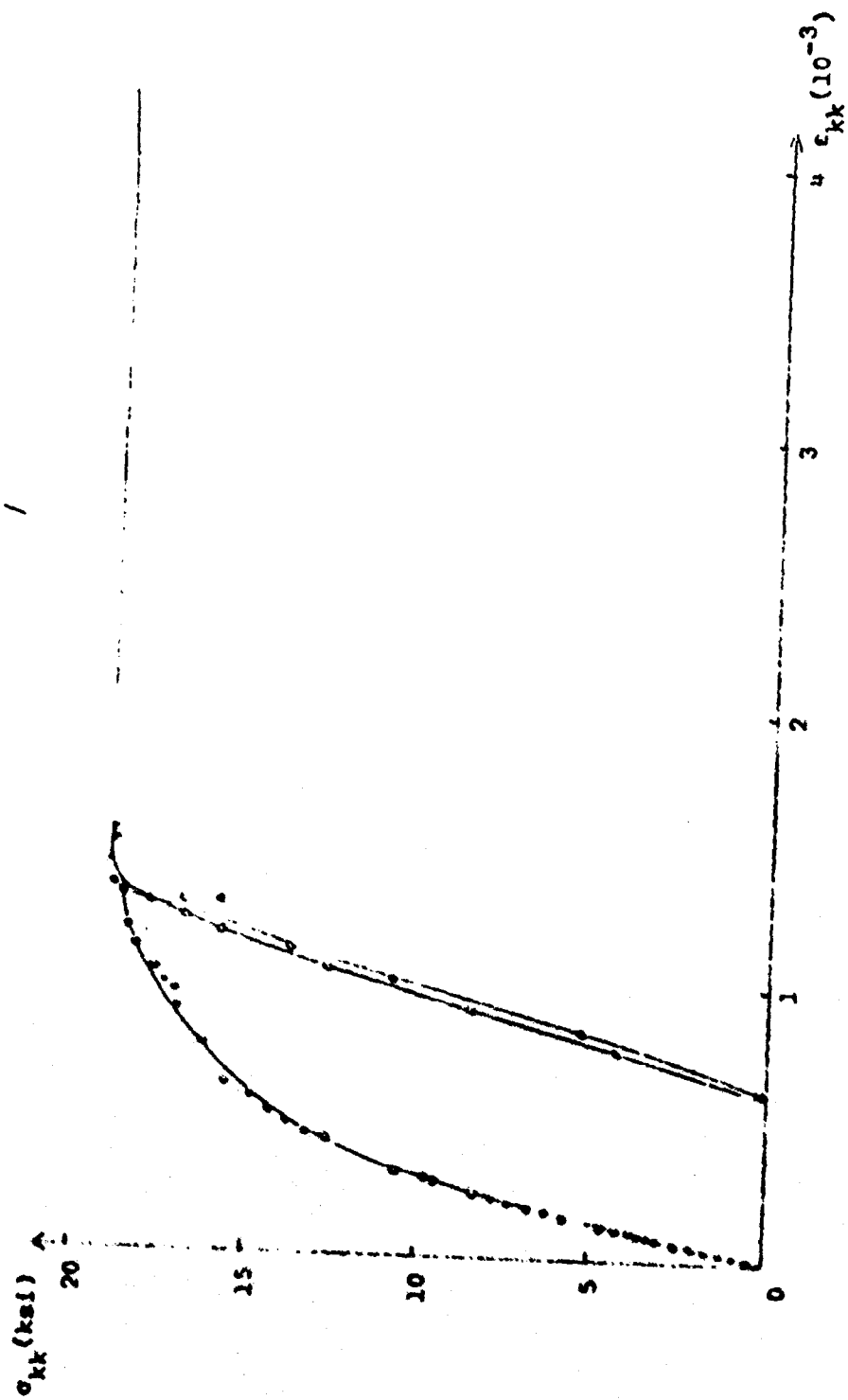


Figure 12 Hydrostatic stress ( $\times 3$ ) versus volumetric strain for aluminum specimen #6

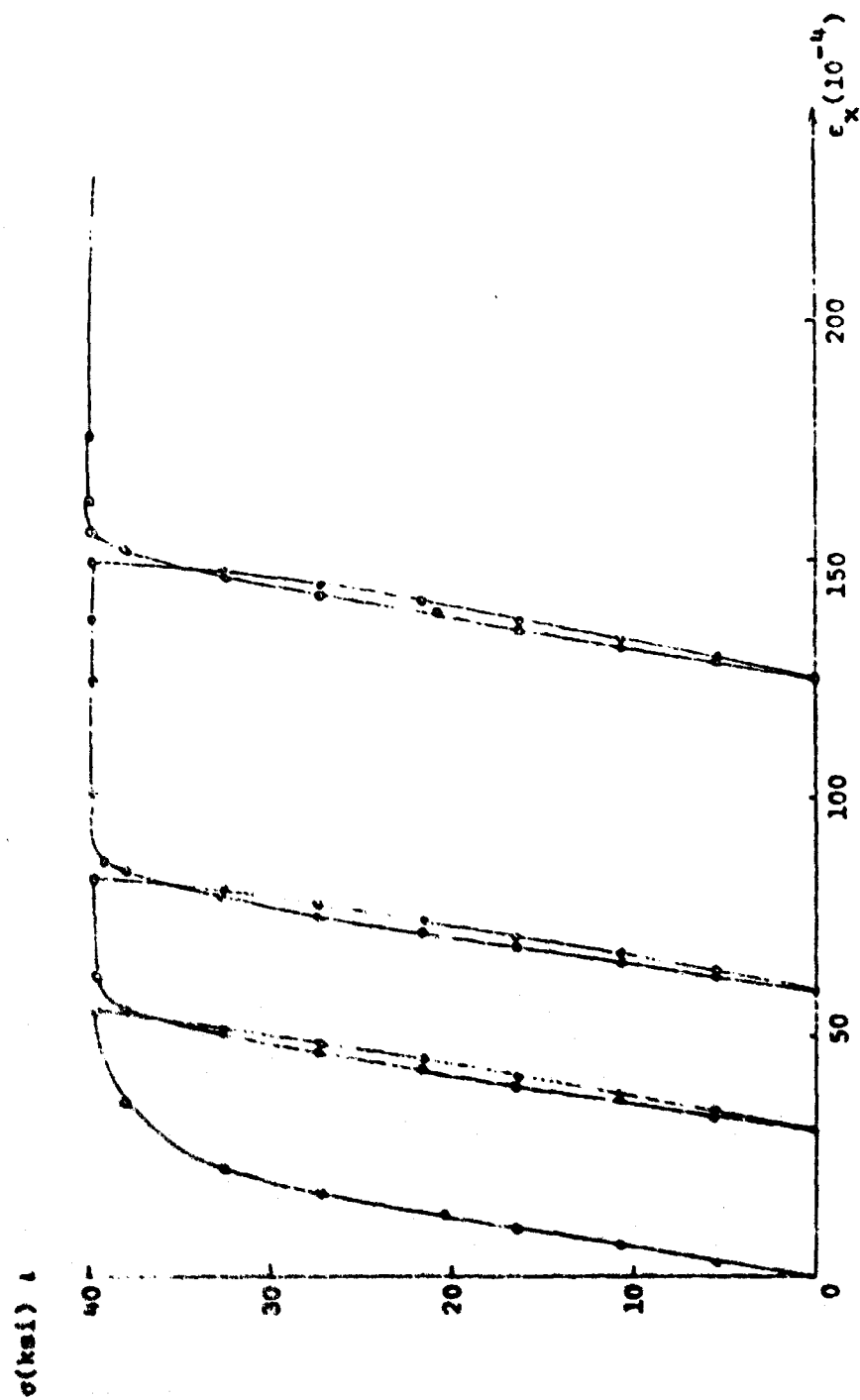


Figure 13 The loading-unloading curve for copper specimen #1

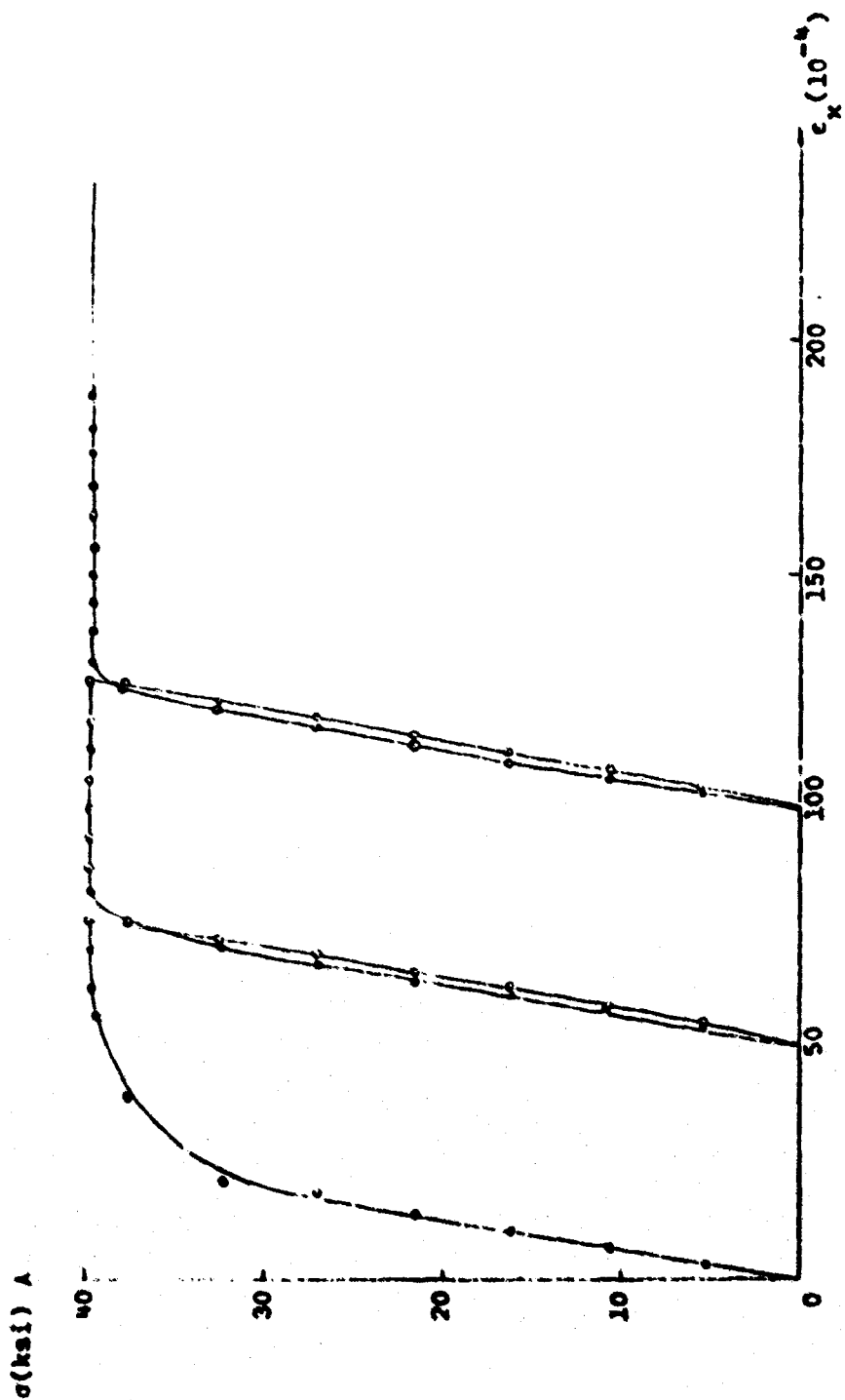


Figure 14. The loading-unloading curve for copper specimen #2

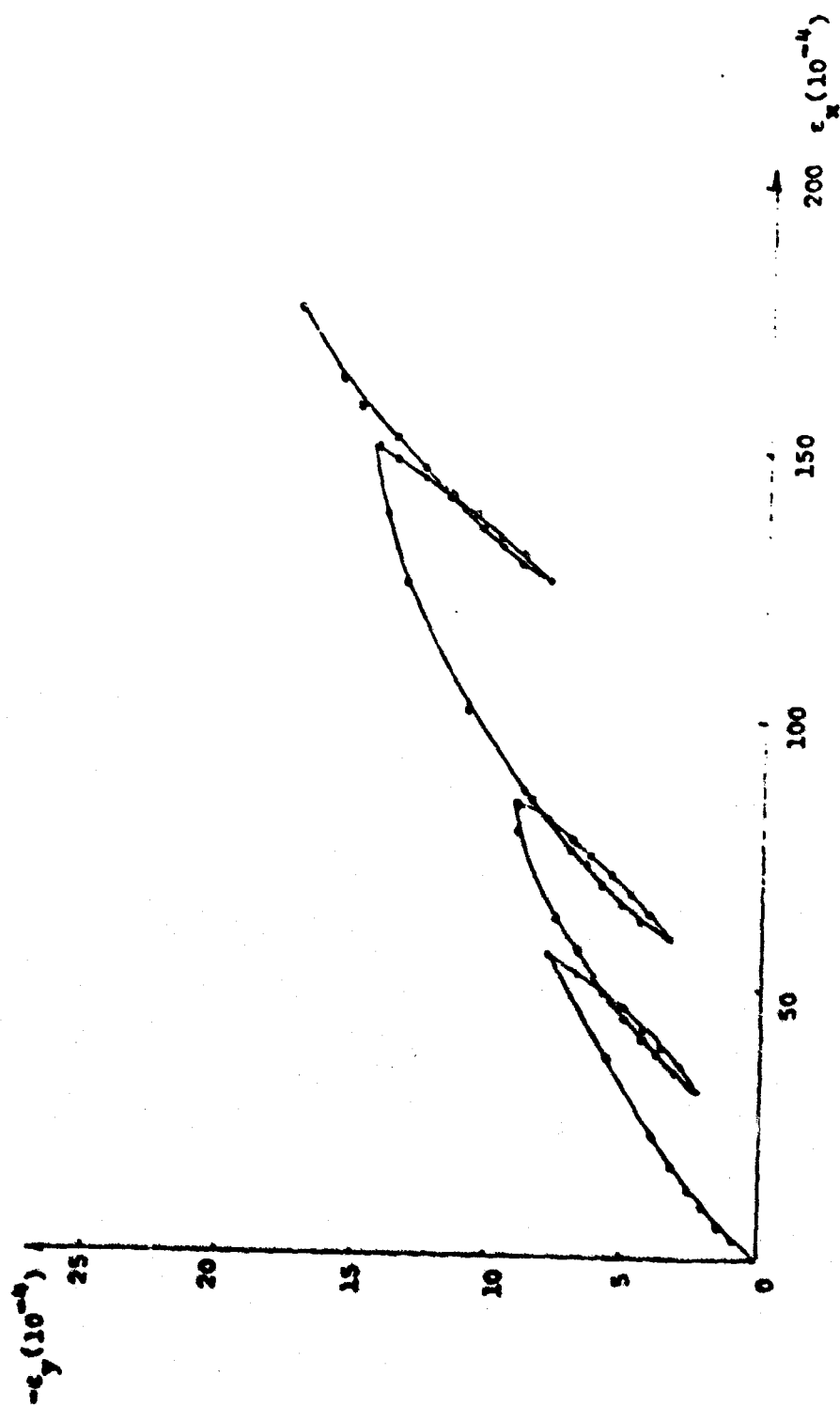


Figure 15. Relation between transverse and longitudinal strain for copper specimen #1

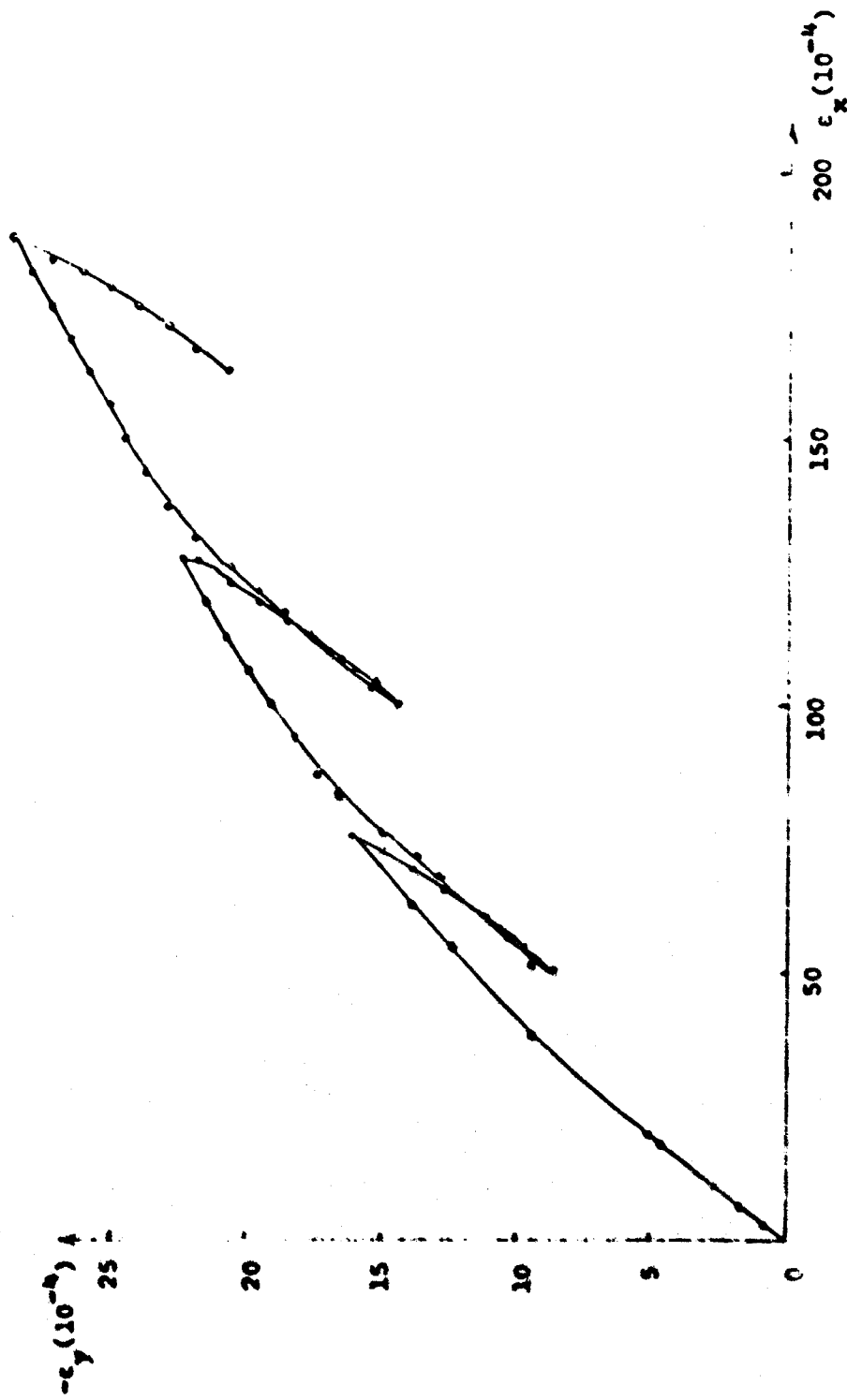


Figure 16. Relation between transverse and longitudinal strain for copper specimen #2

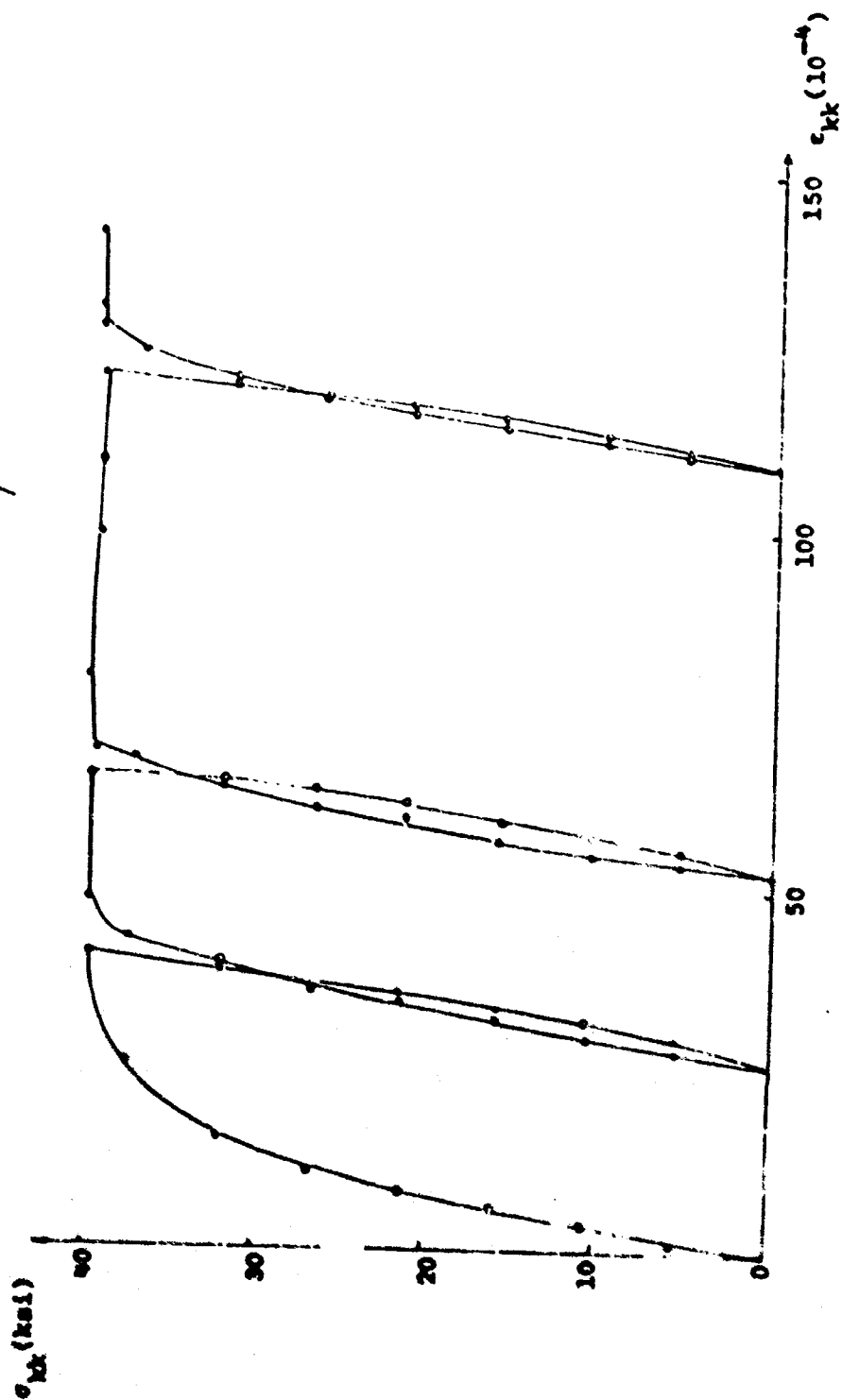


Figure 17 Hydrostatic stress ( $\times 3$ ) versus volumetric strain for copper specimen #1



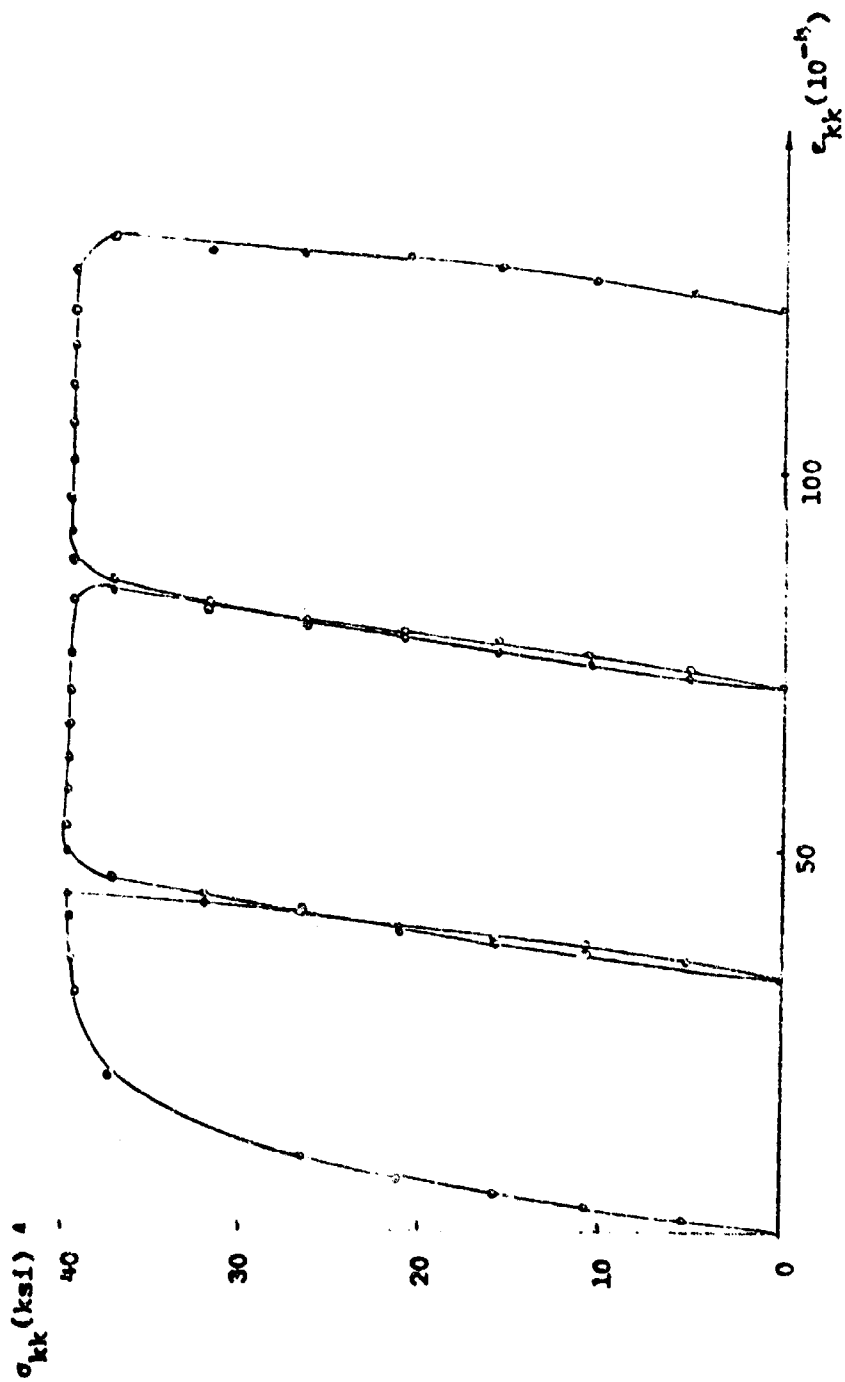


Figure 18 Hydrostatic stress ( $\times 3$ ) versus volumetric strain for copper specimen #2

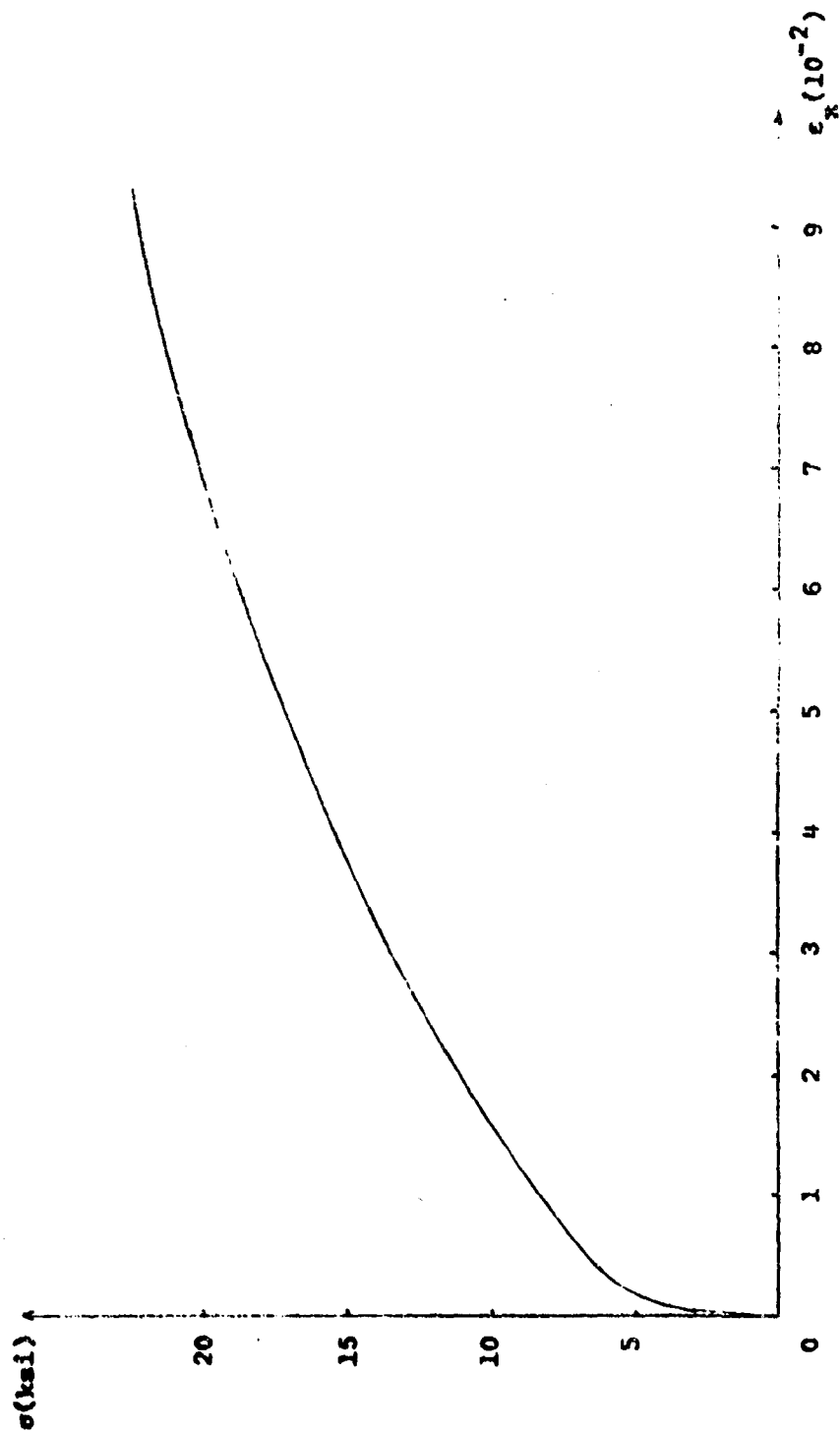


Figure 19 The stress-strain  
curve for copper of group II

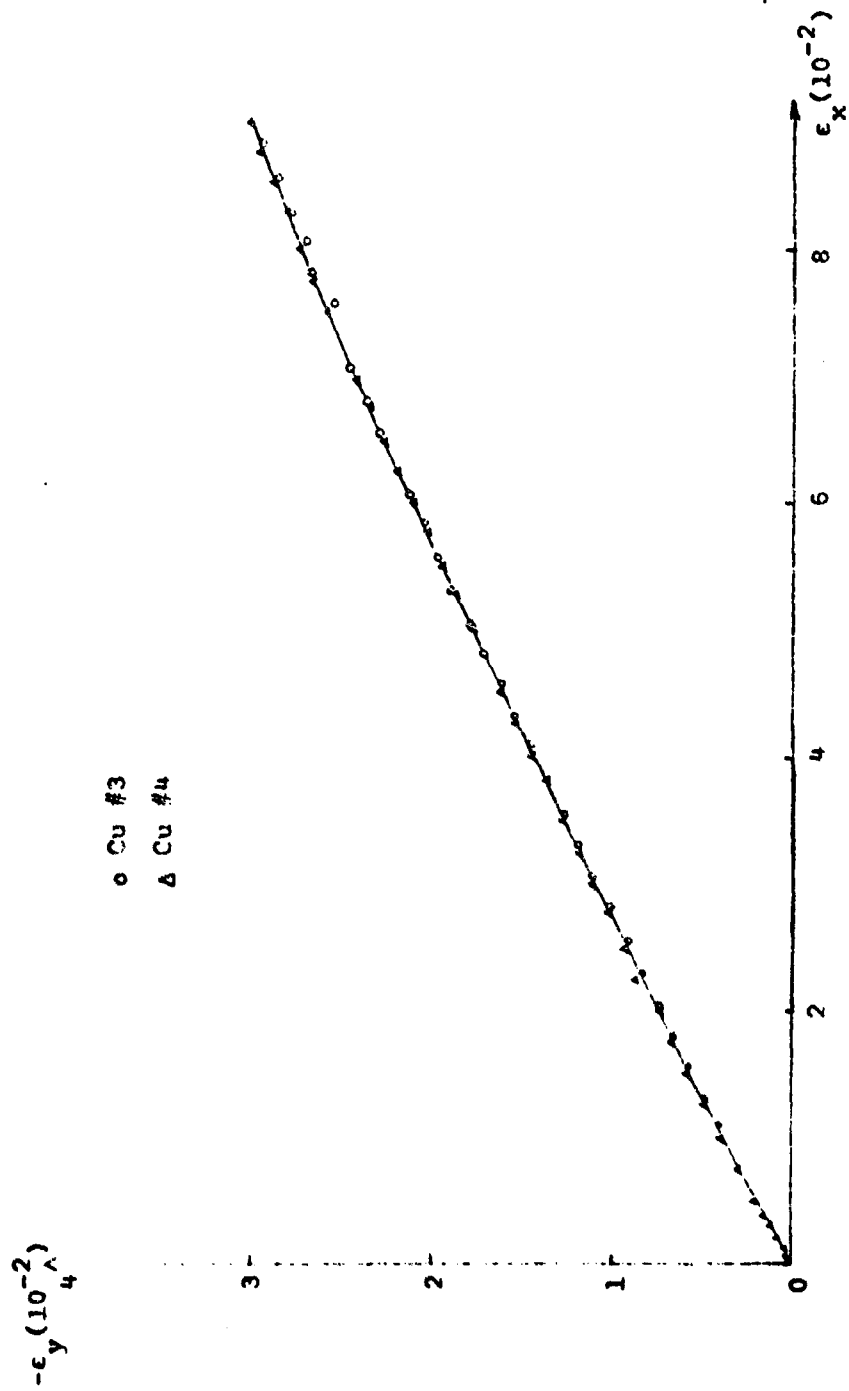


Figure 20 Relation between transverse and longitudinal strain for copper of group II

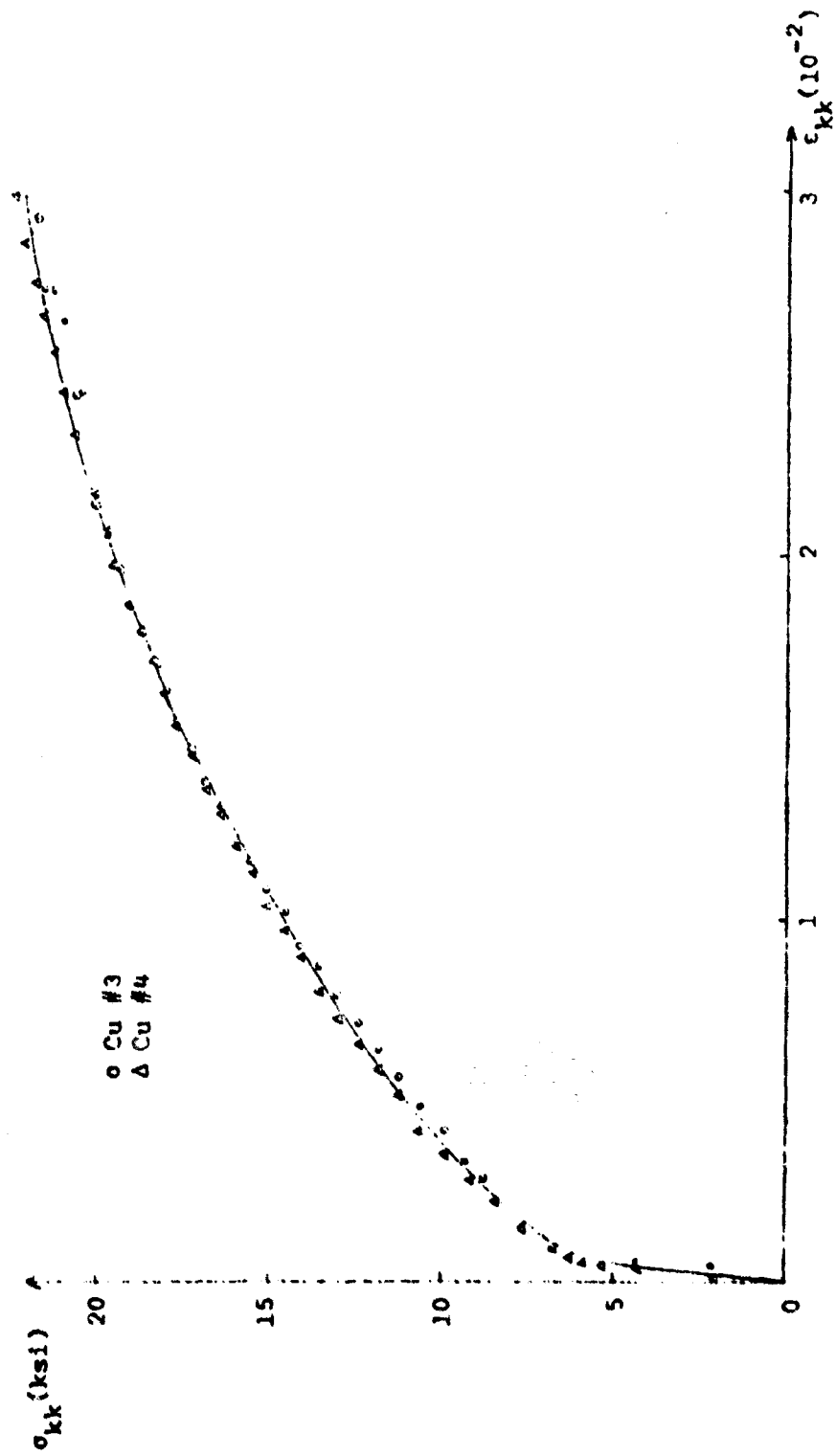


Figure 21. Hydrostatic stress ( $\times 3$ ) versus volumetric strain for copper of group II

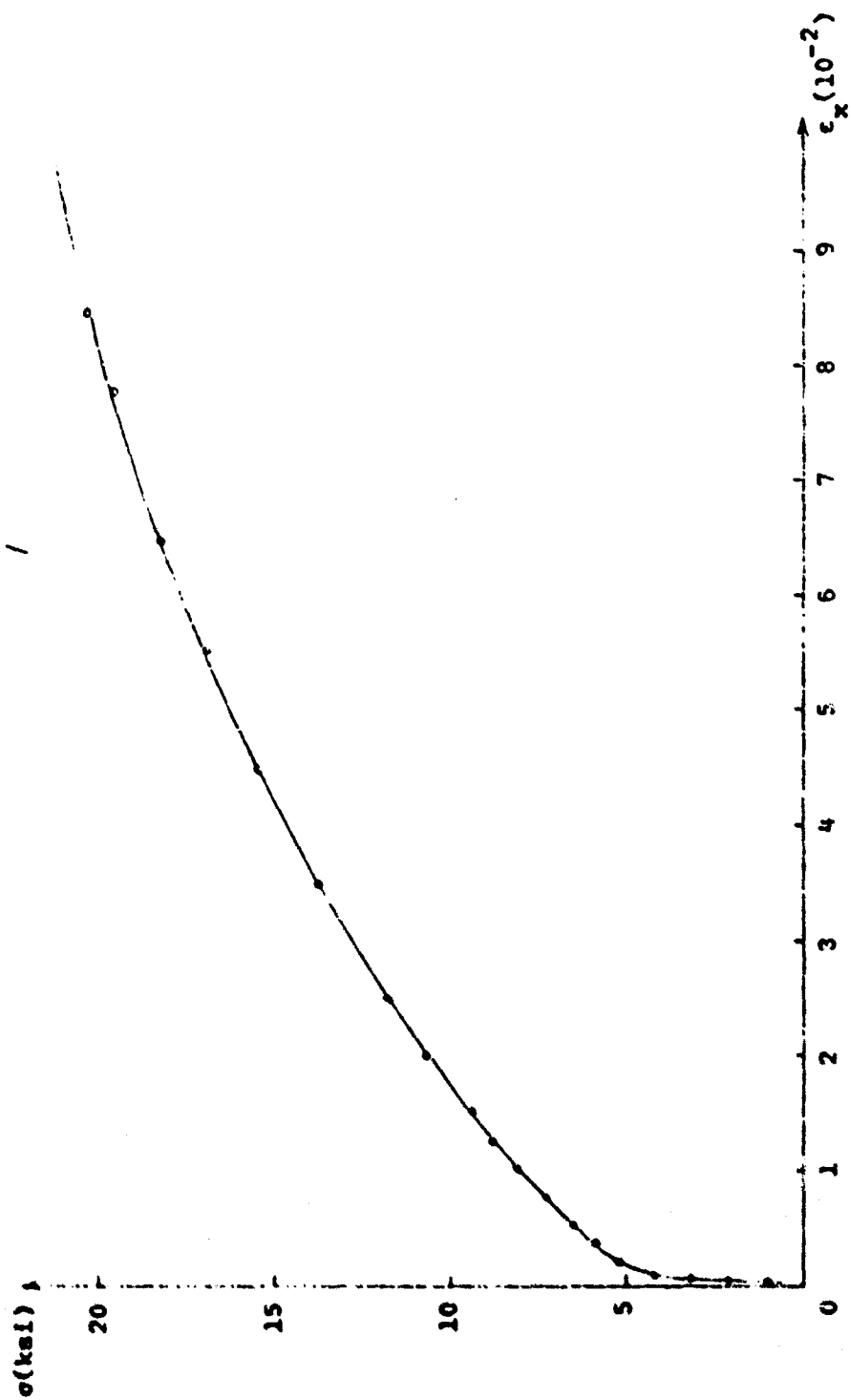


Figure 22 The stress-strain curve for copper of group III

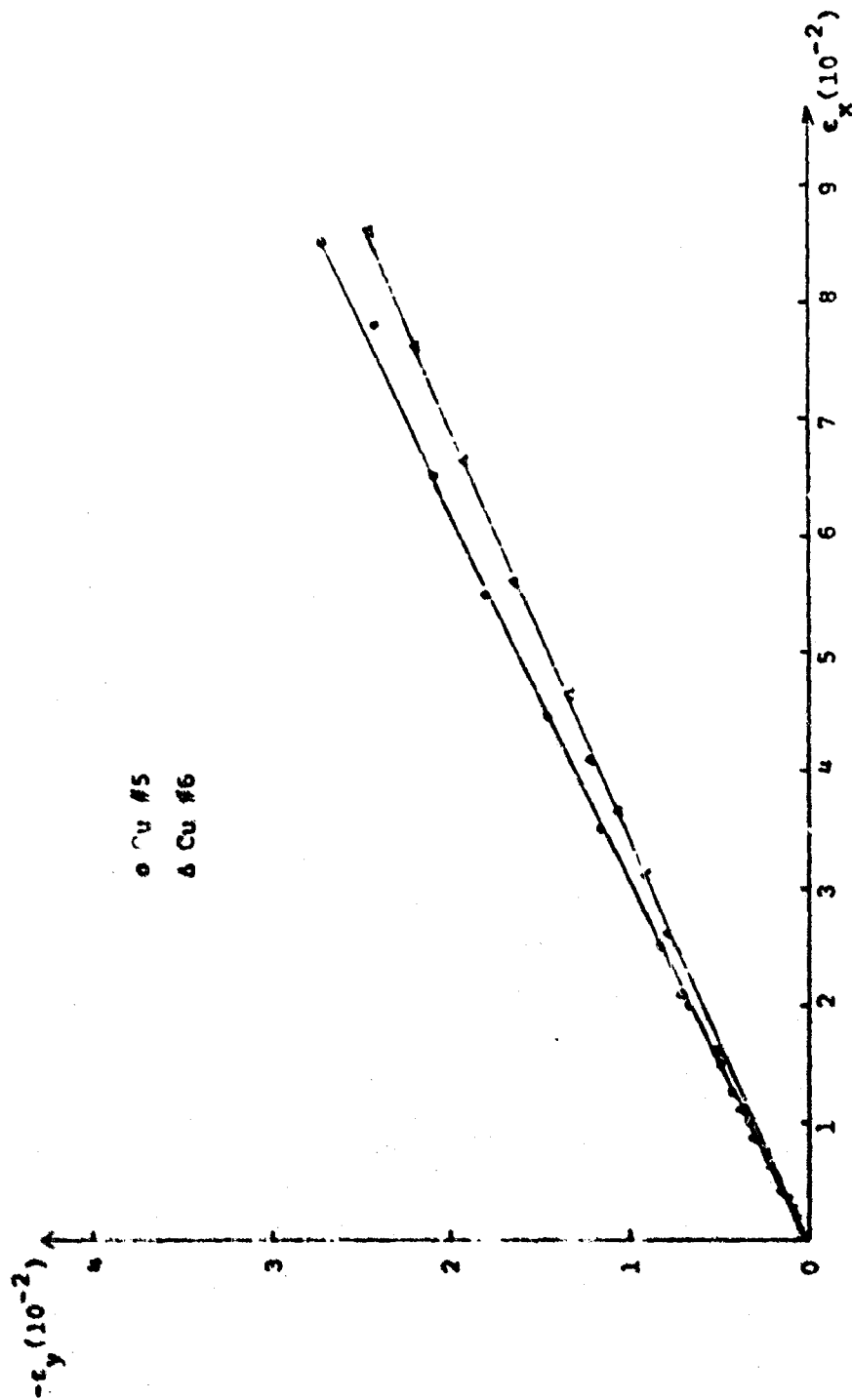


Figure 23 Relation between transverse and longitudinal strain for copper of group III

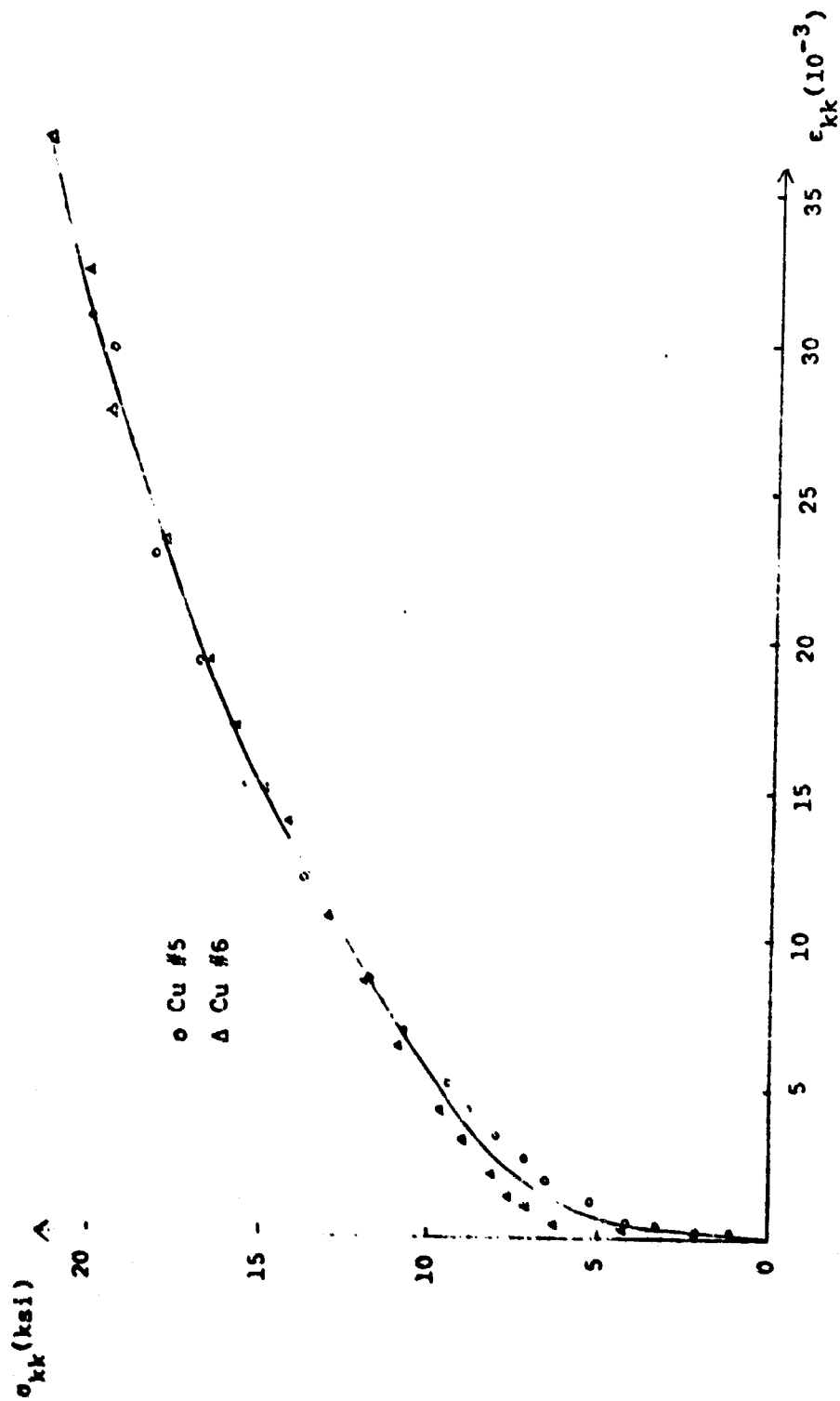


Figure 24 Hydrostatic stress ( $\times 3$ ) versus volumetric strain for copper of group III

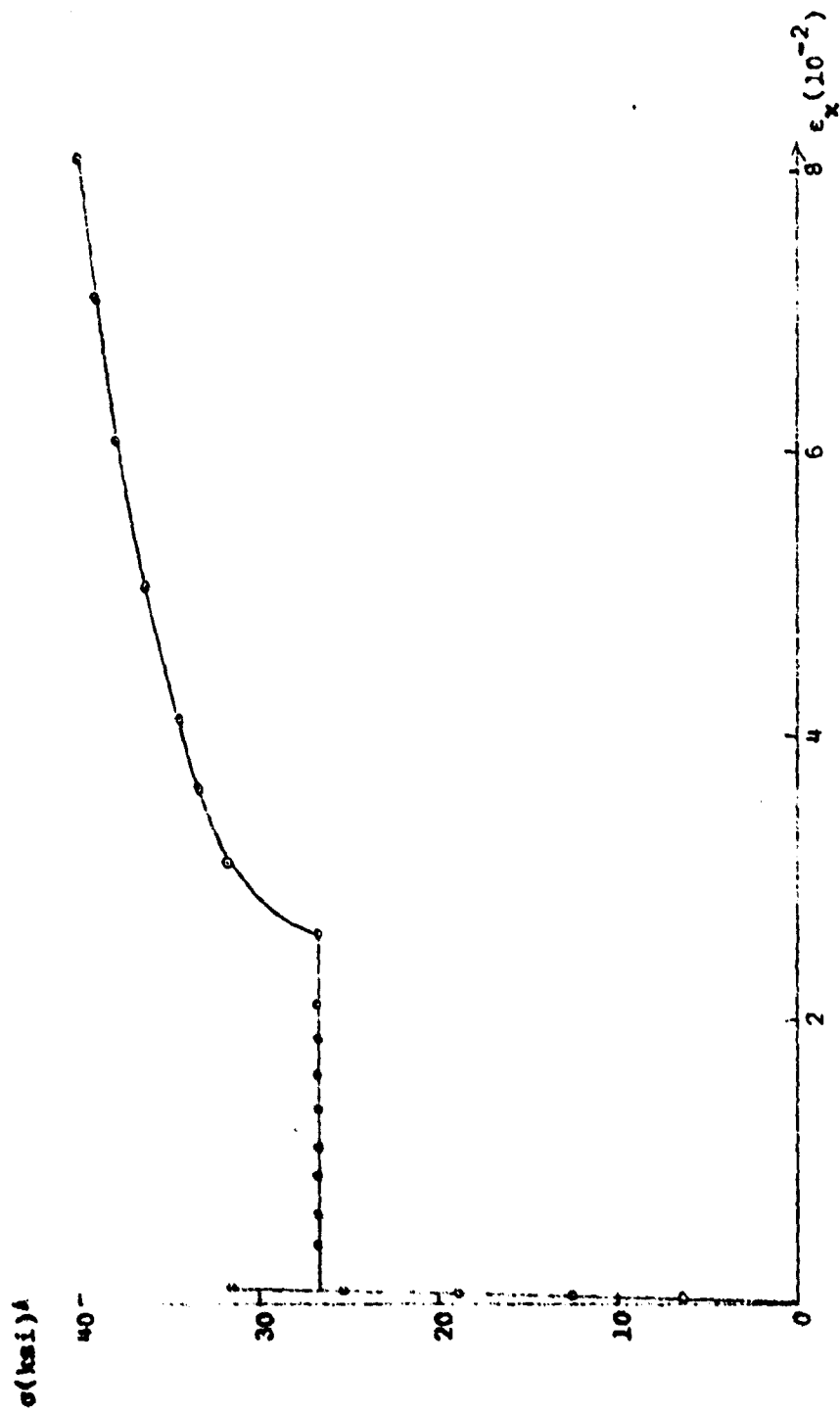


Figure 25 A typical stress-strain curve for low-carbon steel



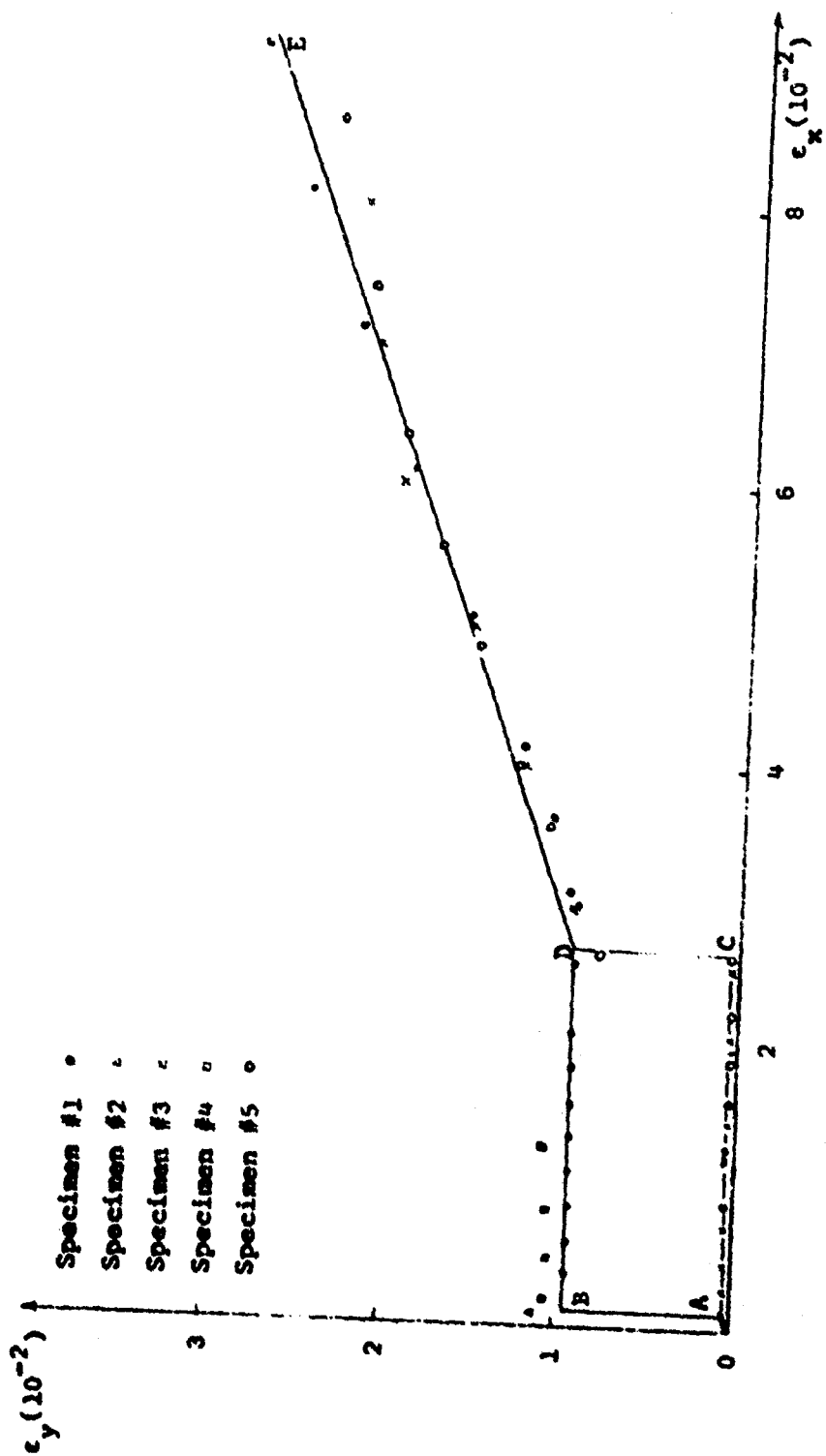


Figure 26 Relation between transverse and longitudinal strain for low-carbon steel

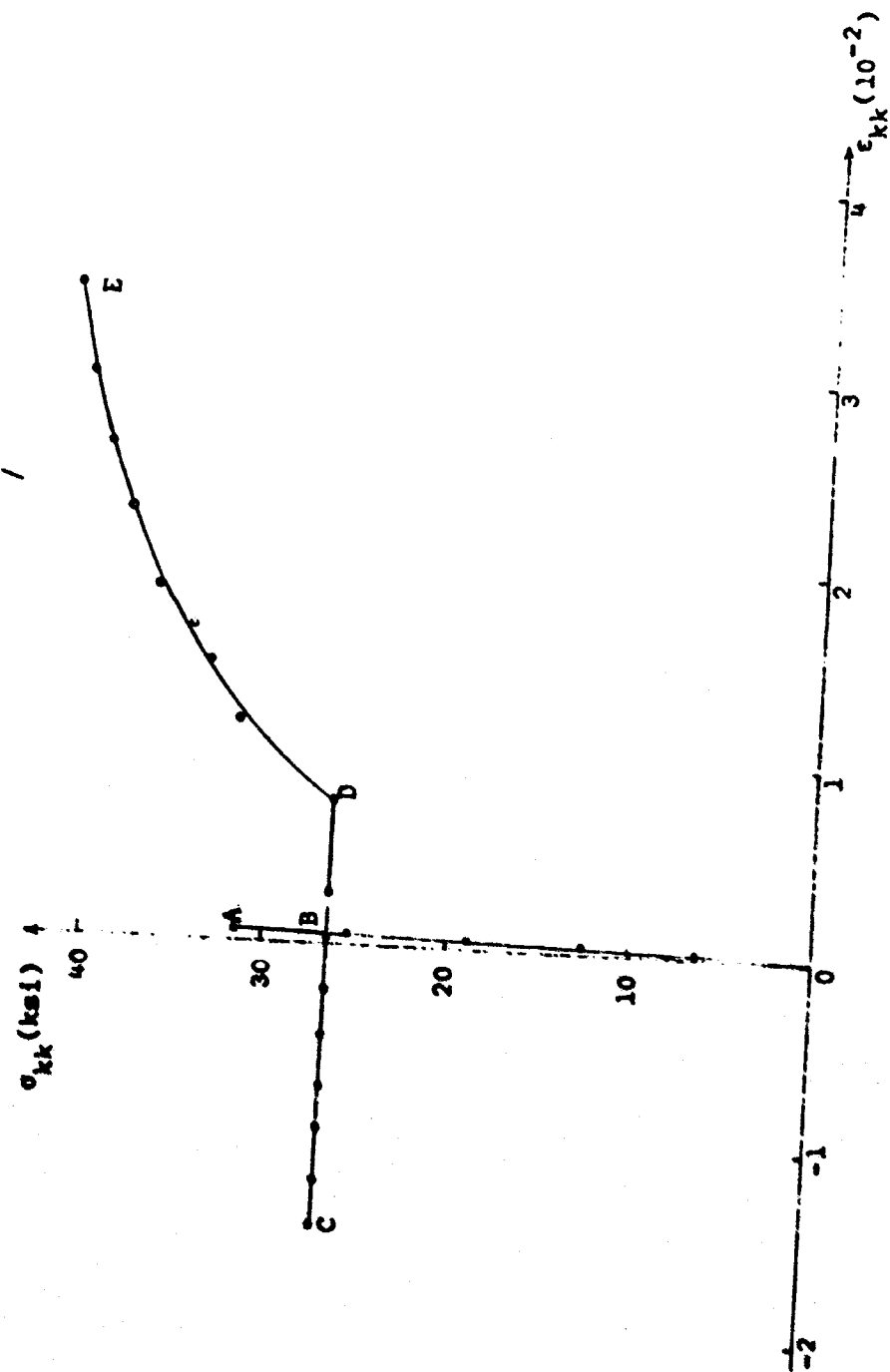


Figure 27 Hydrostatic stress ( $\times 3$ ) versus volumetric strain for steel specimen #1

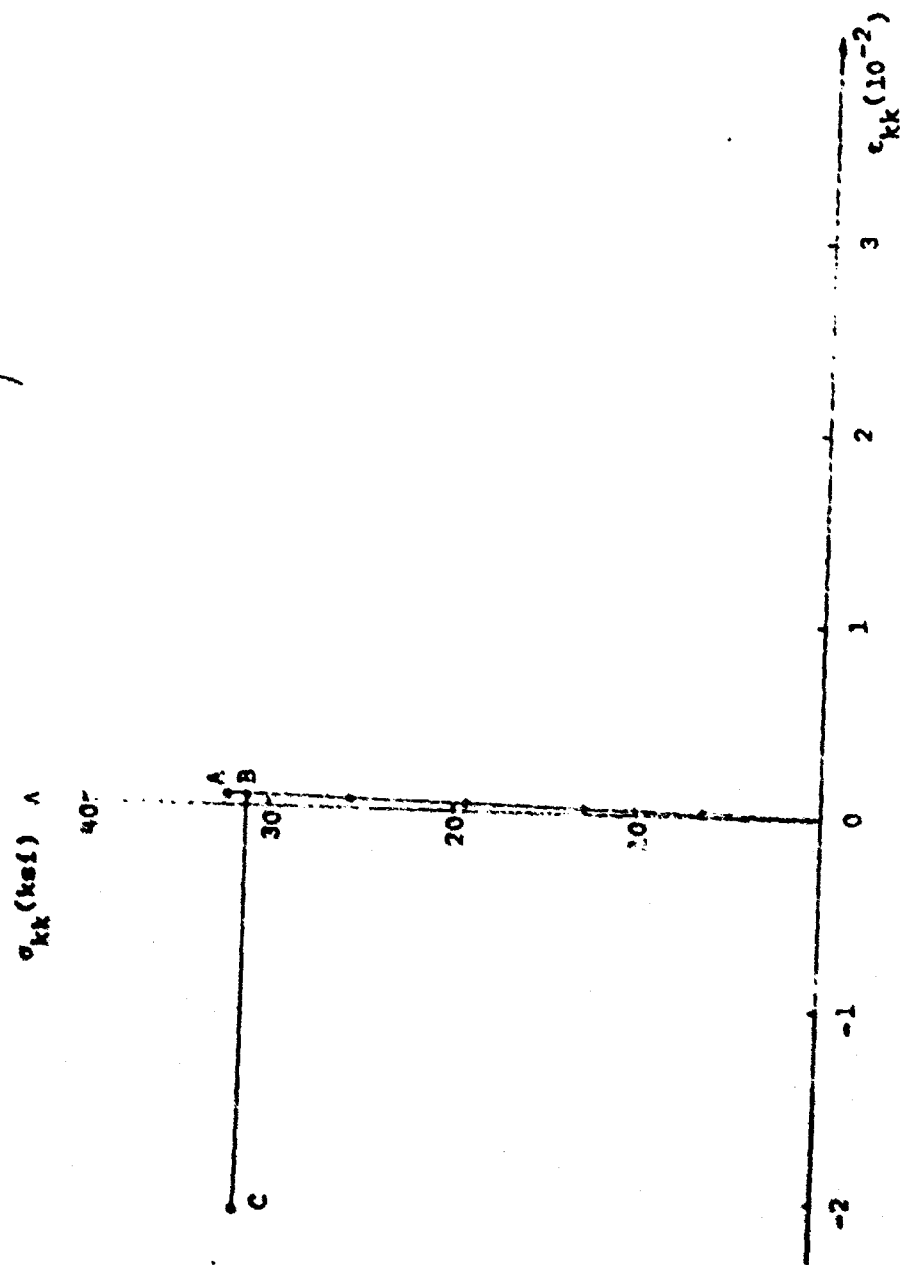


Figure 28 Hydrostatic stress ( $\times 3$ ) versus volumetric strain for steel specimen #2

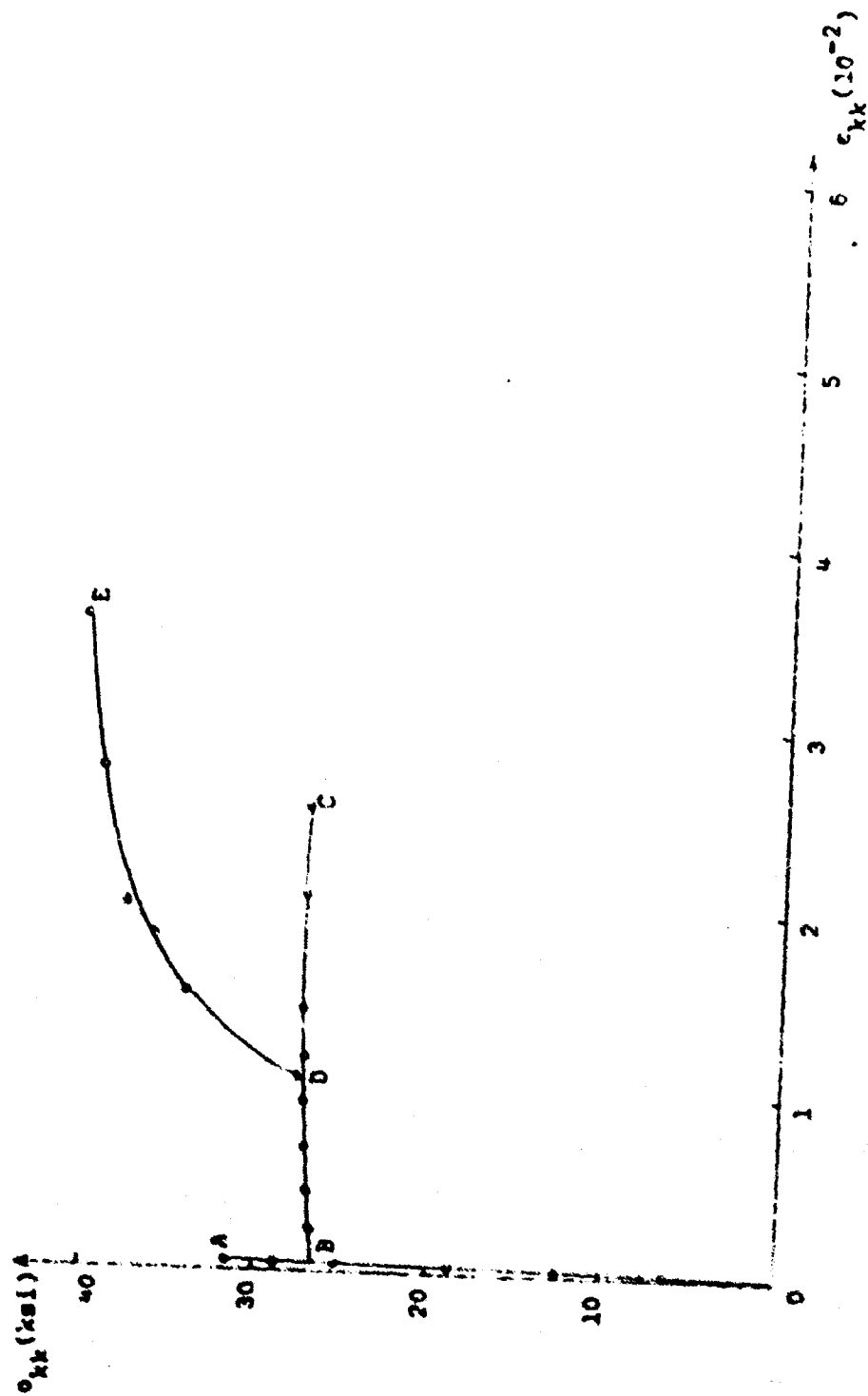


Figure 29 Hydrostatic stress ( $\times 3$ ) versus volumetric strain for steel specimen #3

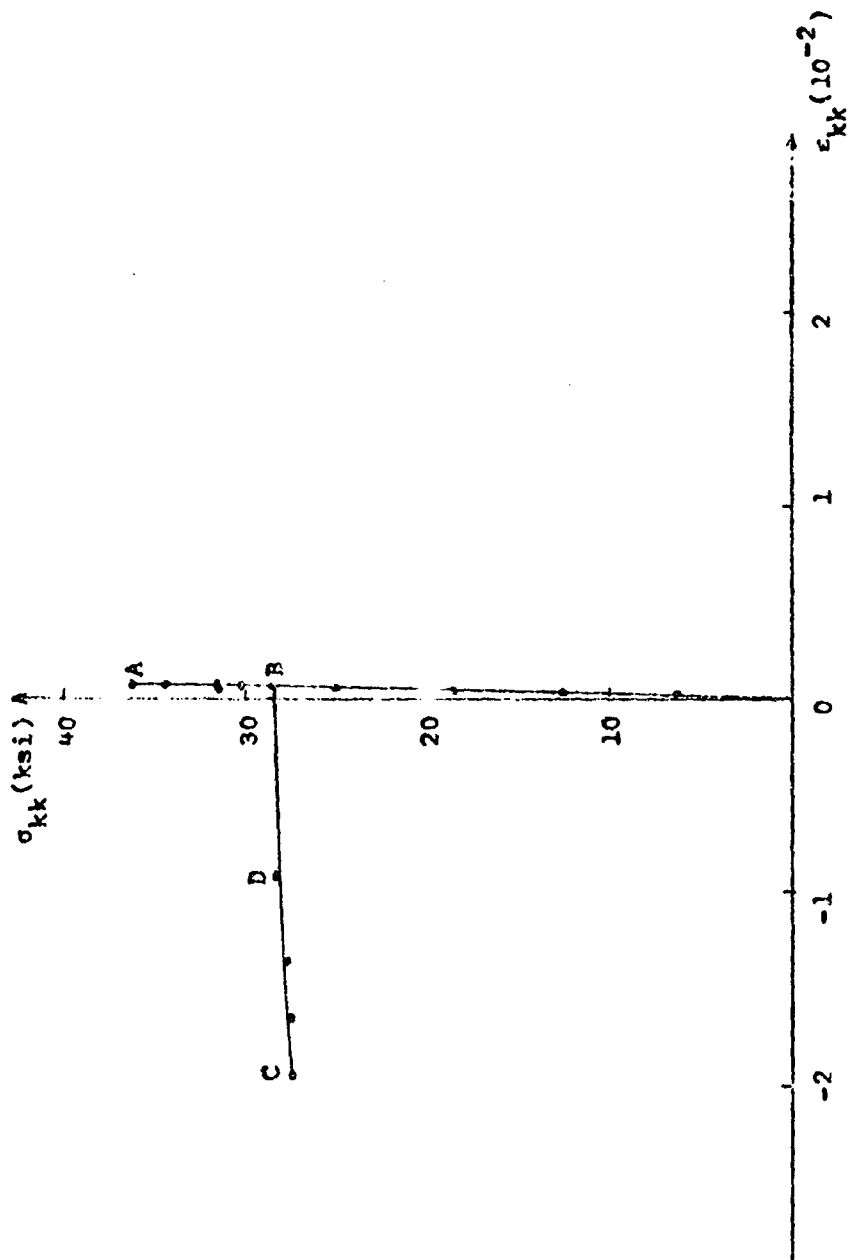


Figure 30 Hydrostatic stress ( $\times 3$ ) versus  
volumetric strain for steel specimen #4

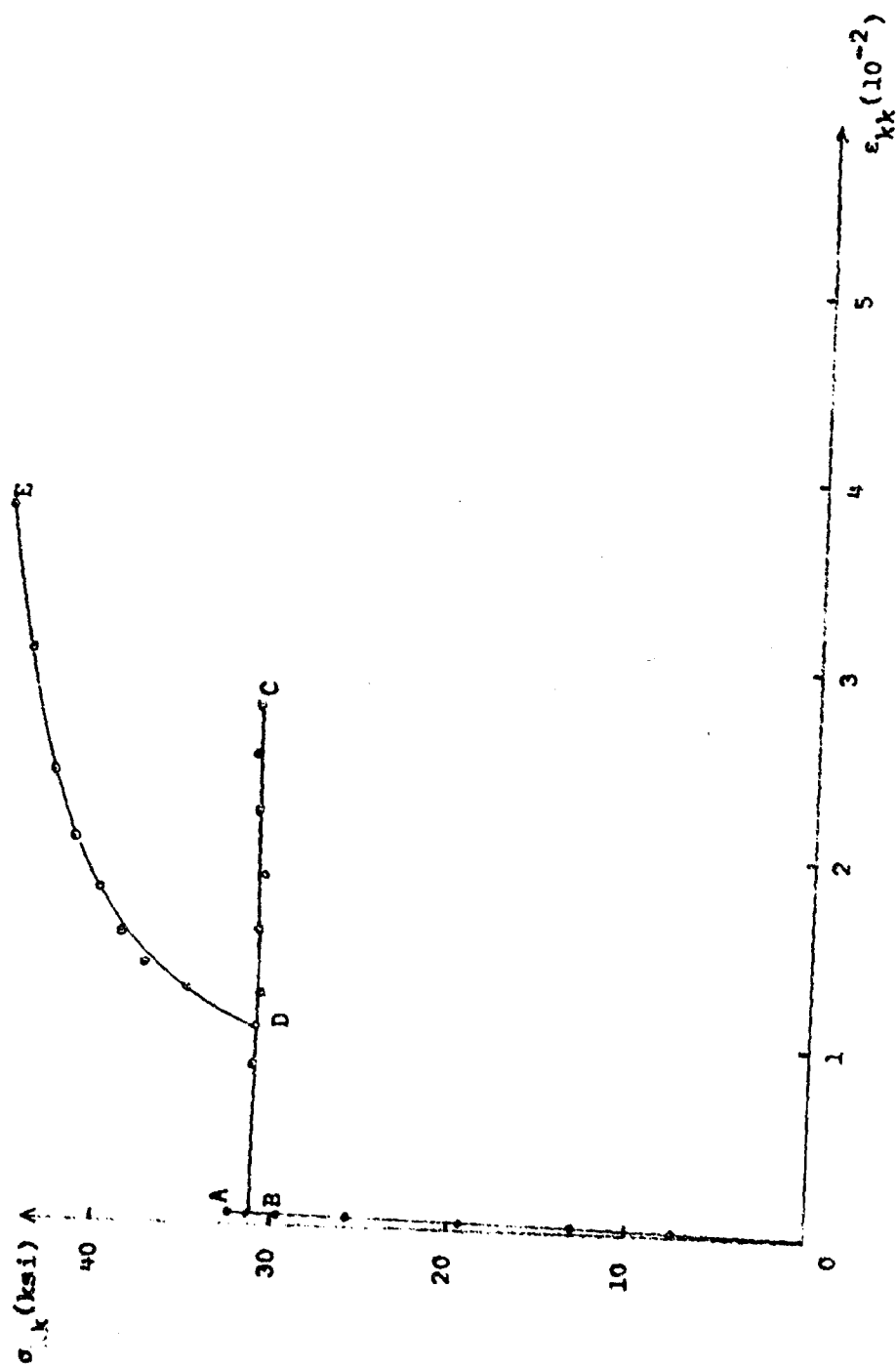


Figure 31 Hydrostatic stress ( $\times 3$ ) versus volumetric strain for steel specimen #5

Heredity Functions of the Endochronic  
Theory of Plasticity  
for Copper and Aluminum

K. C. Valanis

Department of Chemistry and Chemical Engineering  
Stevens Institute of Technology  
Hoboken, New Jersey 07030

and

Han-Chin Wu

Department of Mechanics and Hydraulics  
University of Iowa  
Iowa City, Iowa

Research Sponsored by Air Force Office  
of Scientific Research, Office of Aerospace  
Research, United States Air Force, under  
AFSOR Grant, Nr. 70-1916

Heredity Functions of the Endochronic  
Theory of Plasticity  
for Copper and Aluminum

K. C. Valanis

Department of Chemistry and Chemical Engineering  
Stevens Institute of Technology  
Hoboken, New Jersey 07030

and

Han-Chin Wu

Department of Mechanics and Hydraulics  
University of Iowa  
Iowa City, Iowa

Abstract

The endochronic theory of plasticity, developed previously by the first author, has been shown to give an accurate prediction of metallic response in the plastic range. The mechanical behavior of an isotropic material is given in terms of two "heredity" functions similar to those encountered in the theory of linear viscoelasticity. In the present paper the "tensile" and "transverse" heredity functions of copper and aluminum are determined experimentally using the above theory. The properties of these functions are also discussed.



## 1. Introduction

The recently proposed "endochronic theory of plasticity" has been shown to give accurate analytical predictions to a variety of experimental observations on metals such as copper and aluminum<sup>(1)</sup>. This theory differs from previous theories in that a yield surface is not necessary for the development of the constitutive equations and that the stress (under isothermal conditions) is determined by the previous deformation history defined on a time scale which is independent of the real time, but is itself a property of the material at hand.

In a previous paper<sup>(1)</sup> it was shown that diverse phenomena such as cross-hardening\*, loading-unloading loops, cyclic hardening and effects of prestress, can be described quantitatively and accurately with a single constitutive equation.

Specifically, this equation has the following form for small deformation and initially isotropic materials:

$$\sigma_{ij} = \delta_{ij} \int_0^z \lambda(z-z') \frac{\partial \epsilon_{kk}}{\partial z'} dz' + 2 \int_0^z \mu(z-z') \frac{\partial \epsilon_{ij}}{\partial z'} dz' \quad (1.1)$$

where

$$\lambda(z) = \lambda_\infty + \sum_{r=1}^n \lambda_r e^{-\rho_r z} \quad (1.2)$$

$$\mu(z) = \mu_\infty + \sum_{r=1}^n \mu_r e^{-\alpha_r z}$$

where  $\lambda_\infty$ ,  $\lambda_r$ ,  $\mu_\infty$ ,  $\mu_r$ ,  $\rho_r$  and  $\alpha_r$  are positive constants and

$$z=z(\zeta) ; \frac{dz}{d\zeta} > 0, \quad z > 0. \quad (1.4a,b)$$

\* This term means a change in the uniaxial stress-strain relation due to a torsional prestrain or vice-versa.

The symbol  $z$  denotes a positive monotonically increasing time scale with respect to a time measure  $d\zeta$  such that

$$d\zeta^2 = P_{ijkl} d\epsilon_{ij} d\epsilon_{kl} \quad (1.5)$$

where  $P_{ijkl}$  is a material tensor, which is positive definite and which, for the isotropic materials envisioned in Eq. (1.1), has the form

$$P_{ijkl} = k_1 \delta_{ij} \delta_{kl} + k_2 \delta_{ik} \delta_{jl} \quad (1.6)$$

where  $k_1$  and  $k_2$  are material parameters, such that  $k_1 + \frac{k_2}{3} > 0$ ,  $k_2 > 0$ .

Materials described by Eq. (1.1) are strain history dependent but strain-rate independent. The derivation of constitutive equation (1.1) was given in detail in Ref. 1.

It may be seen that eq. (1.1) is uniquely described by means of two material "heredity functions",  $\lambda(z)$  and  $\mu(z)$ . However, eq. (1.1) may be described instead in terms of the function  $\mu(z)$  and  $K(z)$ , the "shear and bulk heredity functions", respectively. Specifically:

$$s_{ij} = \int_0^z \mu(z-z') \frac{\partial e_{ij}}{\partial z'} dz' \quad (1.7a)$$

$$\sigma_{kk} = 3 \int_0^z K(z-z') \frac{\partial \epsilon_{kk}}{\partial z'} dz \quad (1.7b)$$

and  $s_{ij}$  and  $e_{ij}$  are the stress and strain deviators. The functions  $\lambda(z)$ ,  $\mu(z)$  and  $K(z)$  are related as follows:

$$K(z) = \lambda(z) + \frac{2}{3} \mu(z) \quad (1.8)$$

From an experimental viewpoint it is more convenient to relate  $\delta_{ij}(z)$  and  $\epsilon_{ij}(z)$  to the functions  $E(z)$  and  $\nu(z)$ , which we shall call the "tensile" and "transverse" heredity functions. This relationship is:

$$\int_0^z E(z-z') \frac{\partial \epsilon_{ij}}{\partial z'} dz' = \sigma_{ij} + \int_0^z v(z-z') \frac{\partial \sigma_{ij}}{\partial z'} dz' - \delta_{ij} \quad (1.9)$$

$$\int_0^z v(z-z') \frac{\partial \sigma_{kk}}{\partial z'} dz'$$

The functions  $E(z)$  and  $v(z)$  are related to the previous functions through their Laplace transforms as follows:

$$p\bar{v} = \frac{1}{2} - \frac{1}{6} \frac{\bar{E}}{\bar{K}} \quad (1.10)$$

$$\bar{E} = \frac{3\bar{\mu}}{1 + \frac{\bar{\mu}}{3\bar{K}}} \quad (1.11)$$

where a bar over a function denotes its Laplace transform with respect to the parameter  $p$ .

In the present paper we present forms of the functions  $E(z)$ ,  $v(z)$  that have been determined experimentally in the case of copper and aluminum; these will be discussed in later sections. The experimental measurements necessary to determine the above functions were also used to evaluate critically the implications of the assumption of plastic incompressibility, normally made in the classical theory of plasticity. These experiments are reported in detail in Ref. 2.

As is well known, this assumption leads to the result that Poisson's ratio tends to  $\frac{1}{2}$  as the plastic strain\* increases. Our experimental results do not support this conclusion. In the classical theory of plasticity, plastic incompressibility has also been interpreted to mean that the hydrostatic stress

---

\* The term "plastic strain" is used in the content of the classical theory of plasticity. The endochronic theory does not recognize the dichotomy of strain into elastic and plastic parts.

is a linear function of the hydrostatic strain; our experimental data do not support this either.

Of course in its broader aspect, plastic incompressibility may imply a reversible, though non-linear, volumetric response. However, the observed volumetric response was decidedly irreversible. Consequently our experimental measurements do not support the assumption of plastic incompressibility, at least when the hydrostatic stress is of tensile character. (A non-linear irreversible volumetric response in simple compression has also been reported in the literature by Bridgman<sup>(3)</sup>.)

It is significant that the endochronic theory can predict plastic compressibility, exactly, provided that the heredity function  $K(z)$  is chosen appropriately, or is determined experimentally.

## 2. Experimental determination of the heredity functions.

In the case of the simple tension test eq. (1.9) reduces to the following two eq.'s:

$$\sigma_x = \int_0^z E(z-z') \frac{\partial \epsilon_x}{\partial z'} dz' \quad (2.1)$$

$$-\epsilon_y = \int_0^z \nu(z-z') \frac{\partial \epsilon_x}{\partial z'} dz' \quad (2.2)$$

In Ref. 1, the time scale  $z$  was related to the intrinsic time  $\zeta$  by the equation

$$z = \frac{1}{\beta} \log (1 + \beta \zeta) \quad (2.3)$$

which proved very satisfactory in providing agreement between the theory and a variety of experiments as discussed in the Introduction. For this reason eq. (2.3) will be retained in this paper.

As a result of eq.'s (1.5) and (1.6)

$$d\zeta^2 = k_1^2 (d\epsilon_x + 2\epsilon_y)^2 + k_2^2 (d\epsilon_x^2 + 2d\epsilon_y^2) \quad (2.4)$$

Because  $k_1$  and  $k_2$  are not known and to illustrate the methodology of the theory, we have taken  $k_1 = 0$ . In this event

$$d\zeta = k_2 \left\{ 1 + 2 \left( \frac{d\epsilon_y}{d\epsilon_x} \right)^2 \right\}^{1/2} d\epsilon_x \quad (2.5)$$

If, in addition, an experimental relation between  $\sigma_x$  and  $\epsilon_x$  as well as between  $\epsilon_y$  and  $\epsilon_x$  were known, then from eq.'s (2.3) and (2.5)  $\epsilon_x$  would be a known function of  $z$ , in which case  $\sigma_x$  and  $\epsilon_y$  would also be known functions of  $z$ .

Equations (2.1) and (2.2), which are Volterra integral equations, would then be solved to yield the functional form of the kernels (heredity functions)  $E(z)$  and  $v(z)$ .

In the particular case where  $\epsilon_x$  is a linear function of  $z$  (experiments show that this is a very good approximation as will be shown later) eq.'s (2.1) and (2.2) can be solved exactly to yield the relations:

$$E(z) = h \left\{ \frac{d\sigma}{dz} - \beta\sigma(z) \right\} \quad (2.6)$$

$$-v(z) = h \left\{ \frac{d\epsilon_y}{dz} - \beta\epsilon_y(z) \right\} \quad (2.7)$$

where

$$dz = h d\epsilon_x \quad (2.8)$$

and

$$h = k_2 \left\{ 1 + 2 \left( \frac{d\epsilon_y}{d\epsilon_x} \right)^2 \right\}^{1/2} \quad (2.8a)$$

In Ref. 2 we presented experimentally obtained uniaxial stress-strain curves for a large number of copper and aluminum specimens\*. We also presented experimental curves showing the relation between  $\epsilon_y$  and  $\epsilon_x$  for these same

\* Electrolytic tough pitch copper and commercially pure aluminum.

specimens. In Fig.'s 1-4 we show such typical curves<sup>\*\*</sup>.

Now, using the experimental curves of Fig.'s 3 and 4, eq. (2.5)  $\epsilon_x$  was determined as a function of  $\zeta$  for copper and aluminum and the curves of these functions are shown in Fig. 5, with  $k_2$  remaining undetermined. Similar curves were obtained for  $\epsilon_y$  as a function of  $\zeta$  and appear in Fig. 6.

One can see in Fig. 5 that the relation between  $\epsilon_x$  and  $\zeta$  is linear to a very good approximation for both copper and aluminum. Therefore, eq.'s (2.6) and (2.7) may be considered as approximate solutions of the Volterra integral equations (2.1) and (2.2) and may be used to determine the form of the heredity functions  $E(z)$  and  $v(z)$ . This was done as follows: Eq.'s (2.6) and (2.7) may be written in the alternative form:

$$E(z) = \frac{d\sigma}{d\epsilon} e^{\beta z} - h\beta\sigma(z) \quad (2.9)$$

$$-v(z) = \frac{d\epsilon_y}{d\epsilon_x} e^{\beta z} - h\beta\epsilon_y(z) \quad (2.10)$$

where now  $h$  is taken for consistency to be the mean value of the slope of the approximate linear relation between  $\epsilon_x$  and  $\zeta$ . Using eq.'s (2.9) and (2.10) and Fig.'s (1-4),  $E(z)$  and  $v(z)$  were calculated for copper and aluminum; these appear in Fig.'s 7-8 and 9-10 for various values of  $\beta$ .

#### Discussion of the heredity functions

(a) Copper: Two characteristics of the tensile heredity function  $E(z)$  merit discussion. In the region of small  $z$ ,  $E(z)$  exhibits a point of inflexion; this implies that the second derivative of  $E(z)$  changes sign at that point.

---

<sup>\*\*</sup> For copper specimen 4 and aluminum specimen 4 of Ref. 3.

This behavior is not predicted by the current form of the theory, according to which

$$E(z) = \sum_{r=1}^n E_r e^{-a_r z} \quad (2.11)$$

where  $E_r$  and  $a_r$  are positive constants. Evidently  $\frac{d^2 E}{dz^2}$ , as calculated from the above equation, is always positive. However, except for this small region in the vicinity of  $z=0$ , the experimental curve assumes a shape not unlike the one predicted by the eq. (2.11). On the other hand the form of the function  $E(z)$  does not appear to be particularly sensitive to changes in  $\beta$ , particularly at moderately small values of  $z$ .

The transverse heredity function  $v(z)$  decreases slowly as  $z$  increases but remains virtually constant (over the range of  $z$  shown) if  $\beta$  is small. Therefore, as far as copper is concerned the assumption of constant Poisson's ratio is true, to a very good approximation.

(b) Aluminum: The tensile heredity function for aluminum is very similar to that of copper. The transverse heredity function, however, exhibits a strikingly different behavior. At moderate strains it decreases from its initial value quite rapidly, until it becomes virtually zero; then, at higher strains it increases abruptly to a value which is three times the initial value. Then it decreases again and at still higher strains, it tends to a constant value, which is nearly equal to the initial value.

No physical explanation can be offered at this time for this behavior, which is certainly not due to necking of the specimen; quite definitely, necking did not occur in the range of deformation indicated in Fig. 8.

### 3. Material compressibility under hydrostatic tension

In this section we shall discuss the experimental measurements which led to the conclusion that the assumption of plastic incompressibility (normally made in the classical theories of plasticity) is not tenable.

The experiments, simple in nature, consisted in monitoring the axial stress as well as the axial strain and one transverse strain of a thin flat bar in uniform uniaxial tension<sup>\*</sup>. This simple test has enjoyed a great deal of popularity but we could find only one instance<sup>(4)</sup> where "transverse strain" measurements were made in the plastic range. This is surprising, since this test affords a very critical evaluation of the assumption of plastic incompressibility.

The classical plasticity theory yields the following result, assuming elastic compressibility and a Von Mises yield surface:

$$-\frac{d\epsilon_y}{d\epsilon_x} = \frac{1}{2} - \left(\frac{1}{2} - \nu_0\right) \frac{E_t}{E_0} \quad (3.1)$$

where  $\epsilon_x$  and  $\epsilon_y$  are the longitudinal and transverse strains respectively,  $E_0$  and  $\nu_0$  are the elastic Young's modulus and Poisson's ratio respectively, and  $E_t$  is the tangent modulus of the tensile stress-strain curve.

Eq. (3.1) can be integrated numerically to yield a relation between  $\epsilon_y$  and  $\epsilon_x$ . This has been done for aluminum and copper.

The aluminum specimens were sheared from a 1100-0 aluminum sheet and annealed at 600°F for two hours and then oven cooled to room temperature. The copper specimens were cut out from an electrolytic tough pitch copper 110(99.9 + % cu) bus bar and annealed at 750°F and then oven cooled to room temperature.

<sup>\*</sup> Detailed description of the apparatus and the experimental procedure is to be found in Ref. 2.



he results are shown in Fig.'s 3 and 4. It may be seen that the classical plasticity theory gives a poor prediction of transverse strain response, particularly for aluminum.

On the other hand the assumption of constant Poisson's ratio is quite good over a wide range of axial strain for aluminum and is almost exactly true in the case of copper. For this reason the assumption of constant Poisson's ratio was adopted in the analysis.

Also shown in Fig.'s 11 and 12 are plots of  $\sigma_{kk}$  versus  $\epsilon_{kk}$ . These plots show very vividly that hydrostatic response is not elastic, at least when the hydrostatic stress is tensile. If one extrapolates from one's experience in elasticity, the effect of this assumption is likely to be large in the case of kinematically constrained configurations.

#### References

1. Valanis, K. C. "A Theory of Viscoplasticity without a Yield Surface," Archives of Mechanics, 23, 517 (1971).
2. Valanis, K. C. and Wu, Han-Chin, "Material Instabilities in the Experimental Study of Some Important Metals," Mech. and Hydr. Report 1.03, Univ. of Iowa (1971).
3. Bridgman, P. W., "Volume Changes in Simple Compression," J. App. Phys., 20, 1241 (1946).
4. Stang, A. H., Greenspan, M., and Newman, S. B., "Poisson's Ratio of Some Structural Alloys for Large Strains," J. of Res. Nat. B. Stand., 37, 211 (1946).

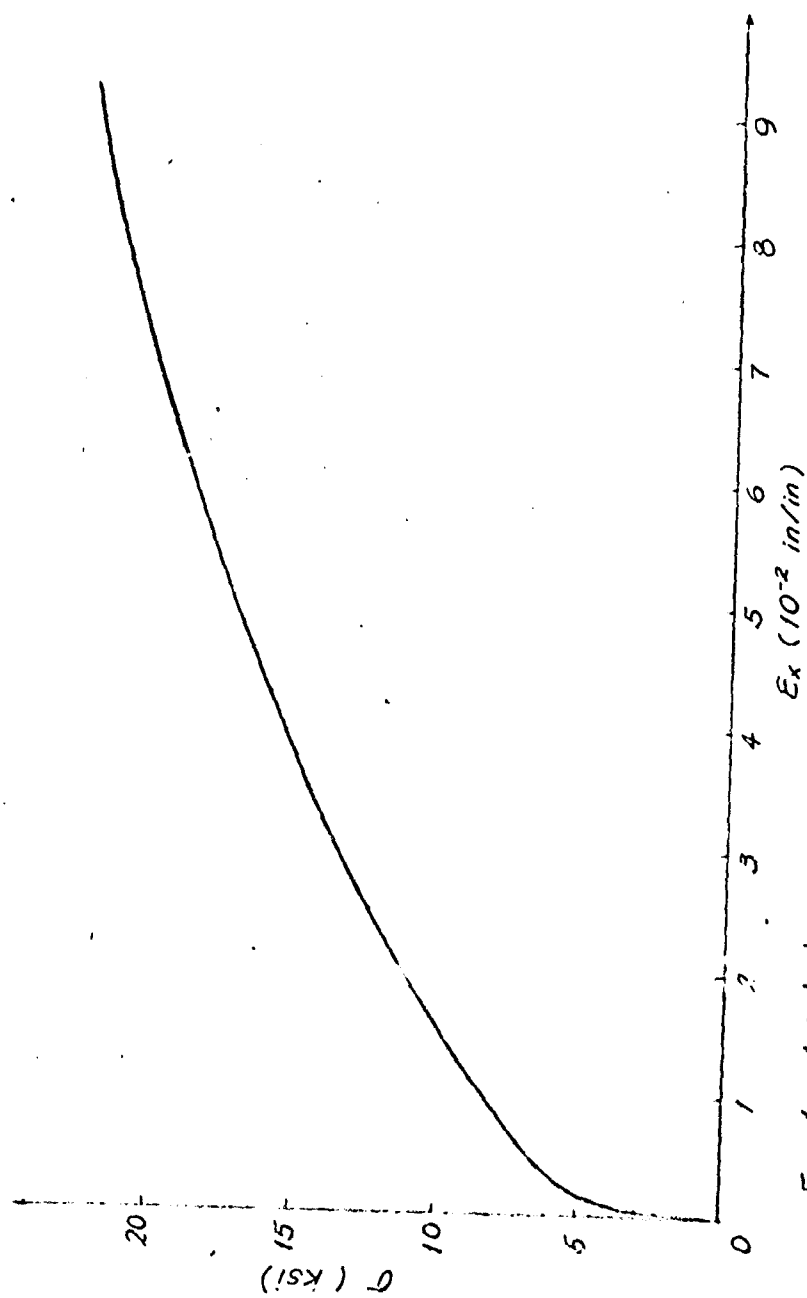


Fig 1 Axial stress vs. axial strain for copper

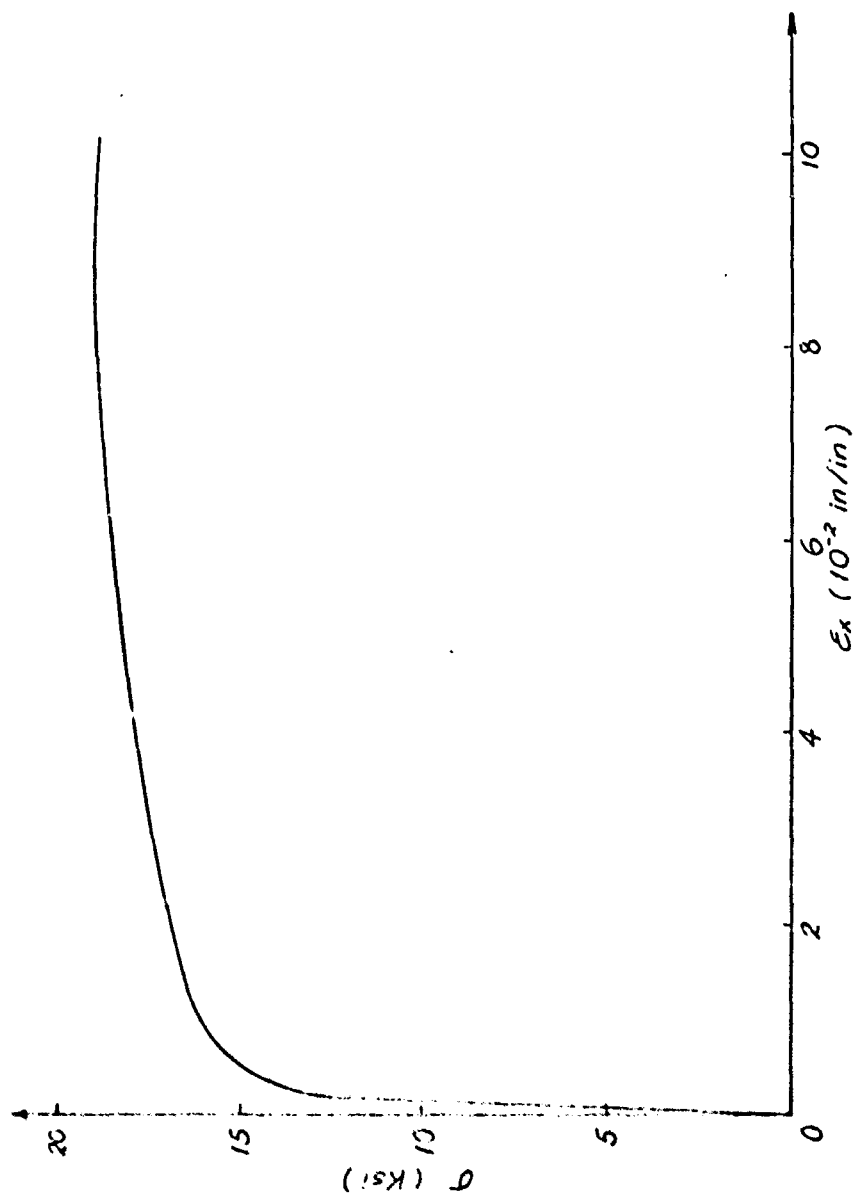


Fig 2 Axial stress vs. axial strain for aluminum

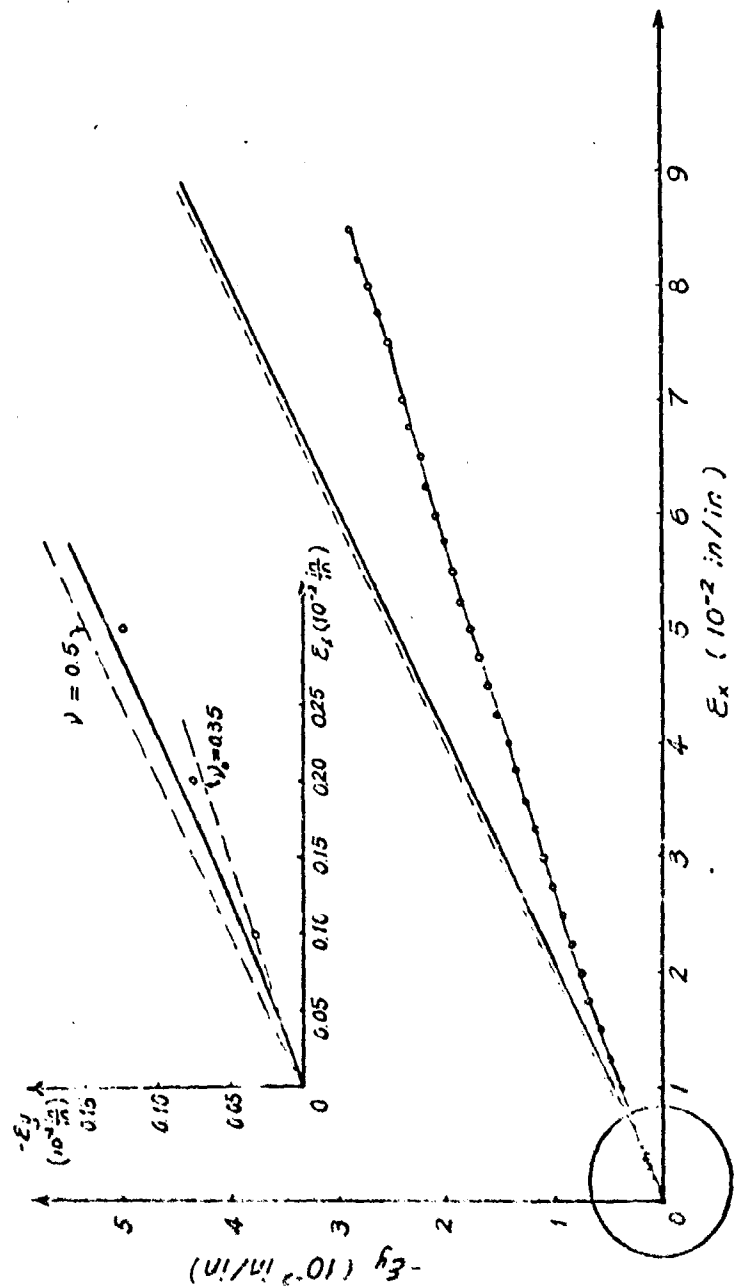


Fig 3 Transverse strain vs. axial strain for copper

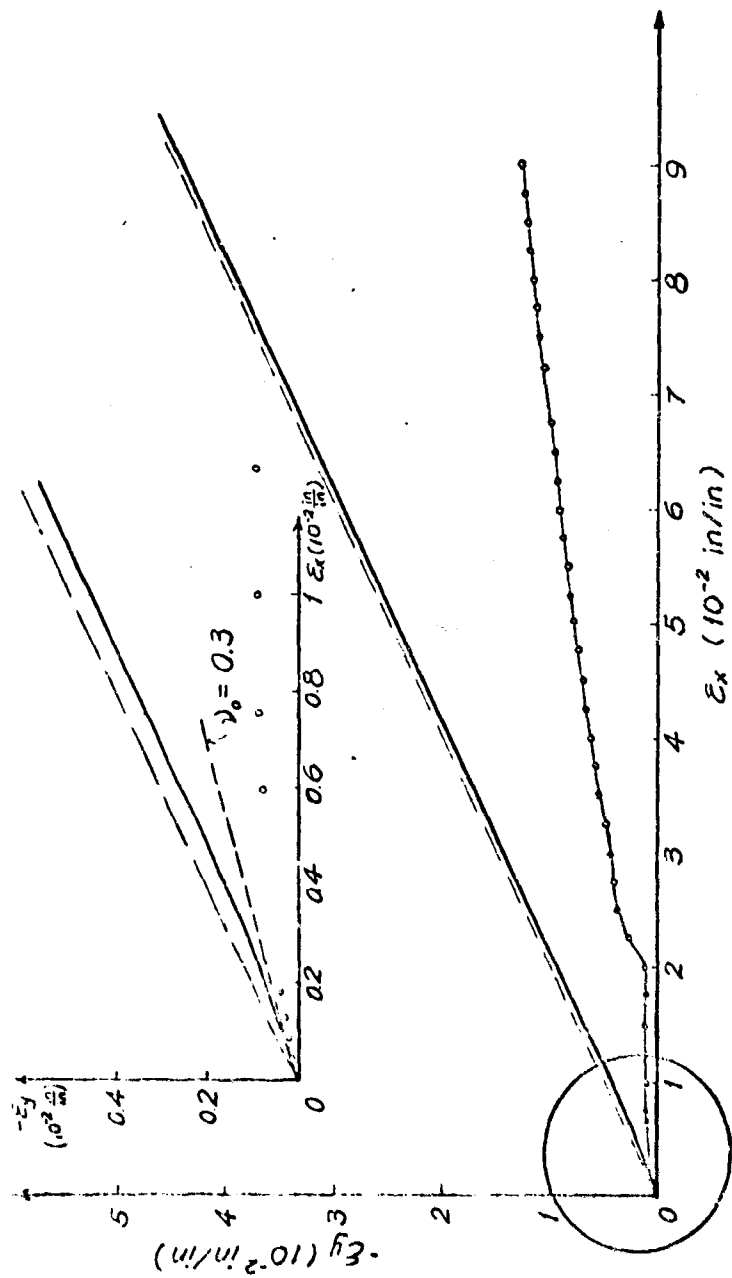


Fig. 4 Transverse strain vs. axial strain for aluminum

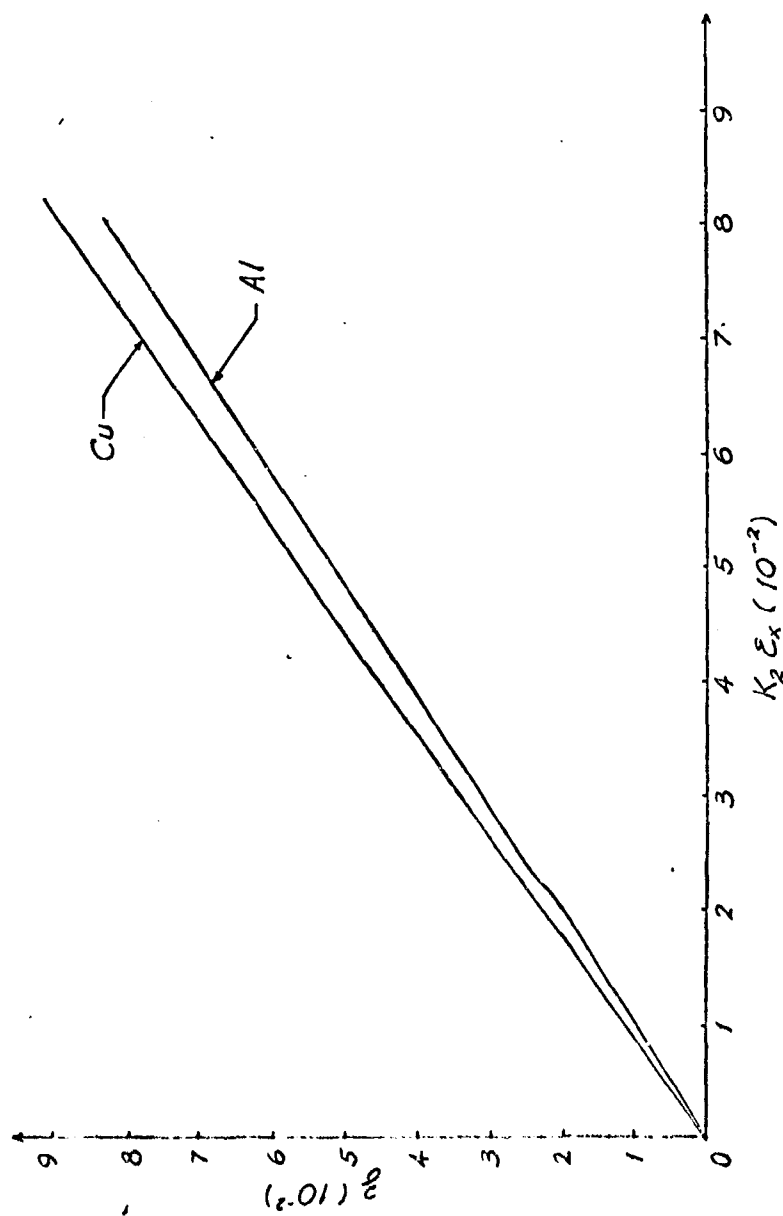


Fig. 5 Axial strain vs. intrinsic time  $\epsilon$  for copper and aluminum

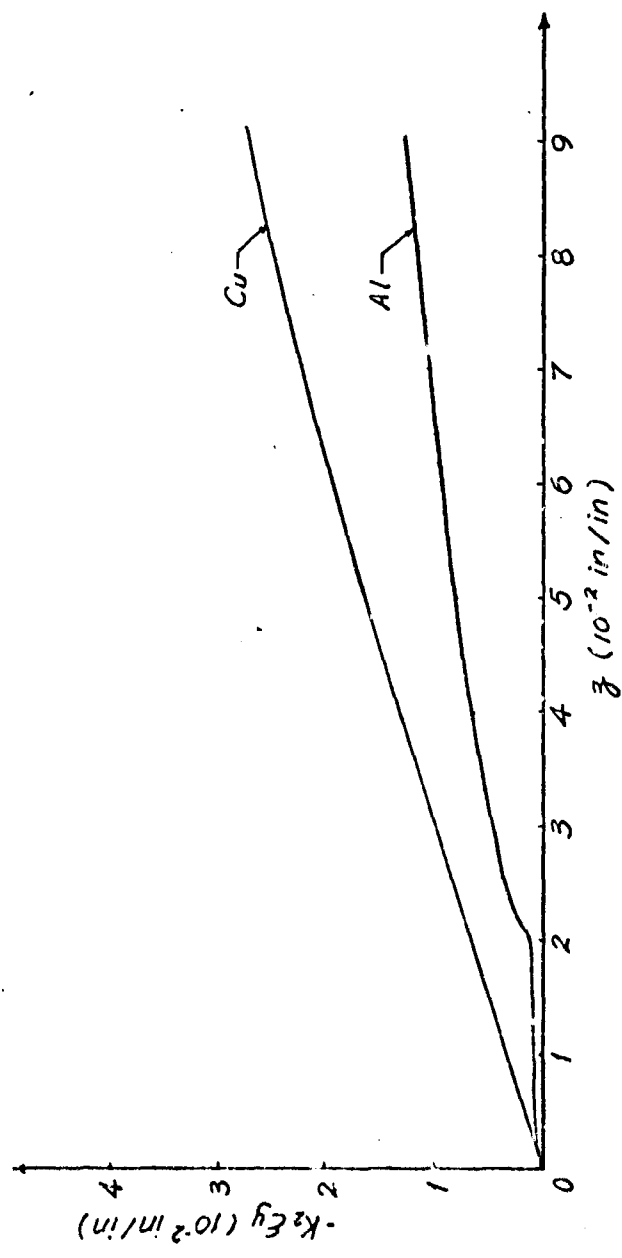


Fig. 6 Transverse strain vs. intrinsic time  $z$  for copper and aluminum

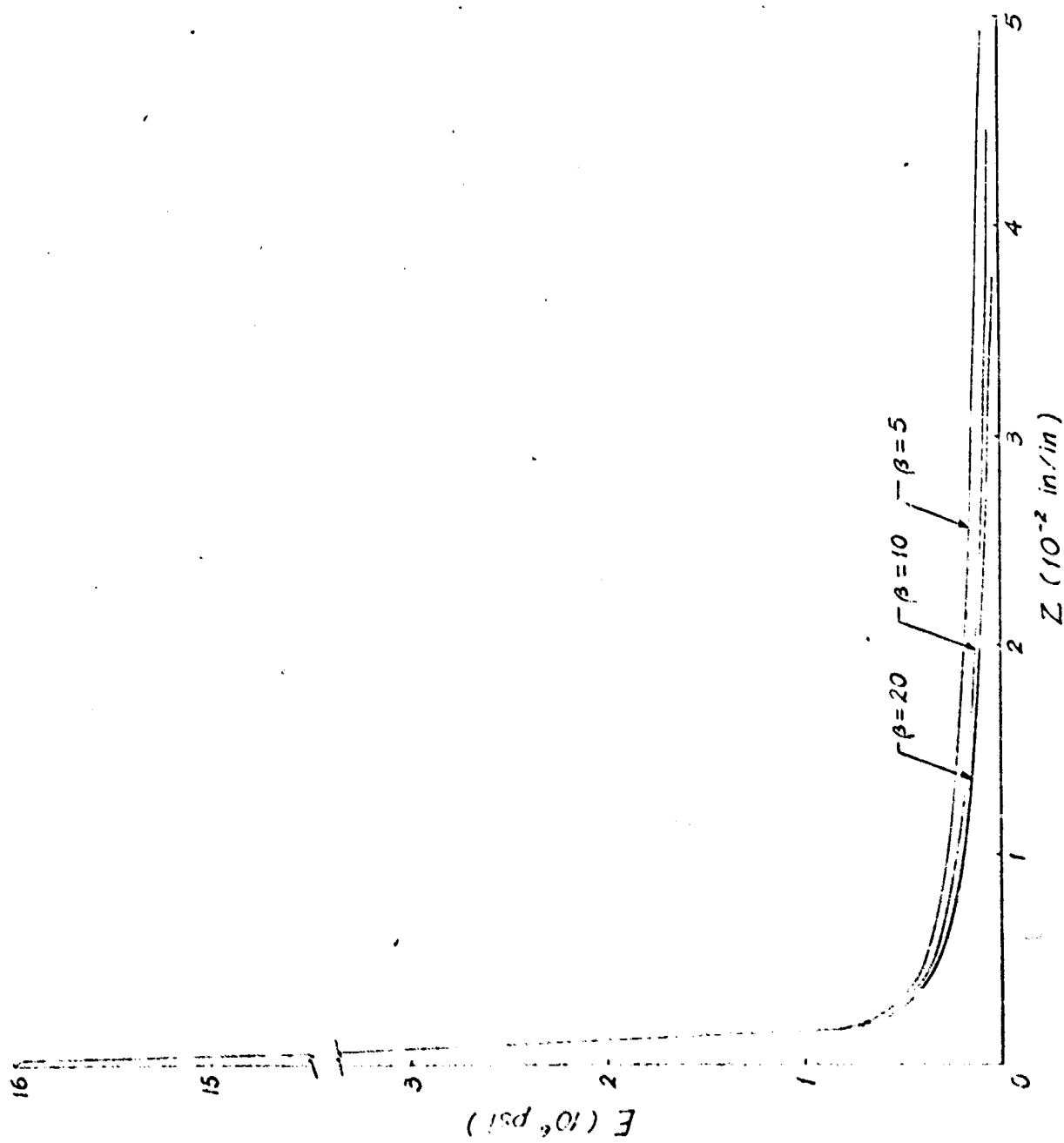


Fig. 7 Tensile heridity function vs. intrinsic time  $Z$  for copper



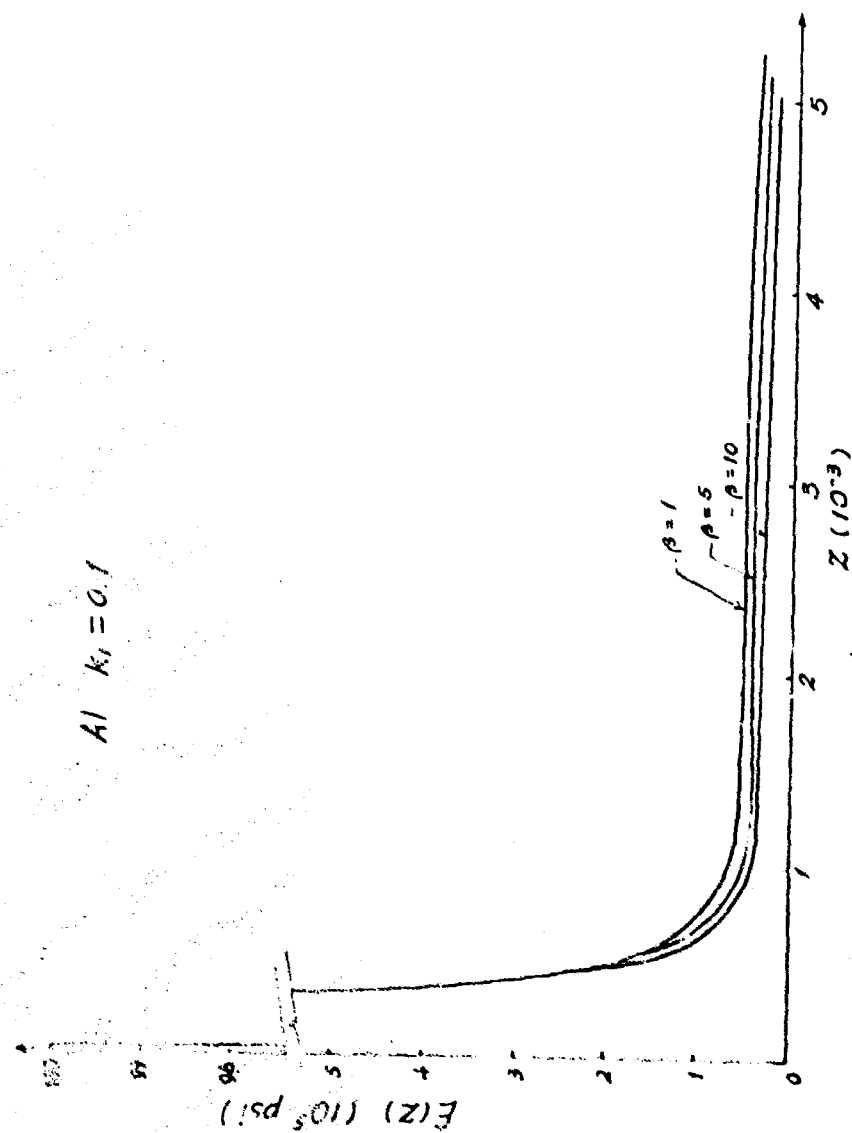


Fig. 8 Tensile hereditary function vs. intrinsic time  $z$  for aluminum

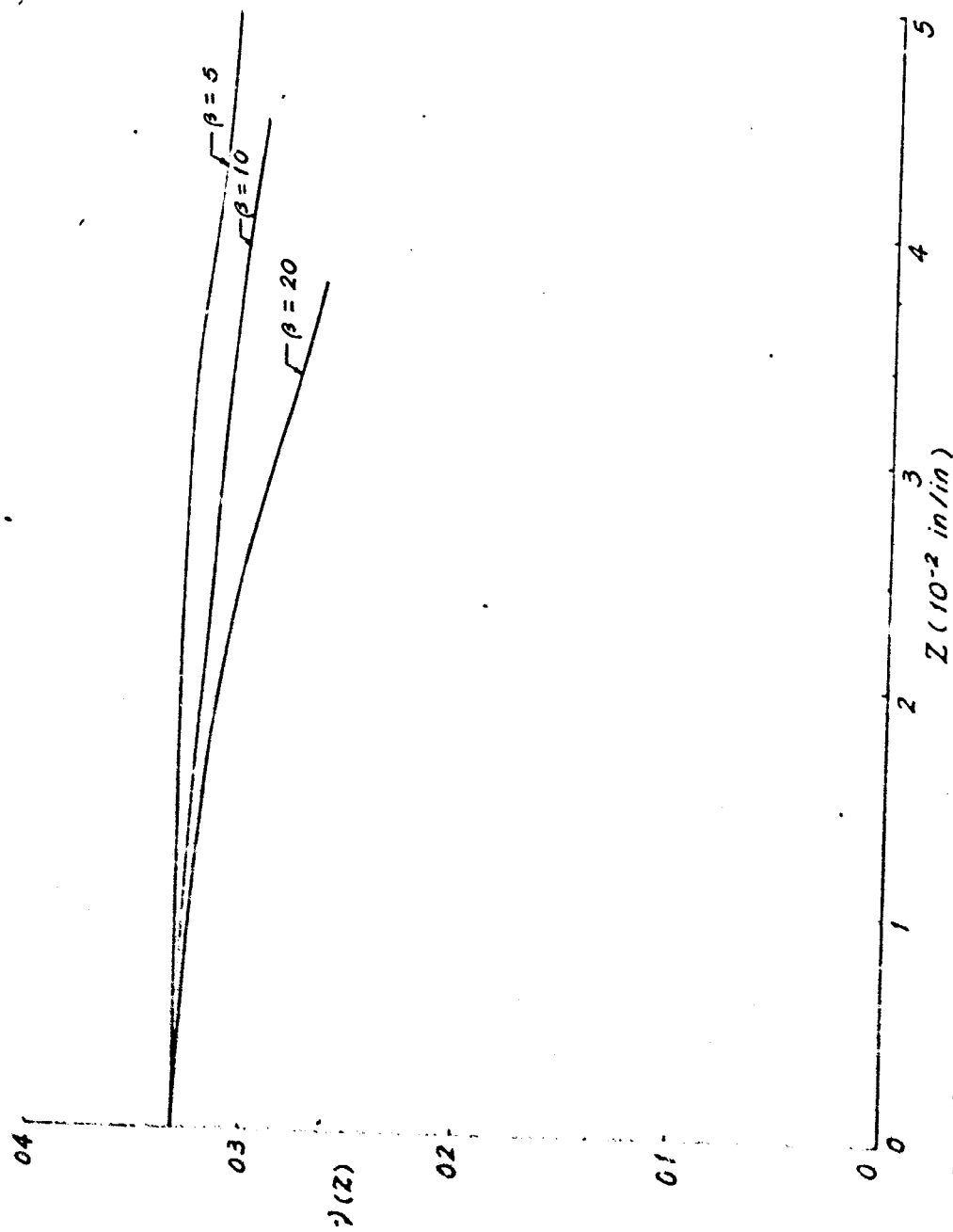


Fig 9 Transverse heredity function vs. intrinsic time  $z$  for copper

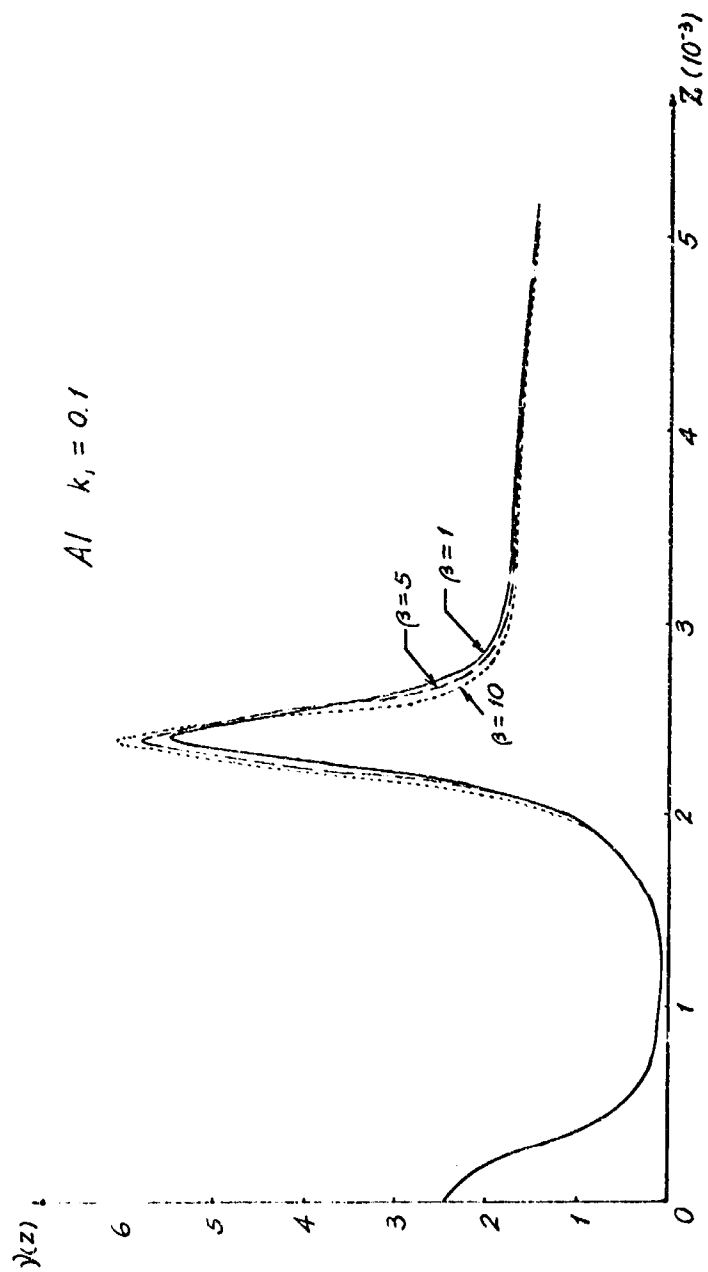


Fig. 10 Transverse heredity function vs. intrinsic time  $z$  for aluminum

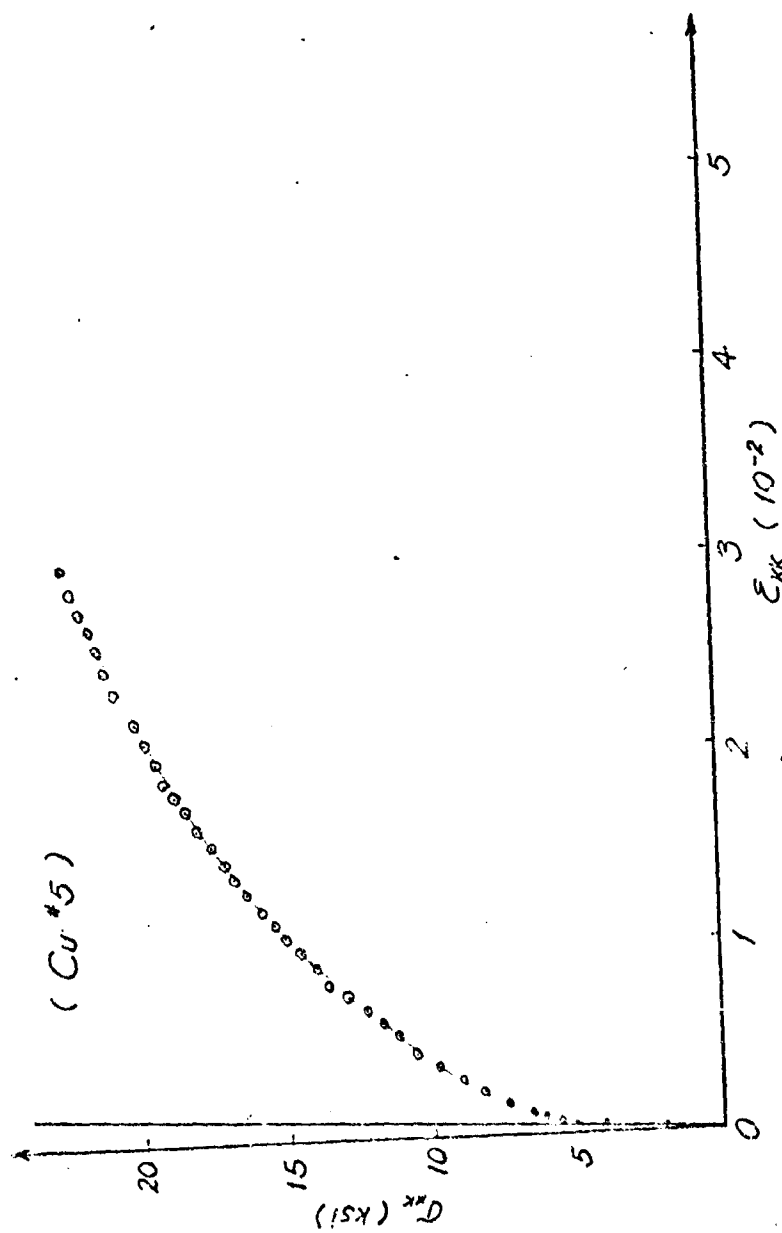


Fig. 11 Hydrostatic stress vs hydrostatic strain for copper

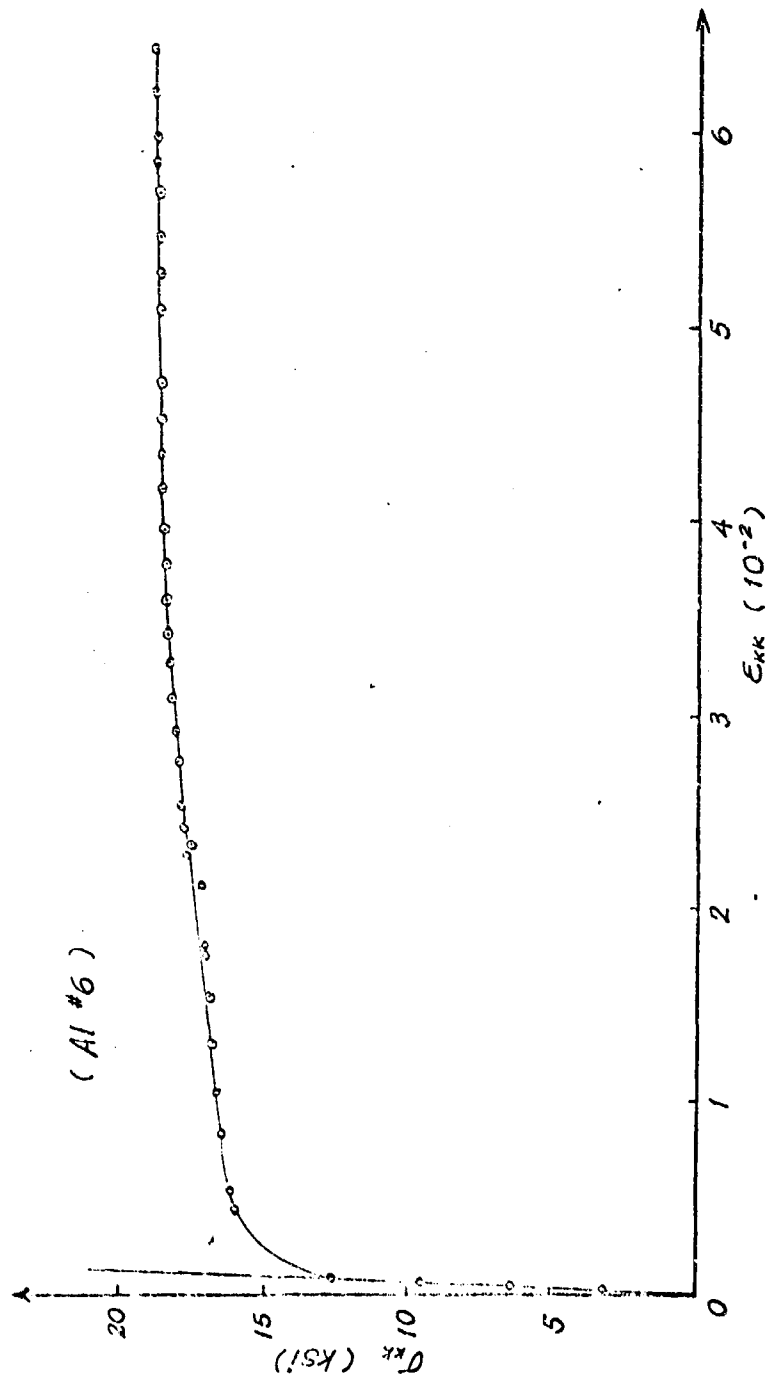


Fig. 12 Hydrostatic stress vs hydrostatic strain for aluminum